DIN: 67SD4405
11 SEPTEMBER 1967

VOYAGER THERMAL INSULATION SYSTEMS
PHASE II SUMMARY REPORT

N68-11264

BY

S. J. BABJAK
M. J. CARPITELLA
R. W. CARR
A. D. COHEN
F. A. FLORIO
C. S. LANKTON
R. LUDWIG
T. F. SMYTH
A. TWEEDIE
A. RICCI

PREPARED FOR

JET PROPULSION LABORATORY
PASADENA, CALIFORNIA
UNDER JPL CONTRACT NO. 951537

GENERAL ELECTRIC
MISSILE AND SPACE DIVISION
Valley Forge Space Technology Center
P. O. Box 8555 • Philadelphia, Penna. 19101

CR-91-55867

DIN: 67SD4405
11 SEPTEMBER 1967

VOYAGER THERMAL INSULATION SYSTEMS
PHASE II SUMMARY REPORT

BY

S. J. BABJAK
M. J. CARPITELLA
R. W. CARR
A. D. COHEN
F. A. FLORIO
C. S. LANKTON
R. LUDWIG
T. F. SMYTH
A. TWEEDIE
A. RICCI

PREPARED FOR

JET PROPULSION LABORATORY
PASADENA, CALIFORNIA
UNDER JPL CONTRACT NO. 951537

THIS WORK WAS PERFORMED FOR THE JET PROPULSION LABORATORY, CALIFORNIA INSTITUTE OF TECHNOLOGY, AS SPONSORED BY THE NATIONAL AERONAUTICS AND SPACE ADMINISTRATION UNDER CONTRACT NAS 7—100.

GENERAL ELECTRIC
MISSILE AND SPACE DIVISION
Valley Forge Space Technology Center
P. O. Box 8555 • Philadelphia, Penna. 19101

This report was prepared by the General Electric Company under Contract No. 951537, Voyager Thermal Insulation Systems, for the Jet Propulsion Laboratory. The work was administered under the technical direction of the Voyager Project Section, Engineering-Mechanics Division of the Jet Propulsion Laboratory, with Mr. Donald Ting acting as Technical Director.

Submitted by: A. D. Cohen

A. D. Cohen, Program Manager (VTIS)
General Electric Company

Approved by: Donald Ting

Donald Ting, Technical Director (VTIS)
Jet Propulsion Laboratory

ABSTRACT

This report summarizes the results of the work performed during Phase II of the subject contract. It contains a description of the test fixtures and insulation systems to be used in the full scale thermal vacuum tests of Phase IV. (The detailed procedure for Phase IV tests has been approved by JPL and has been issued separately as document PVTIS 27.) The results of a detailed thermal analysis are reported.

Several evaluation tests were performed during Phase II. A second set of rapid depressurization tests were performed using an insulation system with vent holes. The results of these tests determined the required vent hole size and spacing to prevent excessive ballooning during launch ascent. Shock, vibration, and acoustic tests were performed to evaluate the ability of the insulation system to withstand these environments. A description of these tests and the results are given. Final results of the long term environmental test will be submitted after the test is completed.

TABLE OF CONTENTS

LIST OF ILLUSTRATIONS

LIST OF TABLES

SECTION 1

INTRODUCTION

The objective of this program, sponsored by the Jet Propulsion Laboratory, is to conduct a research and development effort that will establish techniques of applying superinsulation to planetary vehicles of the Voyager spacecraft/capsule size class. The insulation system should limit the loss of internal energy to space to acceptable values and should protect the vehicle from solar energy at earth and Mars intensity. The program, initiated in October of 1966, is divided into four phases as follows.

Phase I	Study
Phase II	Design
Phase III	Fabrication
Phase IV	Testing

This report covers the major portion of work performed in Phase II. The Phase I results have been discussed in the Phase I Summary Report dated 3 March 1967. A supplement to this present report will be issued in November of 1967 to present the results of a long duration vacuum storage and vibration test.

During Phase II, the full scale thermal vacuum test fixture and insulation systems were designed. The insulation blankets will be comprised of vapor deposited gold on 1/4 mil Mylar and vapor deposited gold on 1/2 mil Kapton. As was shown in Phase I, gold coatings are necessary to withstand the humid ethylene oxide decontamination environment specified in JPL Specification VOL-50530 ETS.

A detailed thermal analysis of the spacecraft and capsule was performed to aid in the prediction of the Phase IV thermal vacuum test results. Steady state analyses were performed for two external environments: near-earth cruise and Mars orbit. The insulation blanket requirements have been generated, and a source of supply identified to insure the procurement of gold on Mylar and Kapton with the required emissivity and adhesion properties. Evaluation tests were also conducted to specify tape materials and adhesives.

In Phase I, a series of rapid depressurization tests were run to determine the effects of boost flight on the insulation system. The blankets used in this test were not restrained,and had provision for venting only at the blanket ends. Unsatisfactory ballooning occurred during the tests, inducing tears in the blankets. A second series of tests were conducted during Phase II where restraining fasteners and vent holes of several different configurations were incorporated into the test blankets. The results of these tests have provided guidelines for specifying vent hole and fastening requirements.

As part of the Phase II effort, a series of environmental tests were performed. Shock, acoustic, and vibration tests were performed on typical test blankets prior to exposure to ethylene oxide cycles. After the decontamination exposure, the blankets were subjected to the three environmental tests for a second time. The results of a long duration vacuum storage test will be documented in a supplementary report. This test, currently in process, subjects an insulation blanket to 60 days of vacuum storage at low temperature. Upon the completion of the 60 days, and with no change in the test conditions, the blanket will be vibrated to simulate the start of the orbit insertion motor. In this manner, the effects of prolonged vacuum storage will be evaluated.

SECTION 2

TECHNICAL DISCUSSION

2.1 DESIGN ENGINEERING

2.1.1 FULL SCALE THERMAL TEST MODEL

2.1.1.1 Test Fixture (GE Drawing 47E211776, Figure 2-1)

The Voyager thermal test fixture consists of two major subassemblies: the spacecraft and the capsule. These two sections will be fastened together for the test, but they may be handled separately as required. Between the spacecraft and the capsule there is an insulation barrier which simulates the aft end of the capsule. The barrier will be supported by a sheet metal platform. The weight of the entire assembly has been estimated as 1900 pounds. The final assembly is comprised of 97 parts and subassemblies, exclusive of fasteners and insulation.

2.1.1.1.1 Capsule Structure Assembly (GE Drawing 47R211634, Figure 2-2)

The capsule has a cylindrical base diameter of 220.5 inches and is 22.50 inches high. From this base there is a 54.7 inch long conical section with a dished (12.0 inch radius) nose. Aft of the cylindrical section there is a short conical section 6 inches long, reducing from the 220.5 inch diameter to 144 inches in diameter. The handling loads are carried at the 144 inch diameter by four handling lugs piercing the forward cone to which the handling equipment is fastened. In the center of the capsule structure is a 45 inch diameter, 48 inch long cylindrical heater can which is attached to the outer skin of the forward cone by means of suspension bars and clips, and to the cylinder section by means of suspension cables and internal structure. The entire assembly consists of 194 piece parts and 9 subassemblies. All of the material, except for the bolts, screws, etc., is 6061-T6 aluminum.

2.1.1.1.2 Spacecraft Structure Assembly (GE Drawing 47R211635-90° Segment, Figure 2-3)
The total spacecraft structure is an approximately 100 inch high, 16 sided figure, measuring 144 inches across the points. The structure is designed to be fabricated in four identical 90-degree segments. At a point three inches from the base is a 16 sided sheet metal structure, 240 inches across the points, representing the solar platform. This platform is supported with triangular sheet metal braces and 2 inch diameter struts. In the center, at the base, there is a simulated rocket motor and nozzle throat. The entire assembly, except for screws, bolts, etc., is made from 6061-T6 aluminum. Each 90 degree segment is comprised of 87 piece parts. The total assembly thus requires 348 individual piece parts, excluding fastener hardware.

2.1.1.2 Handling Equipment
Two primary pieces of handling equipment have been designed: a lift sling and a utility dolly.

2.1.1.2.1 Lift Sling (GE Drawing 47E211780, Figure 2-4)
The lift sling is made up of two crossed 3 inch diameter tubular members and a 1-1/2 inch diameter mast held at the center with a saddle member. Cables are strung from the top of the mast (which is 54.00 inches long) to the ends of the crossed members. There are also cables hanging from the underside of the crossed bars at 73 inches from the center. These cables will attach to the four handling lugs on the capsule structure. The sling is capable of being used to hoist the capsule, the spacecraft, or the two together. All parts are made from CRES steel, series 304.

2.1.1.2.2 Utility Dolly (GE Drawing 47E211788, Figure 2-5)
The utility dolly is made up of two crossed aluminum "I" beams welded at the center and set below four extensions to each arm of the crossed members. Wheels are mounted to each of the four arms. The center section is lower than the outer edge to provide clearance for the simulated rocket motor nozzle. The wheels are swivel type and can be locked. The dolly can be used for either the capsule, the spacecraft, or the two together.

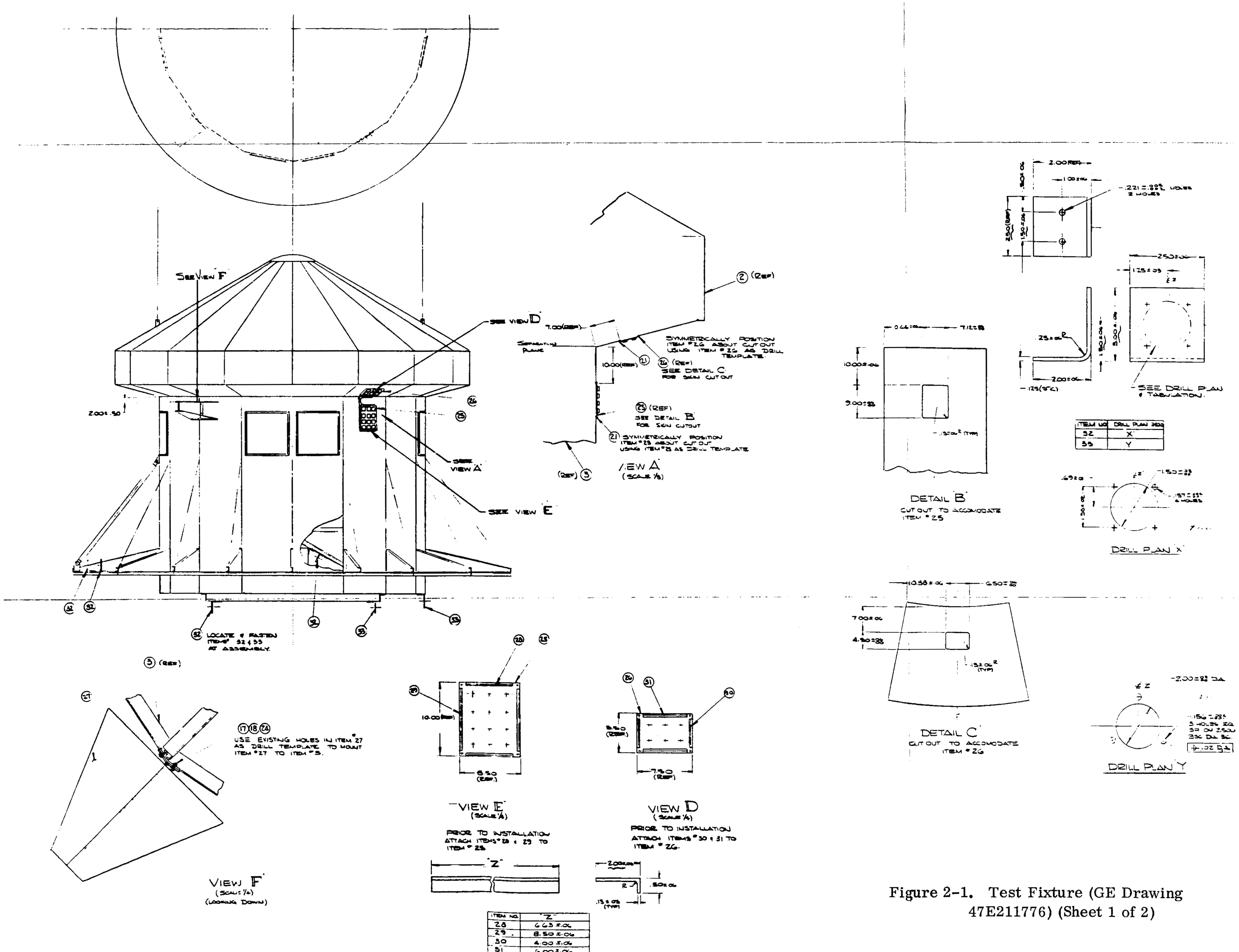

Figure 2-1. Test Fixture (GE Drawing 47E211776) (Sheet 1 of 2)

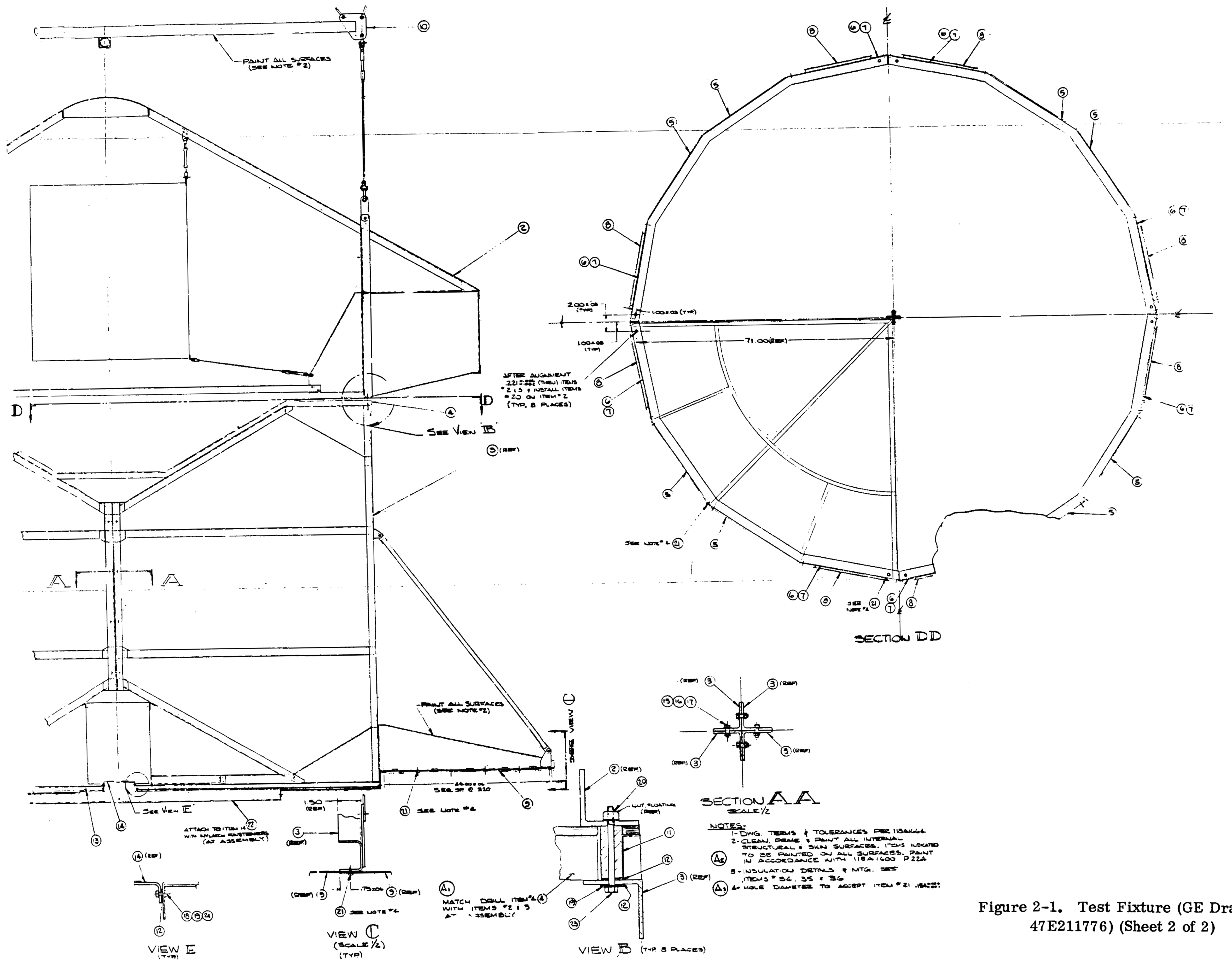

Figure 2-1. Test Fixture (GE Drawing 47E211776) (Sheet 2 of 2)

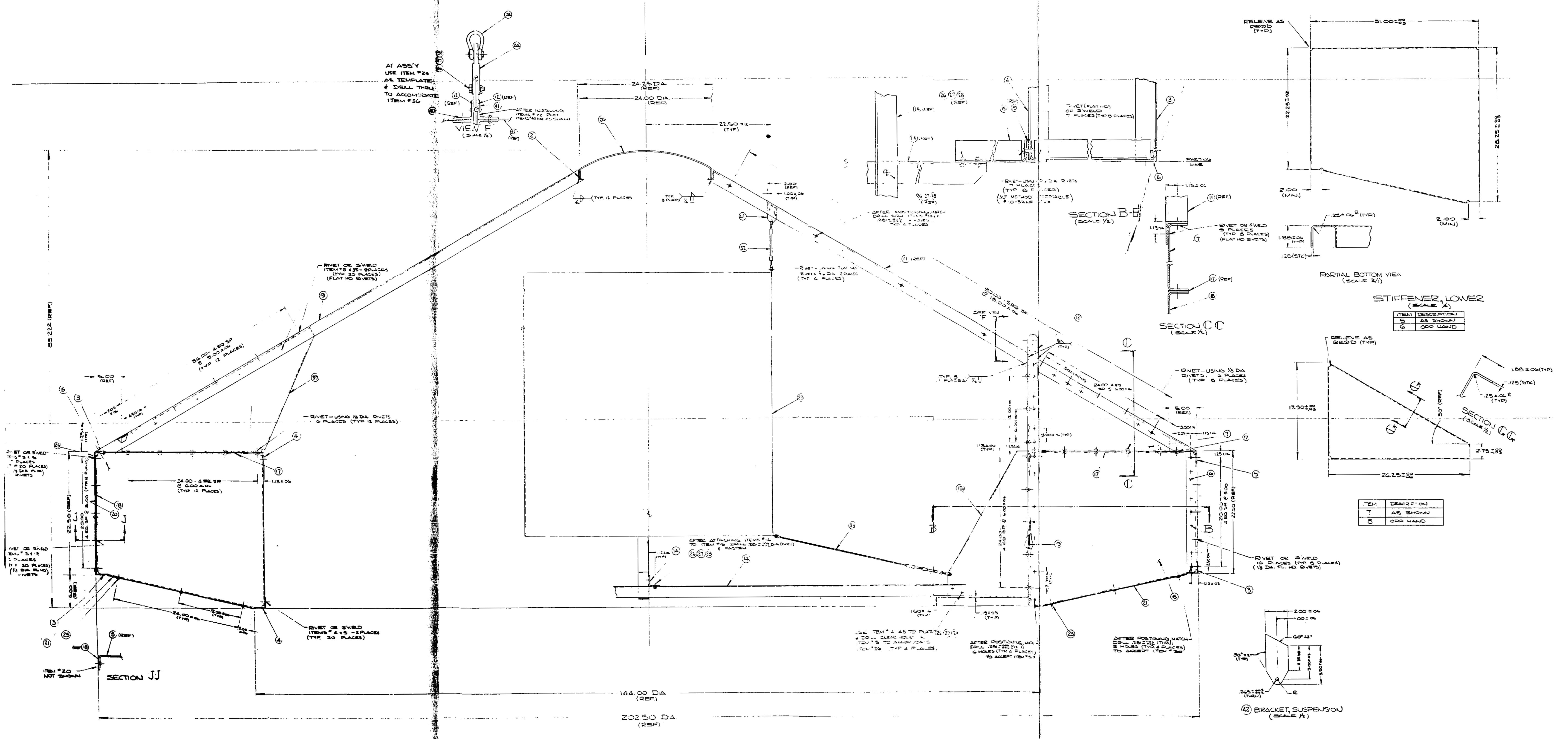

Figure 2-2. Capsule Structure Assembly (GE Drawing 47R211634)

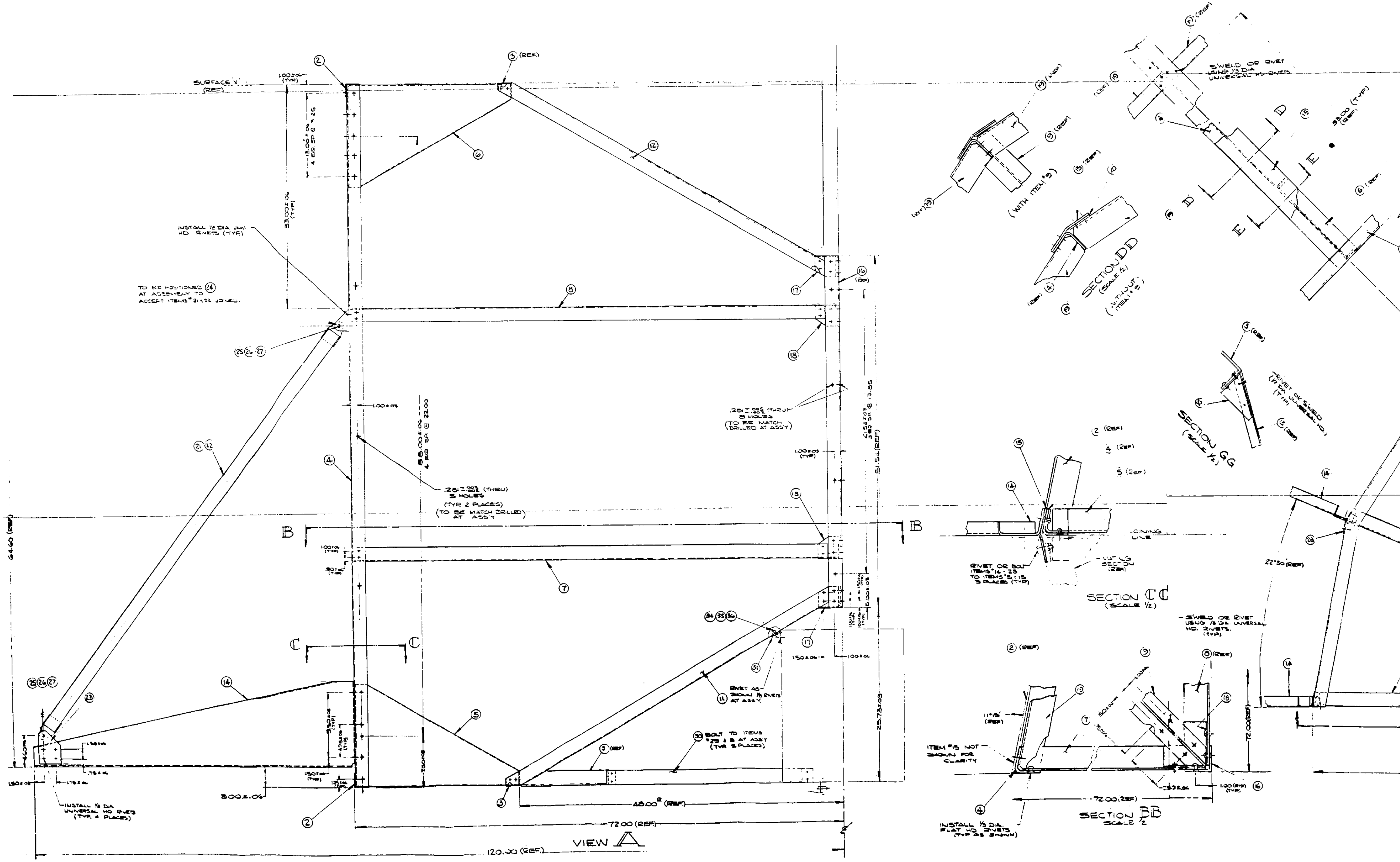

SURFACE 'X' (REF)
INSTALL 1/8 DIA UNIV. HD RIVETS (TYP)
.261 ± .002 (THRU) 3 HOLES (TYP 2 PLACES) (TO BE MATCH DRILLED AT ASSY)
(TO BE MATCH DRILLED AT ASSY)
INSTALL 1/8 DIA UNIVERSAL HD RIVETS (TYP, 4 PLACES)
RIVET AS SHOWN 1/8 RIVETS AT ASSY
120.00 (REF)
72.00 (REF)
48.00 (REF)
VIEW A
SECTION DD (SCALE 1/2)
SECTION GG (SCALE 1/2)
JOINING LINE
SECTION CC (SCALE 1/2)
ITEM #15 NOT SHOWN FOR CLARITY
INSTALL 1/8 DIA. FLAT HD. RIVETS (TYP AS SHOWN)
72.00 (REF)
SECTION BB SCALE 1/2

1

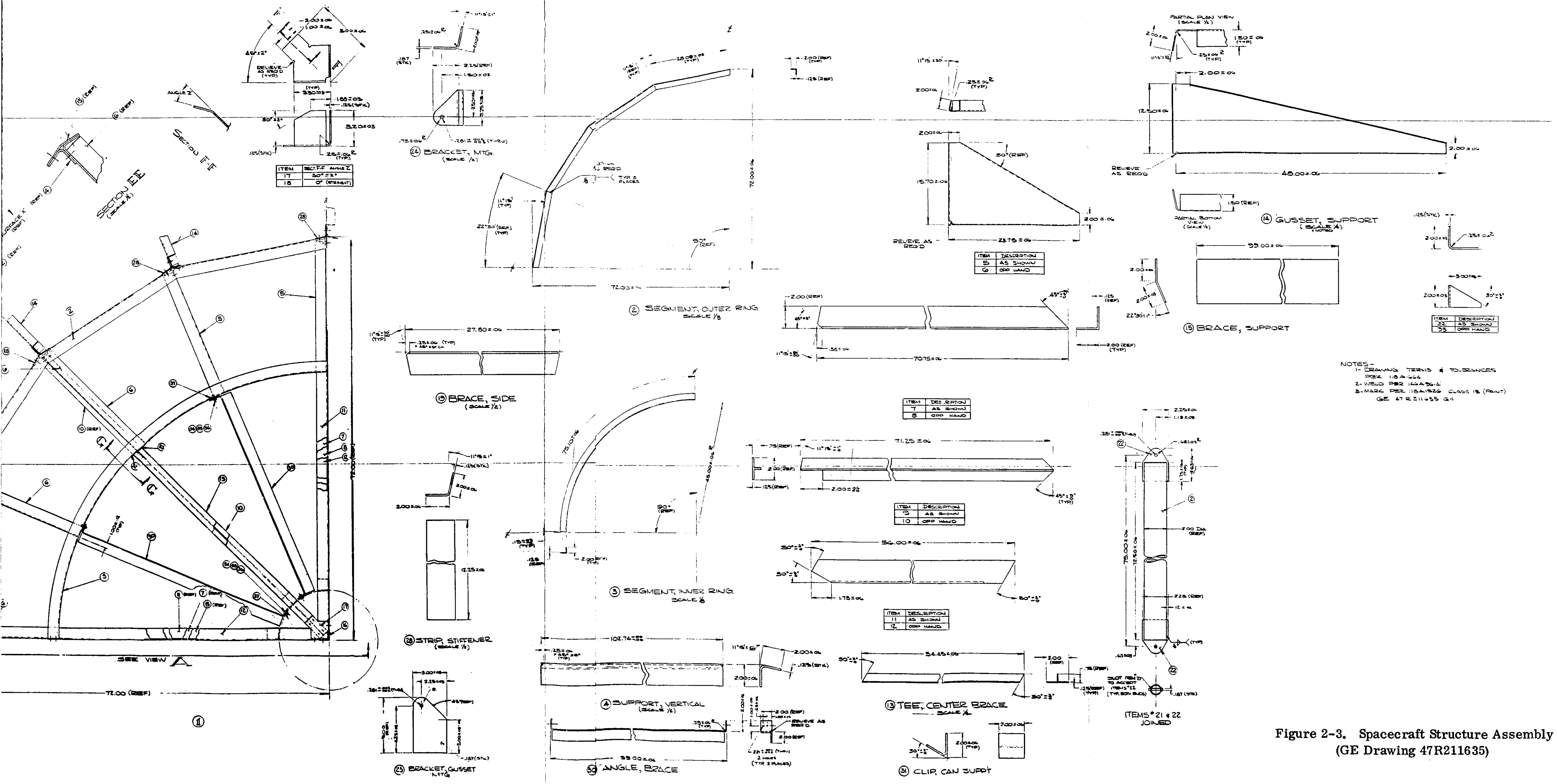

Figure 2-3. Spacecraft Structure Assembly
(GE Drawing 47R211635)

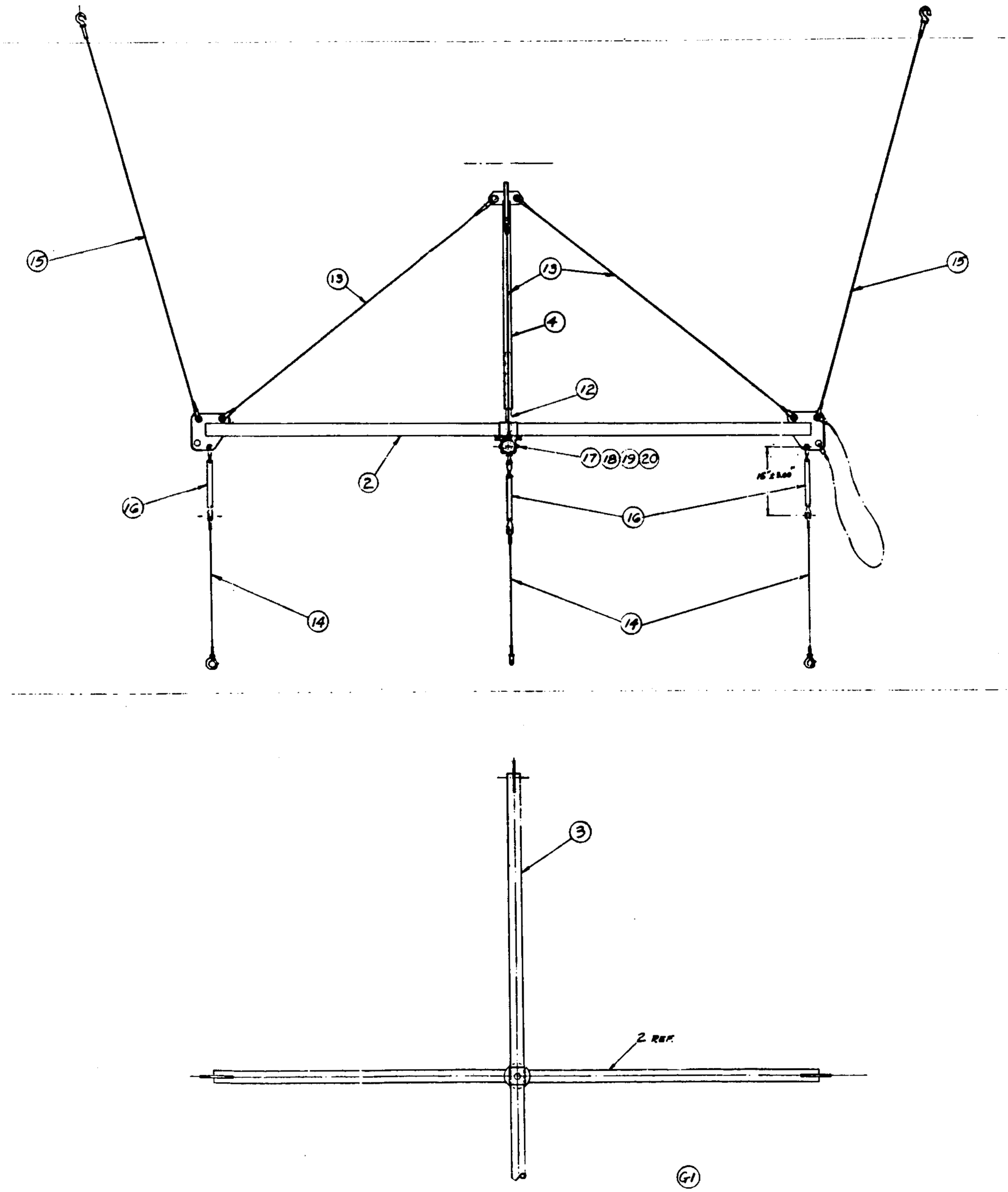

Figure 2-4. Lift Sling (GE Drawing 47E211780)

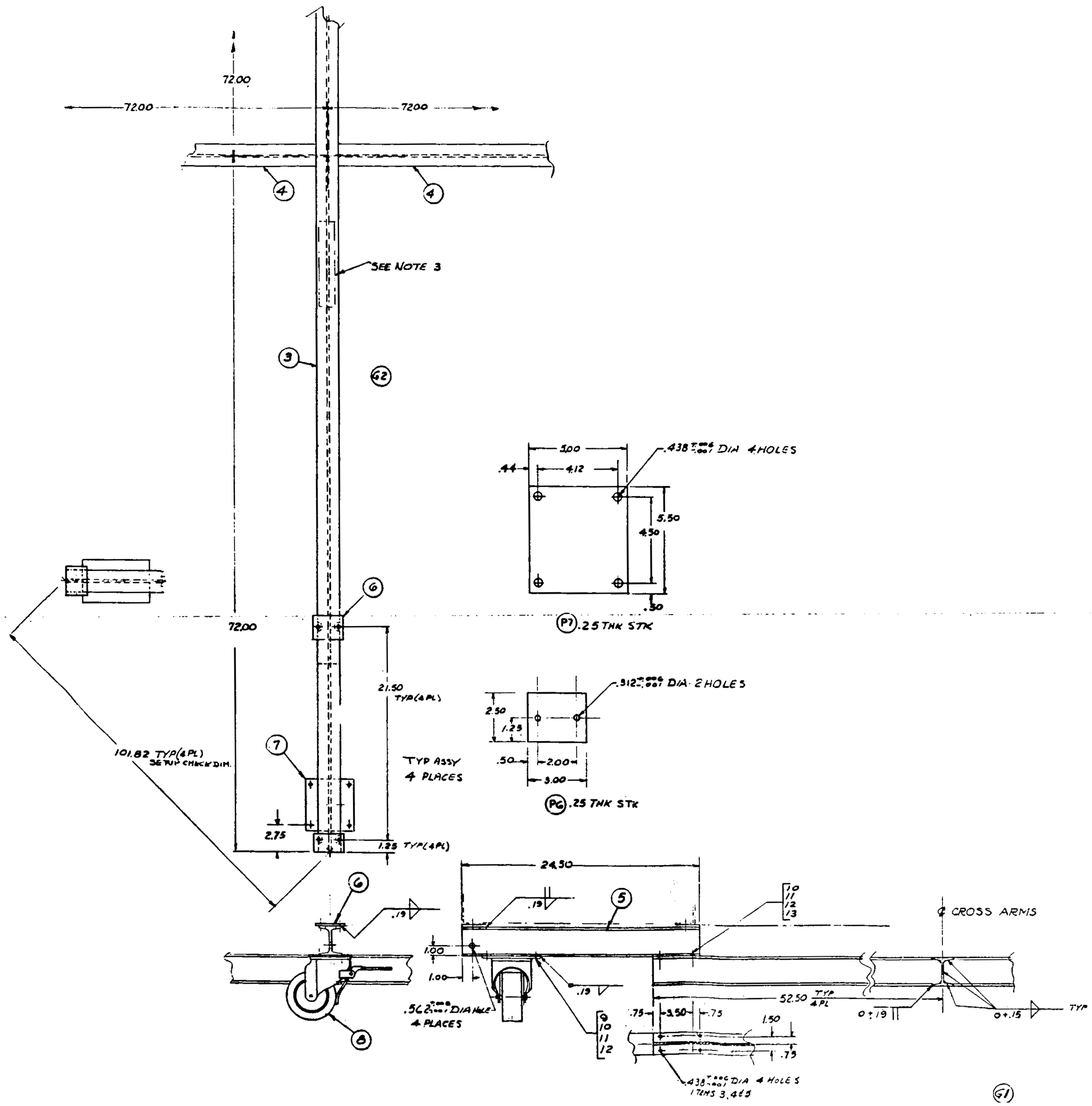

NOTE
1. DRAWING TERMS AND TOLERANCES PER 118A1664
2. WELD PER 14GA9614 CLASS III, VISUAL INSPECTION ONLY.
3. MARK ASSEMBLY GE47E211788G1 PER 118A1526 CLASS 2.

Figure 2-5. Utility Dolly (GE Drawing 47E211788)

2.1.1.3 Insulation Design

The insulation design was divided into four major areas: the insulation for the capsule structure, the spacecraft insulation, the insulation at the top of the spacecraft, and the insulation at the bottom of the spacecraft. In general, a 2 inch overlap step joint was used since its thermal efficiency and ease of manufacturing and handling are superior to the other joint designs considered such as the lap, butt, labyrinth, multistep, knuckle, elbow, reverse elbow, and crush. A significant aspect of the blanket design is that fasteners are being used which will not require disassembly of the fastener to remove the blanket. The fastener, instead, is an integral part of the blanket and is attached to the structure with "Velcro" hook and pile. Two areas of blanket design were resolved; namely, the requirement for relief of internal pressure (venting) and the number of fasteners holding the blanket to the structure. These will be discussed further in this report.

2.1.1.3.1 Capsule Insulation (GE Drawing 47R211785, Figure 2-6)

The capsule insulation blanket dimensions are a 31.5 inch diameter blanket over the nose of the cone, 20 triangular shaped pieces 36 inches across the base and 110 inches long for the conical area, six 109 by 21 inch rectangular pieces around the periphery of the cylindrical section, and seven curved sections 66 inches long and 30 inches wide with an outer radius of 103 inches for the aft cone section.

The triangular blankets covering the forward cone area are wrapped over the upper portion of the cylindrical section for approximately 6 inches in order to prevent gaps at the transition of the cone to the cylinder. In order to assure a good fit by the triangular blanket, slits are required at the large end of the triangular sections. These slits are staggered so that there will be no direct heat loss path, thus minimizing heat losses.

At the present time, four fasteners ("Tingers") are being planned for the nose, 16 for each of the upper cone segments (so that there is no more than 24 inches between fasteners on any one blanket), 19 for each of the cylindrical sections, and 10 for each of the lower cone sections. The fasteners are made from nylon and are shown in Figure 2-7. They have

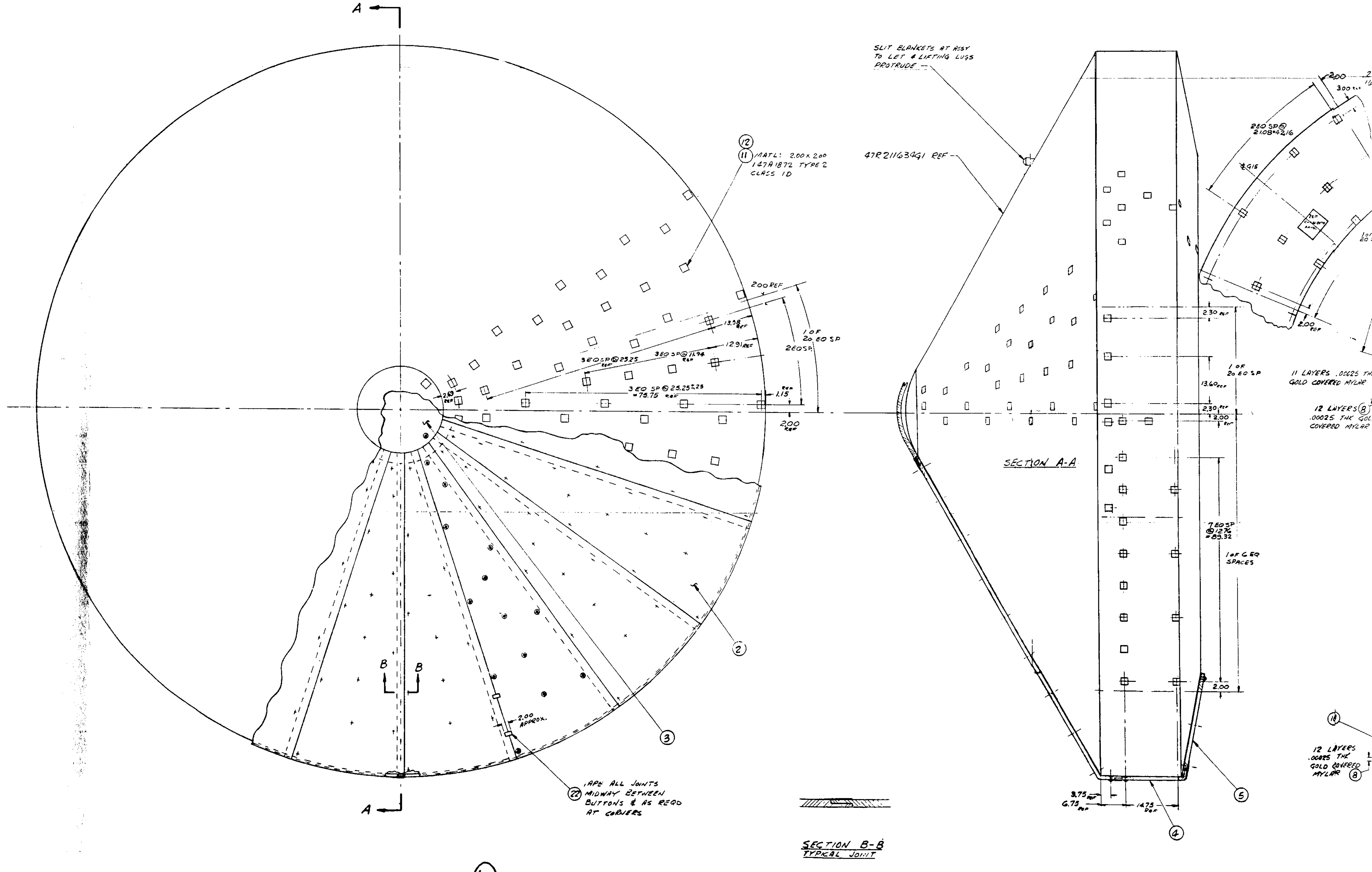

A
A
MATL: 2.00 x 2.00
147A1872 TYPE 2
CLASS 1D
200 REF
1 OF 20 EQ SP
2 EQ SP
3 EQ SP @ 25.25
3 EQ SP @ 11.94
3 EQ SP @ 25.25 = 75.75 REF
1.15
2.00 REF
B
B
2.00 APPROX.
TAPE ALL JOINTS MIDWAY BETWEEN BUTTONS & AS REQD AT CORNERS
SLIT BLANKETS AT ASSY TO LET ¢ LIFTING LUGS PROTRUDE
47R211639G1 REF
SECTION A-A
SECTION B-B
TYPICAL JOINT
2.30 REF
1 OF 20 EQ SP
13.60 REF
2.00
7 EQ SP @ 12.76 = 89.32
1 of 6 EQ SPACES
3.75 REF
6.75 REF
14.75 REF
11 LAYERS .00025 THK GOLD COVERED MYLAR
12 LAYERS .00025 THK GOLD COVERED MYLAR
2 EQ SP @ 21.08 = 42.16
¢ G16
3.00 REF

(1)

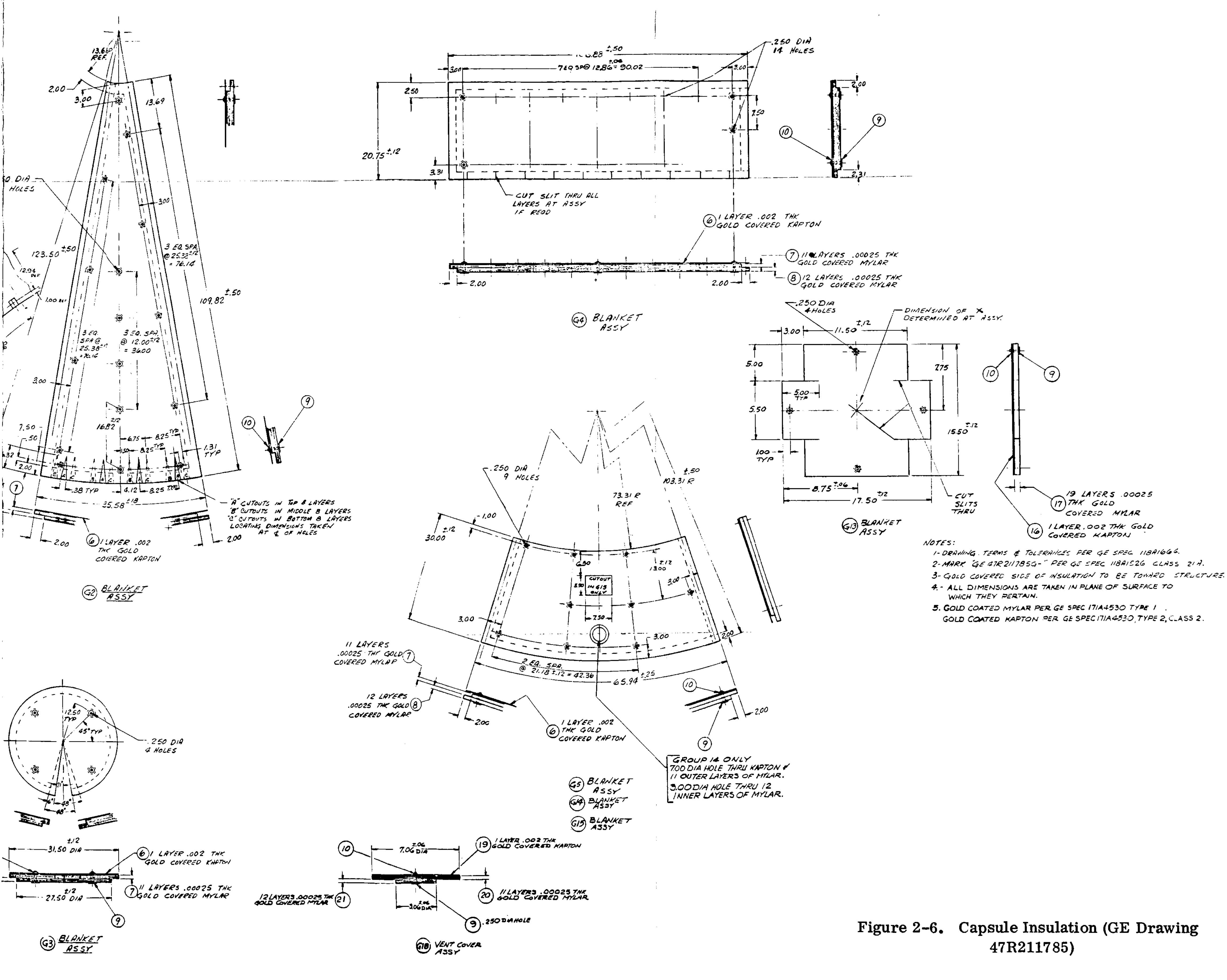

Figure 2-6. Capsule Insulation (GE Drawing 47R211785)

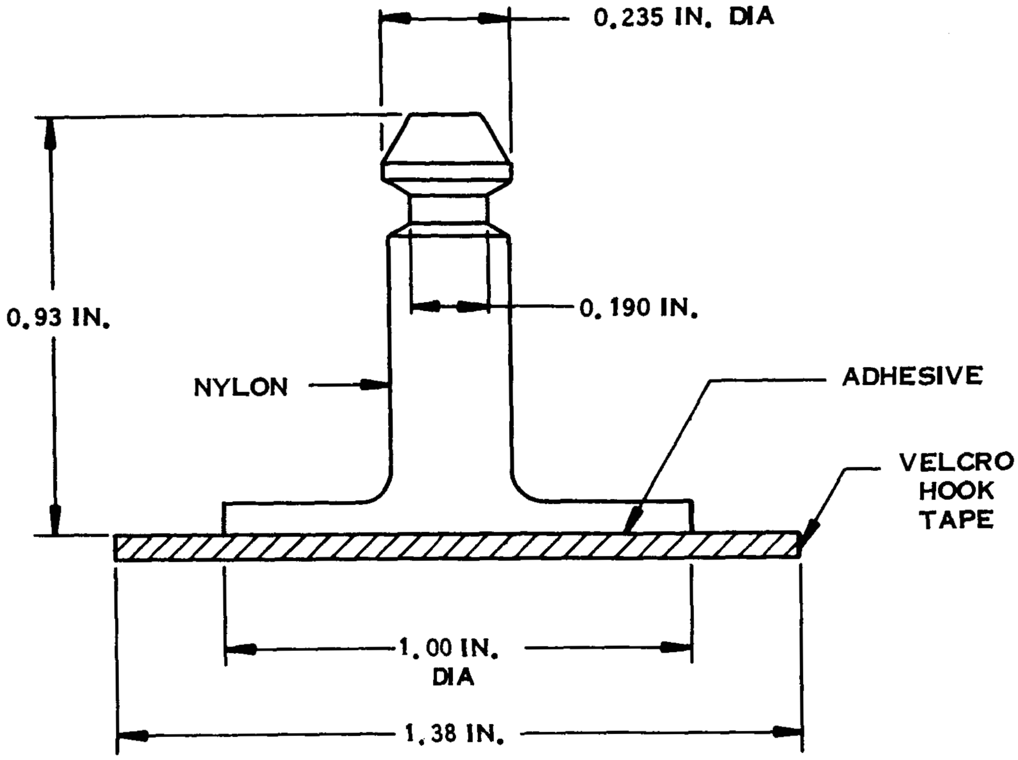

Figure 2-7. Tinger Configuration

1-3/8 inch diameter discs of Velcro hook material cemented to a 1.00 inch diameter base and have a 0.235 inch diameter mast perpendicular to the base. The blanket has a 0.296 inch diameter hole through which the mast is inserted. The mast is undercut at the top to accept a 0.75 inch diameter, 0.06 inch thick nylon washer which holds the fastener in position. There is a corresponding 2 inch square patch of Velcro pile cemented to the structure to which the fastener hook material is assembled.

Generally, penetrations have been held to a minimum. In the capsule blankets, for example, there are four points at which the forward conical blanket is pierced. These splits are for the four handling lugs. Cables and lugs will be insulated with aluminized Mylar (test insulation) prior to the test.

There are no penetrations on either the nose section or the cylindrical blanket section. On the aft conical section there is a cutout for a connector panel. The connector panel, however, has its own blanket which will restrict heat losses from this area. A vent hole is simulated in the aft conical section by a hole cut in the blanket; this hole is covered in turn with a small blanket.

2.1.1.3.2 Spacecraft Insulation (GE Drawing 47R211791, Figure 2-8)
Sixteen individual blankets are to be used to insulate the spacecraft side structure. These blankets are rectangular, 102.5 inches long by 30 inches wide. Eight of the blankets, two each at the principal axes, will have cutouts for simulated thermal panels. At the base of the structure, insulation will consist of nine triangular segments each 34 inches arc length by 41.88 inches long. To complete the insulation on the bottom there are eight sections, each covering two bays which are 26 inches wide. The drawing also calls out the 2 inch diameter strut blanket which is a rectangular piece approximately 10 inches by 72 inches.

The side panels each have 15 fasteners, the bottom interior panels have five each, and the bottom exterior panels have six each. The strut blankets are held to the struts with three fasteners each.

At the top of the spacecraft structure a simulated scan platform penetrates the insulation blanket at the juncture of two bays. The scan platform, however, is also insulated to a point several inches from the outer edge by a blanket. As previously mentioned, eight panels have large cutouts to simulate thermal control panels.

A connector panel also exists at the upper end of the spacecraft, and harnesses from both the capsule and the chamber penetrate here. This penetration is also insulated by a special blanket. At about the middle of the spacecraft, the solar panel support tubes penetrate the blanket. These penetrations are handled by wrapping the upper end lugs with two to three layers of 2 inch wide, 1/4 mil gold coated Mylar for about 12 inches and then installing the tube blanket. The solar panel support brackets penetrate the blankets at the lower outer

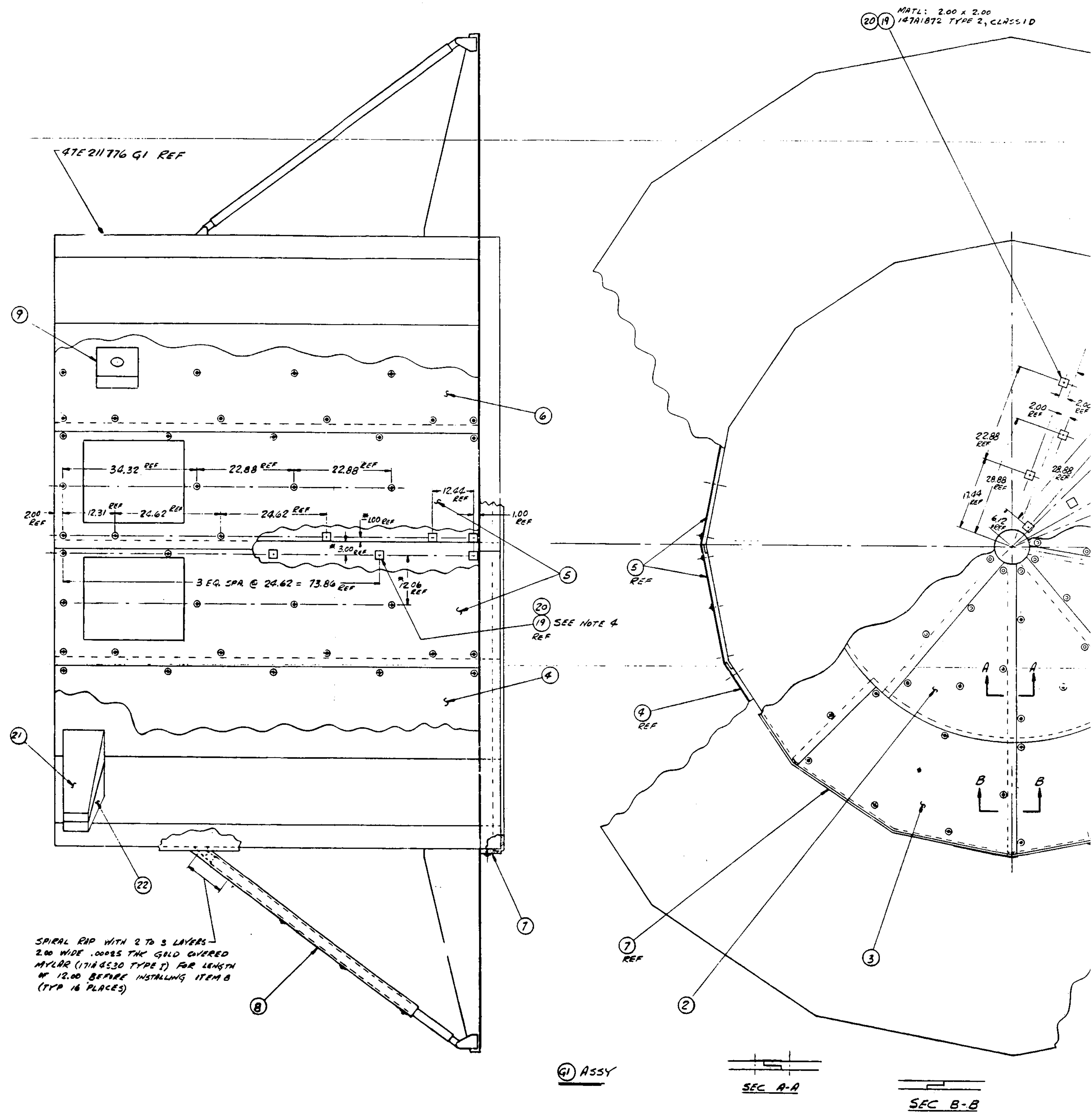

MATL: 2.00 x 2.00
147A1872 TYPE 2, CLASS 1 D
47E 211776 G1 REF
34.32 REF
22.88 REF
12.31 REF
24.62 REF
2.00 REF
12.44 REF
1.00 REF
3 EQ. SPA. @ 24.62 = 73.86 REF
3.00 REF
12.06 REF
SEE NOTE 4
SPIRAL RAP WITH 2 TO 3 LAYERS - 2.00 WIDE .00025 THK GOLD COVERED MYLAR (171A6530 TYPE I) FOR LENGTH OF 12.00 BEFORE INSTALLING ITEM 8 (TYP 16 PLACES)
G1 ASSY
SEC A-A
SEC B-B

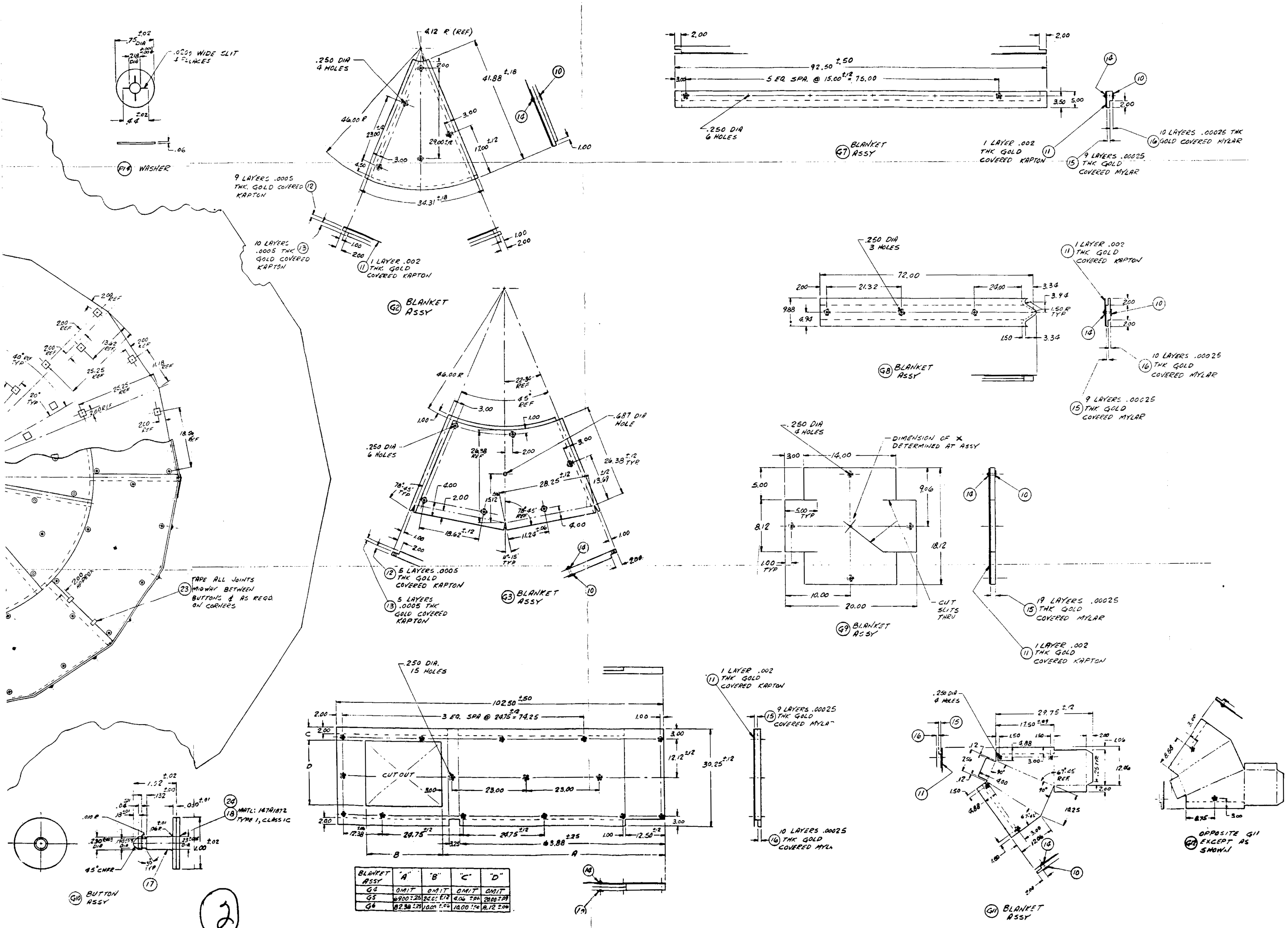

BLANKET ASSY	"A"	"B"	"C"	"D"
G4	OMIT	OMIT	OMIT	OMIT
G5	69.00 ±.25	26.0[illegible] ±.12	4.06 ±.06	20.00 ±.09
G6	82.38 ±.25	10.00 ±.06	10.00 ±.06	8.12 ±.06

NOTES:

1- DRAWING TERMS & TOLERANCES PER GE SPEC 118A1664.
2- MARK "GE47R211791G–" PER GE SPEC 118A1526 CLASS 21A.
3- GOLD COVERED SIDE OF INSULATION TO BE TOWARD STRUCTURE.
4- DIMENSIONS MARKED * ARE TAKEN IN PLANE OF SURFACE TO WHICH THEY PERTAIN
5- GOLD COATED MYLAR PER GE SPEC 171A4530 TYPE 1
GOLD COATED KAPTON PER GE SPEC 171A4530 TYPE 2, CLASS 1 FOR .0005 THK, CLASS 2 FOR .002 THK.

Figure 2-8. Spacecraft Insulation (GE Drawing 47R211791) surface and these are not insulated. The last penetration is on the bottom where the rocket motor penetrates the insulation with an approximate 10 inch diameter hole.

2.1.2 TEST FIXTURES: MECHANICAL TESTS

2.1.2.1 Vibration/Shock/Acoustic Test Fixture (GE Drawing 47R211348, Figure 2-9)

A 30 inch cubic test fixture was used for the vibration, shock and acoustic tests. One plane was used for mounting to the test equipment and the other five surfaces were used for insulation blanket test specimens. The cube is a welded frame made from 4 inch diameter aluminum tubing and covered with thin aluminum skins. The insulation blanket specimens are defined as follows:

Side 1	Nineteen layers of 1/4 mil gold coated Mylar and one layer of 2 mil Kapton, held with four fasteners.
Side 2	Same as side 1 except six fasteners are used.
Sides 3 & 4	Two blankets, one of which covers 1-1/2 sides, the other 1/2 side. A step joint is used between the two. Both blankets are made similar to side 1.
Top	Ten layers of gold coated 1/2 mil Kapton with four fasteners.

The objective of the tests is to evaluate the capability of the blankets and their mounting system to withstand the mechanical environments to which they will be exposed. If the insulation system passes the tests without problems, the full scale thermal test model insulation will not need modification. Problems, if they occur in this series of tests, may require changes to the full scale design.

2.1.2.2 Depressurization Test Fixture (GE Drawing 47E210413, Figure 2-10)

The test fixture is a rectangular frame 120 inches long by 48 inches wide. One side of this frame is covered with an insulation blanket test specimen. The objectives of the test are (1) to evaluate the use of holes for venting the internal layers of the blanket, (2) to determine if the step joint is acceptable for use on large blankets, and (3) to obtain information on the need for intermediate fasteners. Four specimens were used in this test. Three of the specimens had a different number of holes (4, 9 and 16 holes per square foot, all 1/8 inch in diameter) and the fourth specimen had additional posts along with four 1/8 inch diameter holes per square foot. The results of this test are reported in Section 2.5.2.

2.1.2.3 Long Term Thermal Vacuum Test Fixture (Figure 2-11)

This test fixture is a 14 inch long by 14 inch diameter right circular cylinder of sheet metal. The cylinder is made in two sections. A sheet metal cone is mounted inside the upper half and the armature of a vibration exciter is mounted to the small end of the cone, inside the lower half of the cylinder. The exciter body is supported by springs from the joint between the upper and lower halves of the cylinder. The external surface of the cylinder is insulated with 20 layers of gold coated Mylar, and Kapton step joints and Tinger support posts were used for assembly. The entire assembly will be supported by springs in the cold walled vacuum chamber.

Although not intended as a definitive thermal performance test, the thermal performance is being monitored to determine if any change occurs when the model is vibrated at the end of a 60 day period. To maintain the fixture at $40^{o}F$ in its liquid nitrogen cooled environment, 3.7 watts is required; chamber pressure is below 2×10^{-8} torr. It is estimated that the net heat leakage from the insulation is less than 2.5 watts, after subtracting from the gross power the leakage from six pairs of thermocouple leads, six heater wires, two accelerometer cables, the exciter power lead, and the three structural supports. The exposed fixture surface area is about 7 square feet, so the net insulation leakage approximates 1.2 Btu/hr-ft^2.

It is expected that the thermal performance of the full scale insulation system will be considerably better than the insulation on this relatively small model. However, this model's thermal performance, when extrapolated directly for the larger surface area, is sufficient to satisfy the full sized vehicle requirements.

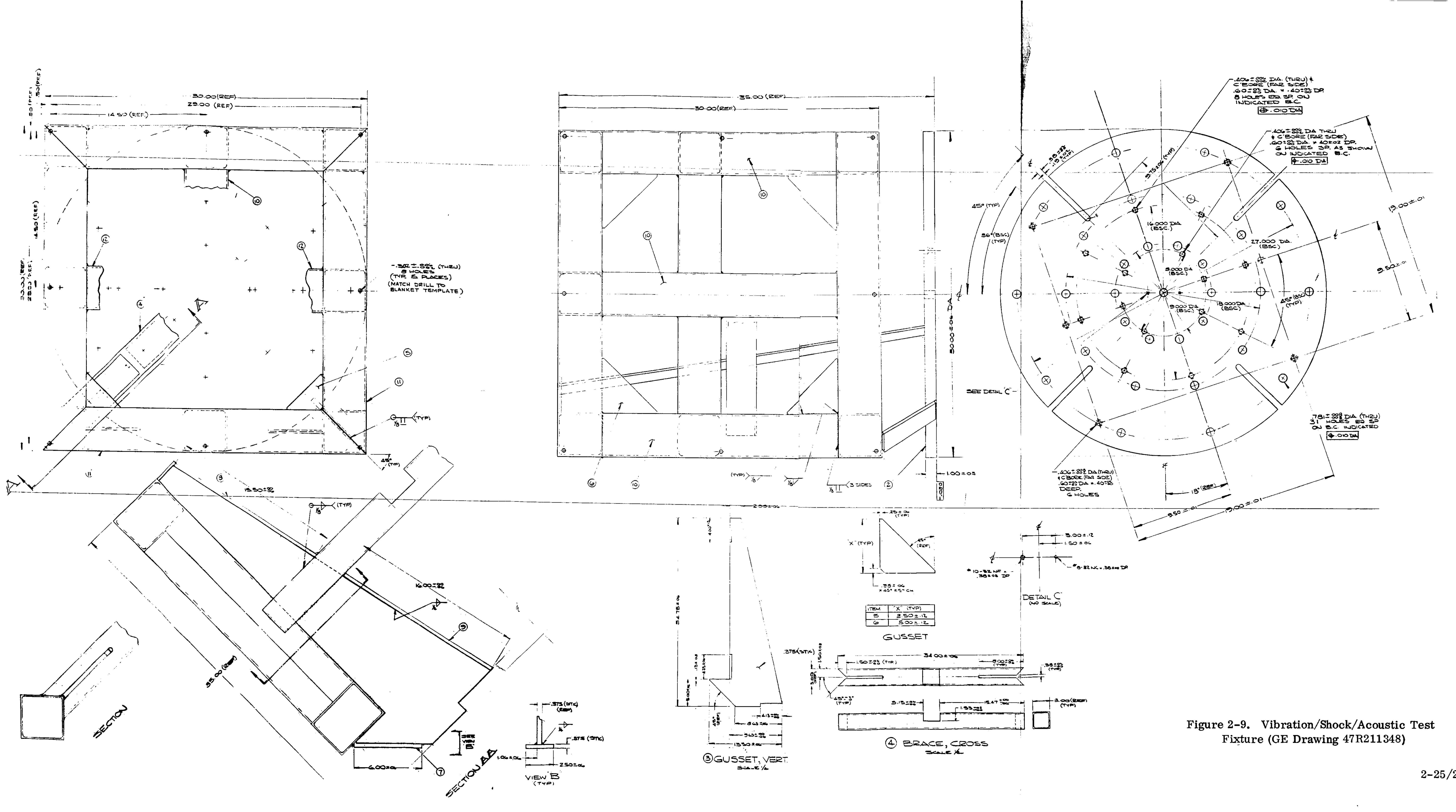

Figure 2-9. Vibration/Shock/Acoustic Test Fixture (GE Drawing 47R211348)

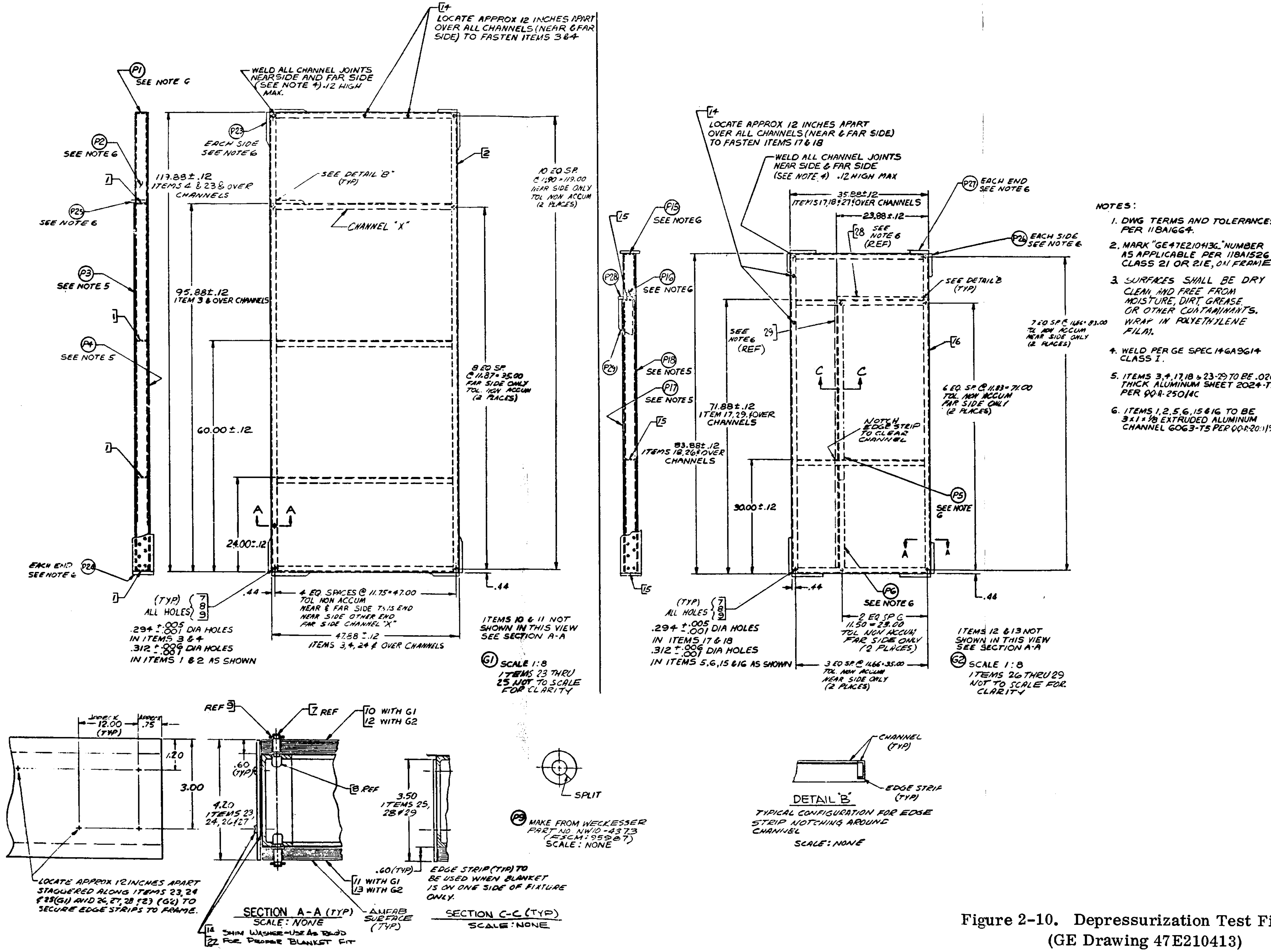

Figure 2-10. Depressurization Test Fixture
(GE Drawing 47E210413)

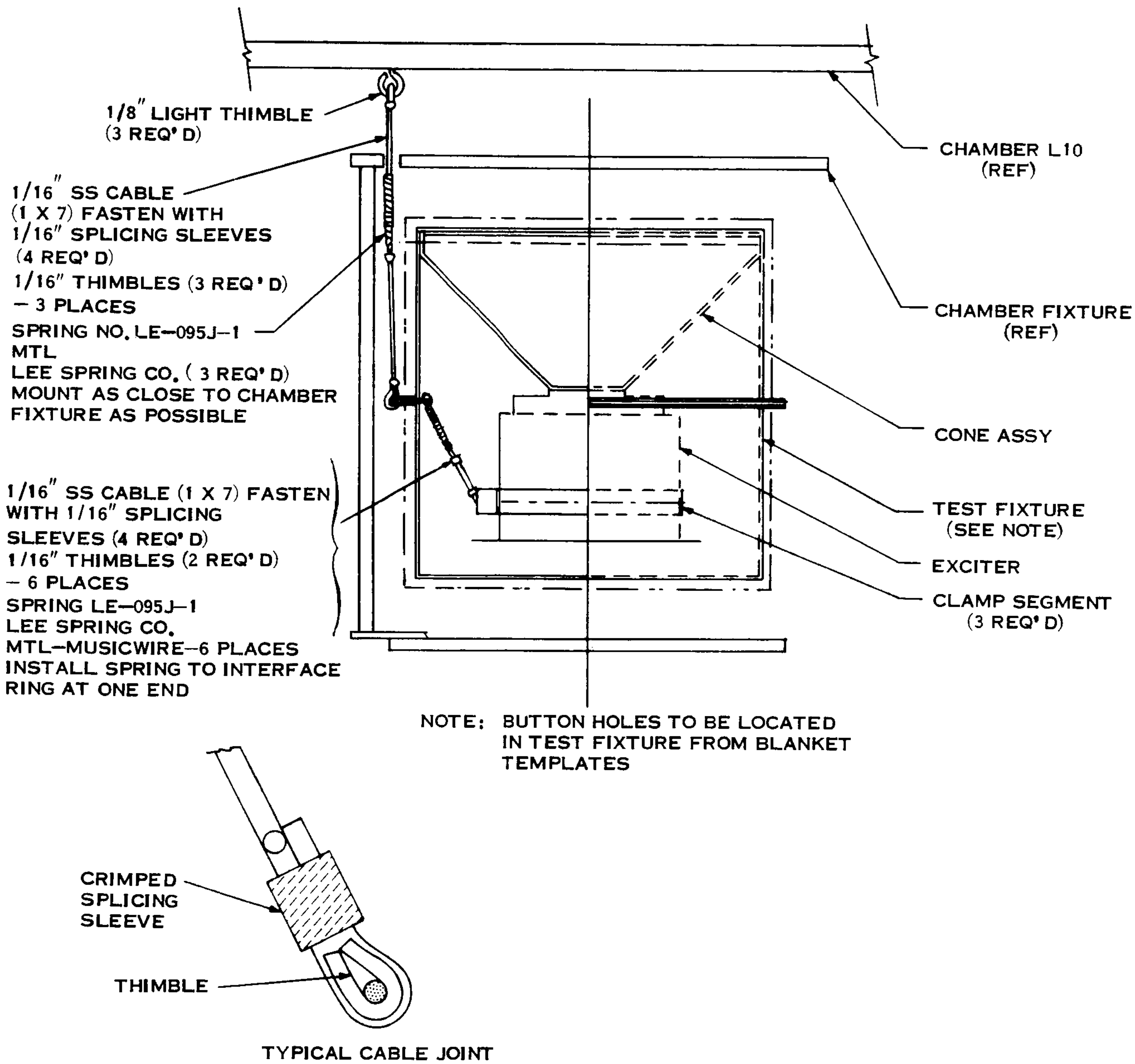

Figure 2-11. Long Term Thermal Vacuum Test Fixture

2.2 THERMAL ANALYSIS

The objectives of the thermal analysis conducted during Phase II were to determine the temperature patterns that are to be expected in the capsule and spacecraft structure with the insulation system designed for the Phase IV tests, and to predict the power required to maintain these structures at desired operating temperatures. The steady state analyses were performed for two external environments: near-Earth cruise and Mars orbit.

2.2.1 CAPSULE ANALYSIS

The capsule analysis was performed for two configurations: one with the nodal division as shown on Figure 2-12, and the other with the heat shield and aeroshell structure removed (nodes 8 to 17). Thus, the first configuration is generally representative of an actual capsule configuration, with the surface laboratory represented by the cylindrical heater of node 1, while the second configuration, which does not incorporate the heat shield and aeroshell structure within the sterilization canister, is similar to the capsule test fixture designed for Phase IV.

All of the capsule nodes are symmetrical about the centerline. Planar nodes 2 and 3 are used to represent the actually conical insulated interface between the capsule and spacecraft. Nodes 2, 3, and 4 are considered adiabatic, since the spacecraft and capsule may be at the same temperature, except for the one low temperature capsule case where the spacecraft is assumed warmer. Nodes 5, 6, 7 and 18 through 22 are assigned to that part of the sterilization canister that is exposed to space. It is assumed that no external radiation is incident on this external surface, since it is shaded from the sun by the spacecraft, and that radiation to space through the surrounding insulation is controlled by an effective emittance term applied to these nodes. Each of the nodes exchanges internal radiation with all other nodes in view, except that radiation between the heat shield and the adjacent canister is restricted to nodes that are immediately opposite; e.g., node 13 to node 18, node 14 to node 19, etc. Table 2-1 shows the details of the internodal connections.

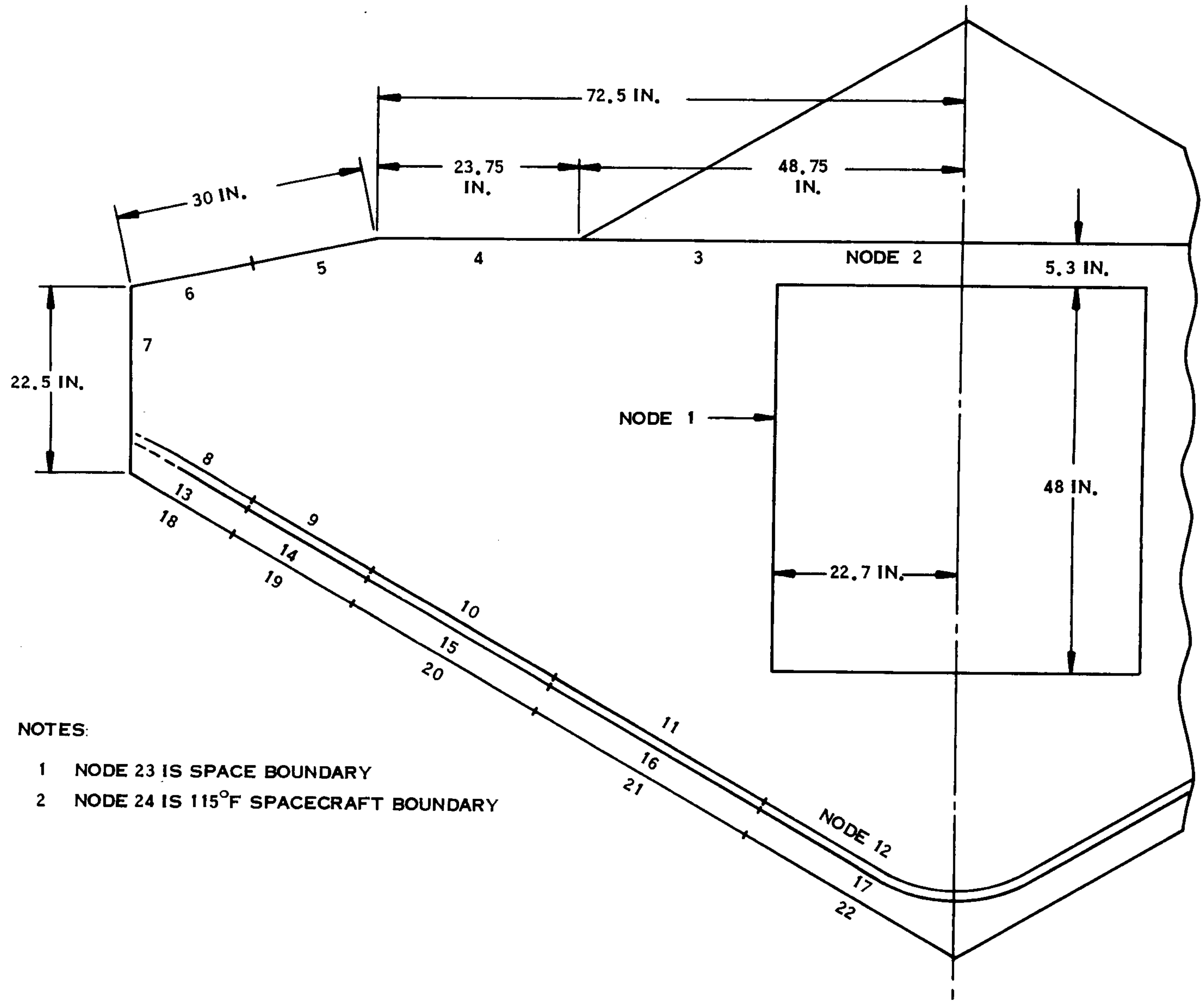

NOTES:

1 NODE 23 IS SPACE BOUNDARY
2 NODE 24 IS 115°F SPACECRAFT BOUNDARY

Figure 2-12. Capsule Nodal Configuration

Table 2-1. Internode Connections for Capsule With Heat Shield

1. Radiation				
Node i	Node j	F_e	$F_{a_{i \to j}}$	A_i (ft^2)
2	1	0.6795	0.81	11.24
2	5	0.810	0.0046	
2	6		0.0082	
2	7		0.0700	
2	8		0.0640	
3	1	0.810	0.186	40.59
3	5		0.0016	
3	6		0.0023	
3	7		0.0661	
3	8		0.110	
3	9		0.140	
3	10		0.271	
3	11		0.223	
4	1	0.810	0.072	61.22
4	5		0.0051	
4	6		0.0029	
4	7		0.099	
4	8		0.224	
4	9		0.192	
4	10		0.255	
4	11		0.130	
4	12		0.020	
5	1	0.810	0.072	51.84
5	7		0.146	
5	8		0.285	
5	9		0.210	
5	10		0.172	
5	11		0.0696	
5	12		0.0105	
5	23	0.0075	1.0	51.84

Table 2-1. Internode Connections for Capsule With Heat Shield (Cont)

1. Radiation				
Node i	Node j	F_e	$F_{a_{i \to j}}$	A_i (ft^2)
6	1	0.810	0.035	61.66
6	7		0.348	
6	8		0.311	
6	9		0.123	
6	10		0.0925	
6	11		0.477	
6	12		0.0099	
6	23	0.0075	1.0	
7	1	0.810	0.074	77.85
7	8		0.149	
7	9		0.0609	
7	10		0.0665	
7	11		0.0401	
7	12		0.0095	
7	23	0.0075	1.0	100.1
8	1	0.810	0.047	71.93
8	9		0.00866	
8	10		0.00992	
8	11		0.00642	
8	12		0.00174	
9	1	0.810	0.089	58.76
9	10		0.0507	
9	11		0.0298	
9	12		0.00363	
10	1	0.81	0.135	68.46
10	11		0.0324	
10	12		0.00647	
11	1	0.81	0.273	46.74
11	12		0.0135	
12	1	0.6795	0.480	12.87

Table 2-1. Internode Connections for Capsule With Heat Shield (Cont)

1. Radiation				
Node i	Node j	F_e	$F_{a_{i \to j}}$	A_i (ft^2)
13	18	0.0345	0.864	71.93
13	7	0.0497	0.136	
14	19	0.0345	1.0	58.76
15	20	0.0345	1.0	68.46
16	21	0.0345	1.0	46.74
17	22	0.0345	1.0	12.87
18	23	0.0075	1.0	62.15
19	23	0.0075	1.0	60.05
20	23	0.0075	1.0	70.87
21	23	0.0075	1.0	49.72
22	23	0.0075	1.0	15.54

2. Conduction		
Node i	Node j	C_{i-j} (Btu/hr-^oF)
7	18	20.77
8	13	8.082
9	14	6.602
10	15	7.692
11	16	5.251
12	17	1.446
18	19	18.950
19	20	12.170
20	21	6.420
21	22	3.152

Figure 2-13 plots temperatures of nodes of the capsule-with-aeroshell for a range of heater power. Heat is assumed to be generated uniformly over the entire heater surface that is represented by node 1. Thus, the figures should be entered at values of heater power and the resulting temperature pattern determined. Figure 2-14 shows similar values for the configuration that does not include the shield and aeroshell. This configuration is representative of the Phase IV test configuration, and demonstrates that the test configuration temperatures within the capsule will be more uniform than would be expected for an actual capsule and aeroshell situation. Table 2-2 gives the interconnection details for this case.

The low power point on Figure 2-14, designated by the symbol ◊, represents the Phase IV test situation where the capsule is colder than the spacecraft. Therefore, nodes 2, 3, and 4, receive heat by radiation through the spacecraft-capsule interface insulation, and node 4 receives conductive heat through the spacecraft-capsule structural connection, with the spacecraft assumed to be at the upper test temperature of $115^{\circ}F$.

The net results for the two capsule configurations considered show that the low effective emittance of the capsule external insulation results in relatively small capsule temperature differences. As expected, the Phase IV configuration without the shield is more nearly isothermal, but the difference is not sufficient to warrant increasing the complexity of the test fixture to include this component.

2.2.2 SPACECRAFT ANALYSIS

The spacecraft configuration includes a liquid fueled midcourse correction and orbit insertion engine. Although internal spacecraft analysis details such as engine piping to tankage connections, and external engine nozzle shading were not included, the spacecraft analysis was more complex than that of the capsule.

The spacecraft analyzed here and shown in Figure 2-15, sheet 1, is a prism comprised of 16 sides. Electronic equipment is mounted to eight of these sides and the heat flow from this equipment is simulated by electrical heaters mounted on the equipment bay panels. Four

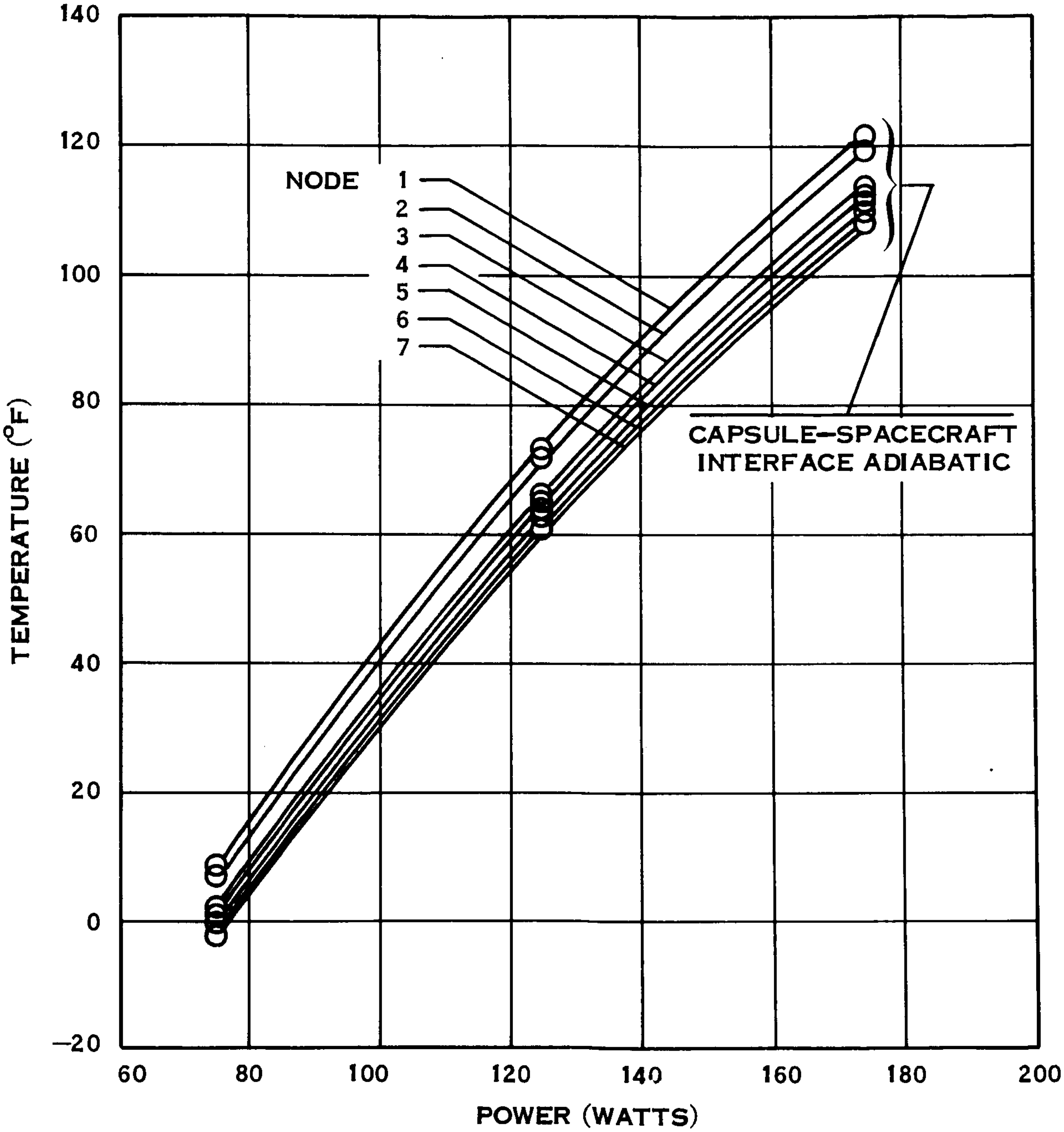

Figure 2-13. Temperature Pattern: Capsule with Heat Shield (Sheet 1 of 3)

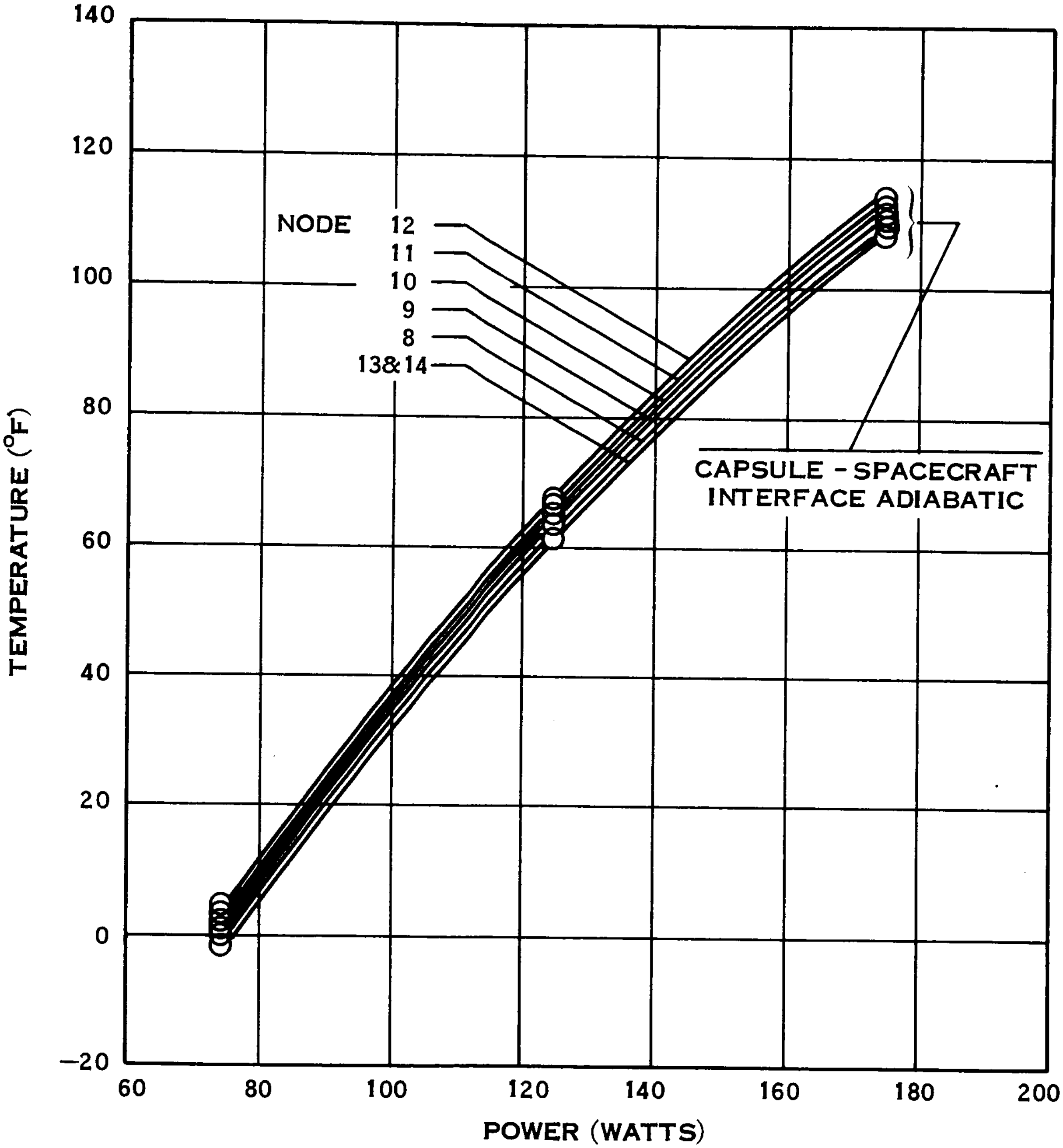

Figure 2-13. Temperature Pattern: Capsule with Heat Shield (Sheet 2 of 3)

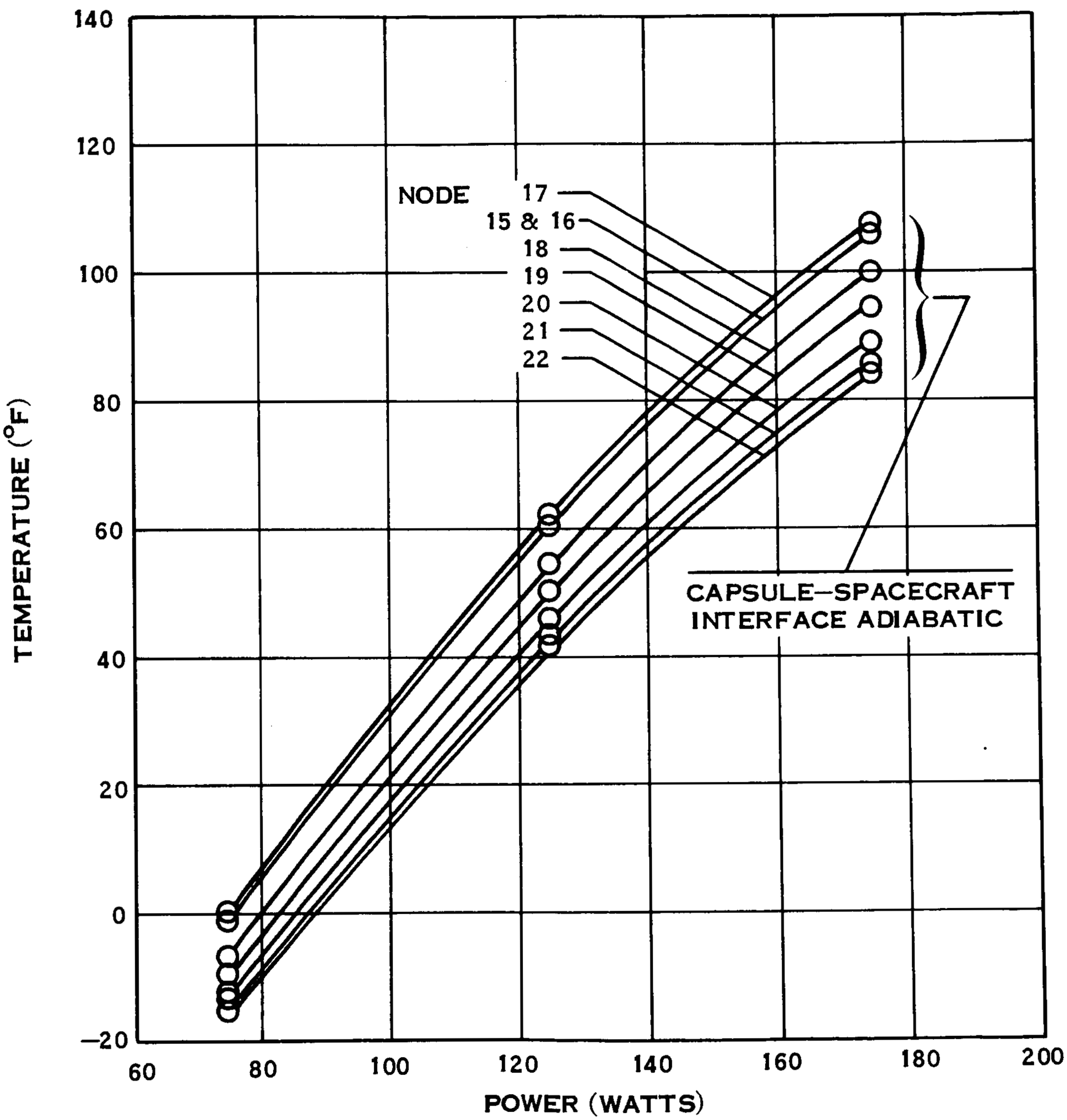

Figure 2-13. Temperature Pattern: Capsule with Heat Shield (Sheet 3 of 3)

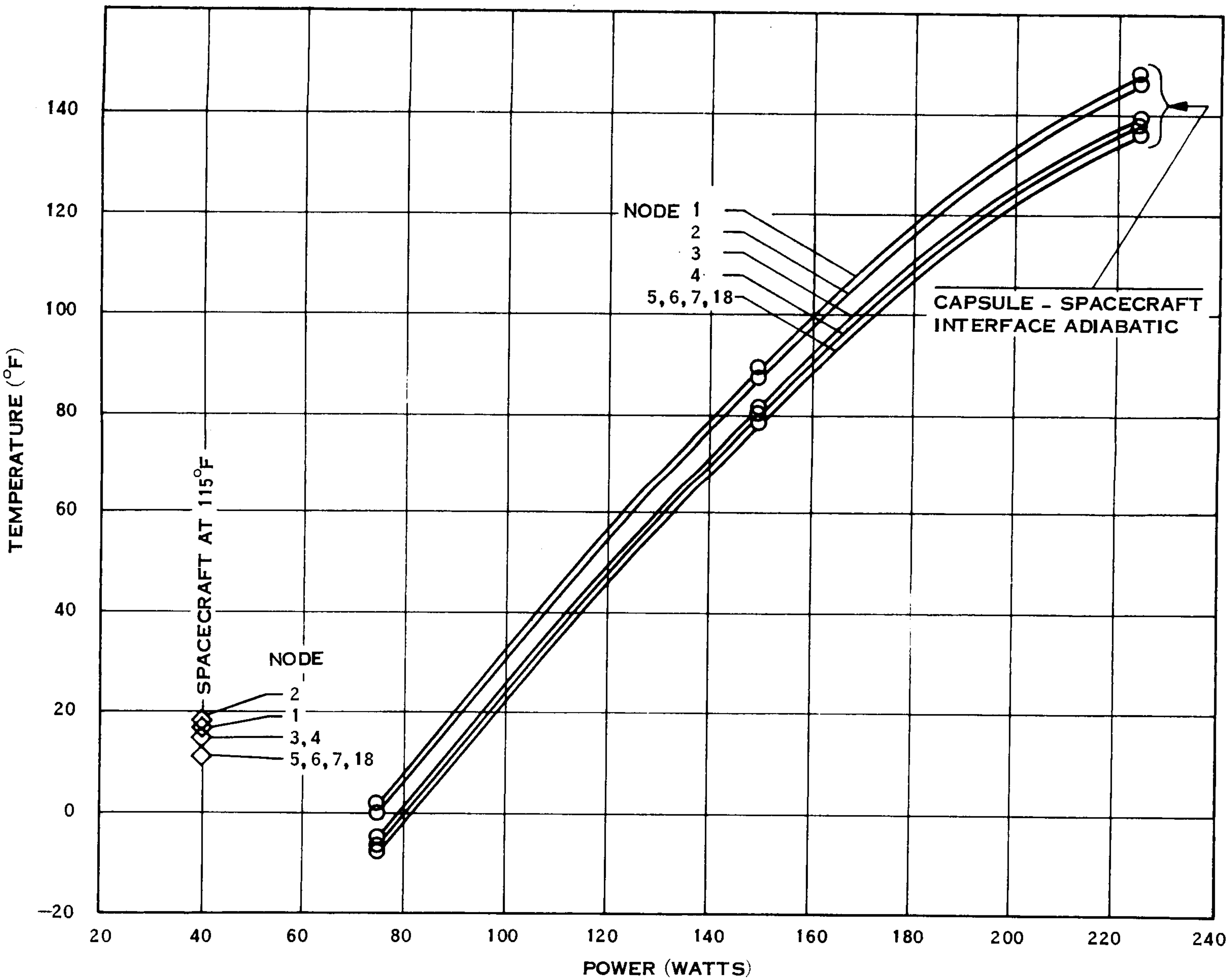

Figure 2-14. Temperature Pattern: Capsule Without Heat Shield (Sheet 1 of 2)

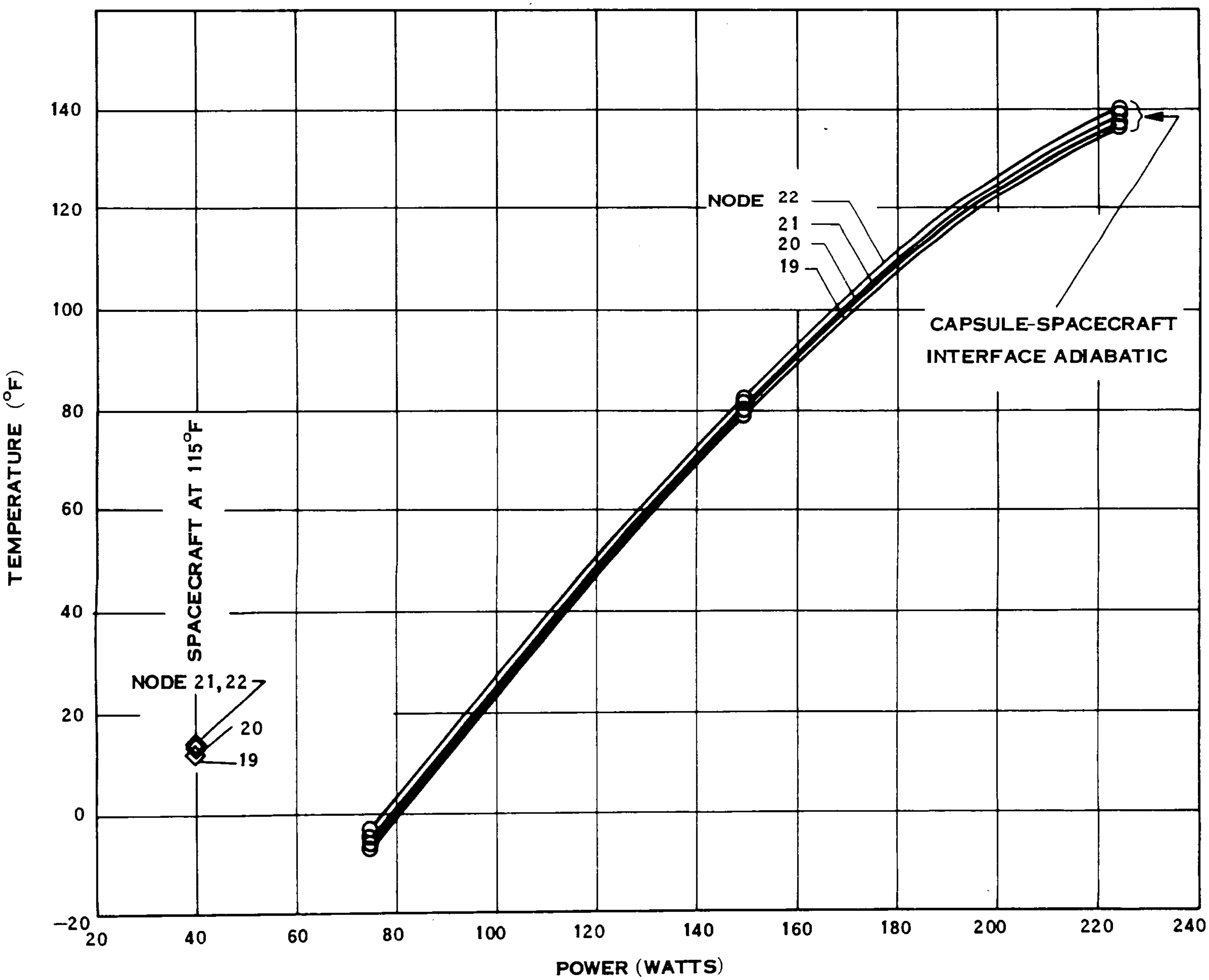

Figure 2-14. Temperature Pattern: Capsule Without Heat Sheild (Sheet 2 of 2)

Table 2-2. Internode Connections for Capsule Without Heat Shield

1. Radiation				
Node i	Node j	F_e	$F_{a_{i \to j}}$	A_i (ft^2)
2	1	0.6795	0.81	11.24
2	5	0.810	0.0046	
2	6		0.0082	
2	7		0.070	
2	18		0.064	
* 2	24	0.009	1.0	12.87
3	1	0.810	0.186	40.59
3	5		0.0016	
3	6		0.0023	
3	7		0.0061	
3	18		0.110	
3	19		0.140	
3	20		0.271	
3	21		0.223	
* 3	24	0.009	1.0	45.18
4	1	0.810	0.072	61.22
4	5		0.0051	
4	6		0.0029	
4	7		0.099	
4	18		0.224	
4	19		0.192	
4	20		0.255	
4	21		0.130	
4	22		0.020	
* 4	24	0.009	1.0	
5	1	0.810	0.072	51.84
5	7		0.146	
5	18		0.285	
5	19		0.210	
5	20		0.172	
5	21		0.0696	
5	22		0.0105	
5	23	0.0075	1.0	

*These internode connections are used only in the case where the capsule is colder than the spacecraft.

Table 2-2. Internode Connections for Capsule Without Heat Shield (Cont)

1. Radiation				
Node i	Node j	F_e	$F_{a_{i \to j}}$	A_i (ft^2)
6	1	0.810	0.035	61.66
6	7		0.348	
6	18		0.311	
6	19		0.123	
6	20		0.925	
6	21		0.0477	
6	22		0.0099	
6	23	0.0075	1.0	
7	1	0.810	0.074	77.85
7	18		0.149	
7	19		0.0609	
7	20		0.0665	
7	21		0.0401	
7	22		0.0095	
7	23	0.0075	1.0	100.1
18	1	0.810	0.047	62.15
18	19		0.00866	
18	20		0.00992	
18	21		0.00642	
18	22		0.00174	
18	23	0.0075	1.0	
19	1	0.810	0.089	60.05
19	20		0.0507	
19	21		0.0298	
19	22		0.00363	
19	23	0.0075	1.0	
20	1	0.810	0.135	70.87
20	21		0.0324	
20	22		0.00647	
20	23	0.0075	1.0	

Table 2-2. Internode Connections for Capsule Without Heat Shield (Cont)

1. Radiation				
Node i	Node j	F_e	$F_{a_{i \to j}}$	A_i (ft^2)
21	1	0.810	0.273	49.72
21	22	↓	0.0135	↓
21	23	0.0075	1.0	
22	1	0.0795	0.480	15.54
22	23	0.0075	1.0	↓

2. Conduction		
Node i	Node j	C_{i-j} (Btu/hr-^{o}F)
* 4	24	0.5802
7	18	20.77
18	19	18.950
19	20	12.170
20	21	6.420
21	22	3.152

*These internode connections are used only in the case where the capsule is colder than the spacecraft.

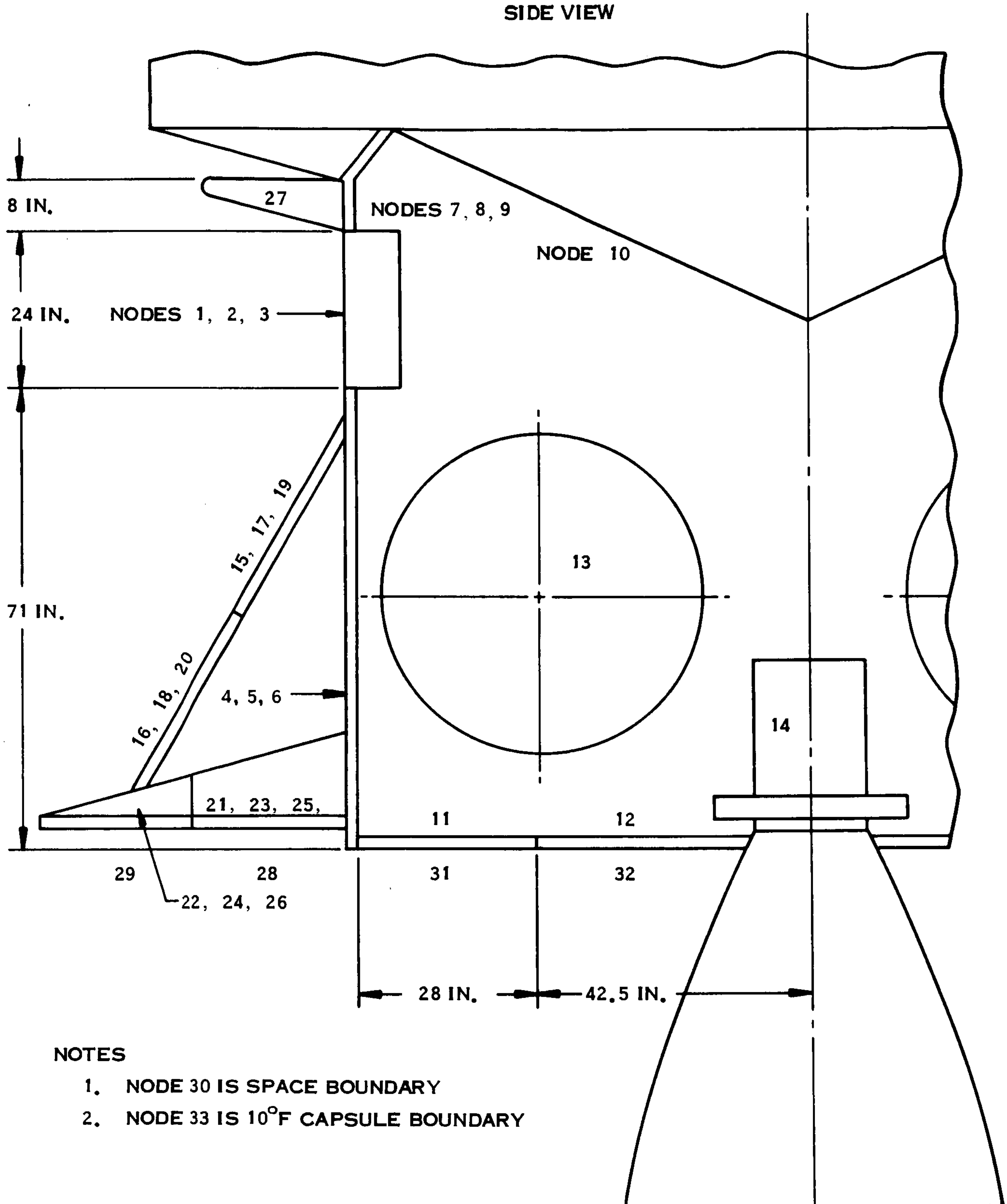

NOTES

1. NODE 30 IS SPACE BOUNDARY
2. NODE 33 IS 10°F CAPSULE BOUNDARY

Figure 2-15. Spacecraft Nodal Configuration (Sheet 1 of 2)

TOP VIEW

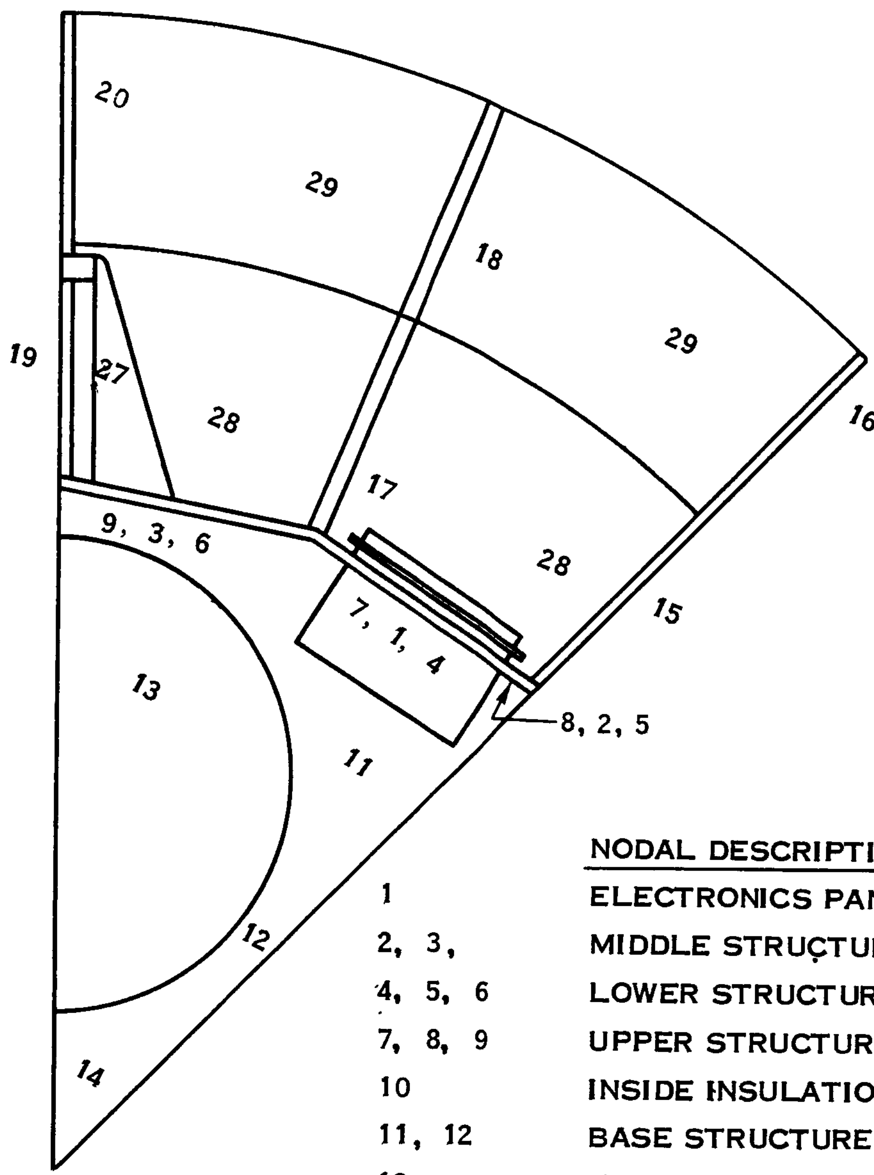

NODAL	DESCRIPTION
1	ELECTRONICS PANEL
2, 3,	MIDDLE STRUÇTURE
4, 5, 6	LOWER STRUCTURE
7, 8, 9	UPPER STRUCTURE
10	INSIDE INSULATION SURFACE
11, 12	BASE STRUCTURE
13	FUEL TANK
15 TO 20	SOLAR ARRAY SUPPORTS
27	SCAN PLATFORM SUPPORT
28, 29	SOLAR ARRAY
31	BASE SOLAR ARRAY
32	OUTSIDE INSULATION SURFACE

Figure 2-15. Spacecraft Nodal Configuration (Sheet 2 of 2)

main engine fuel tanks are located within the body. In an attempt to reduce the number of nodes required to analyze this situation, the spacecraft was divided into eight equal parts. Each part includes an equipment bay panel, an adjacent plain panel, and one half of a fuel tank. The nodal network was made up of of these one-eighth circumferential sections, as shown on Figure 2-15, sheet 2. By using only a one-eighth section, a fewer number of nodes were required for the analysis, but calculating the internal radiation terms became more complex.

In the symmetrical spacecraft, each of the equipment bays will have a radiation connection to each of the fuel tanks. Consequently, radiation from the equipment bay to the tank in the one-eighth section was set up to include the view factor summation of a bay to all the tanks. In like manner, the internal radiation interchange between all nodes of the one-eighth section mathematical model includes the total view factor that would occur between similar type nodes in the full sized case. In this fashion, the spacecraft analysis was performed with 32 nodes whereas several hundred nodes would be required to give this much detail for a whole spacecraft. Table 2-3 gives the spacecraft nodal connection details. Five conditions or cases were considered. In each case the solar flux was assumed incident on nodes 28, 29, 31, and 32. Specific details of each case are given in Table 2-4. In this table, the node 1 (equipment bay panel) heater power is stated as eight times the value actually used in the one-eighth section mathematical model, and is thereby applicable to the entire spacecraft. The nodal temperatures that result for each case are given in Table 2-5.

Cases 3, 4, and 5 of spacecraft analysis included a radiation and conduction term to the capsule instead of the normally assumed adiabatic interface. In case 5, the capsule was assumed to be at $10^{o}F$, and spacecraft power was adjusted to give approximately $115^{o}F$ spacecraft temperature. Thus, this computed point shows the influence of the capsule on the spacecraft in the inverse sense that the effect of the spacecraft on the capsule had been previously shown.

Table 2-3. Internode Connections for Spacecraft

1. Radiation				
Node i	Node j	F_e	$F_{ai \rightarrow j}$	A_i (ft^2)
1	10	0.81	0.373	3.333
1	11	0.81	0.040	↓
1	12	0.81	0.013	↓
1	13	0.81	0.267	↓
*1	28	0.0425	0.020	↓
**1	28	0.0255	0.020	↓
*1	29	0.0425	0.030	↓
**1	29	0.255	0.030	↓
*1	30	0.05	0.950	↓
**1	30	0.30	0.950	↓
2	10	0.81	0.373	0.667
2	11	0.81	0.040	↓
2	12	0.81	0.013	↓
2	13	0.81	0.0275	↓
2	30	0.009	1.0	↓
3	10	0.81	0.373	5.333
3	11	0.81	0.055	↓
3	12	0.81	0.019	↓
3	13	0.81	0.283	↓
3	14	0.90	0.012	↓
3	30	0.009	1.0	↓
4	10	0.81	0.095	9.861
4	11	0.81	0.149	↓
4	12	0.81	0.027	↓
4	13	0.81	0.267	↓
4	30	0.009	1.0	↓

*These connections are for cases where emittance of equipment bay equals 0.05

**These connections are for cases where emittance of equipment bay equals 0.30

Table 2-3. Internode Connections for Spacecraft (Cont)

1. Radiation				
Node i	Node j	F_e	$F_{ai \rightarrow j}$	A_i (ft^2)
5	10	0.81	0.095	1.972
5	11	0.81	0.150	↓
5	12	0.81	0.027	↓
5	13	0.81	0.265	↓
5	30	0.009	1.0	↓
6	10	0.81	0.113	15.78
6	11	0.81	0.170	↓
6	12	0.81	0.028	↓
6	13	0.81	0.349	↓
6	14	0.90	0.001	↓
6	30	0.009	1.0	↓
7	10	0.81	0.430	1.111
7	11	0.81	0.032	↓
7	12	0.81	0.010	↓
7	13	0.81	0.182	↓
7	14	0.90	0.002	↓
7	30	0.009	1.0	↓
8	10	0.81	0.444	0.222
8	11	0.81	0.032	↓
8	12	0.81	0.010	↓
8	13	0.81	0.187	↓
8	14	0.90	0.002	↓
8	30	0.009	1.0	↓
9	10	0.81	0.468	1.778
9	11	0.81	0.031	↓
9	12	0.81	0.010	↓
9	13	0.81	0.183	↓
9	14	0.90	0.002	↓
9	30	0.009	1.0	↓

Table 2-3. Internode Connections for Spacecraft (Cont)

1. Radiation				
Node i	Node j	F_e	$F_{ai \rightarrow j}$	$A_i (ft^2)$
10	11	0.81	0.063	13.55
10	12	0.81	0.031	↓
10	13	0.81	0.282	↓
10	14	0.90	0.019	↓
***10	30	0.009	1.0	14.13
# 10	33	0.009	1.0	14.13
11	13	0.81	0.370	8.624
11	31	0.018	1.0	8.624
12	13	0.81	0.535	4.310
12	32	0.009	1.0	4.651
14	13	0.90	0.443	0.6133
14	30	1.0	1.0	0.0475
15	30	0.009	1.0	0.3952
16	30	0.009	1.0	0.3952
17	30	0.009	1.0	0.7905
18	30	0.009	1.0	0.7905
19	30	0.009	1.0	0.3952
20	30	0.009	1.0	0.3952
21	28	0.765	0.40	1.675
21	30	0.90	0.35	1.675
22	29	0.765	0.40	0.80
22	30	0.90	0.45	0.80

***This connection is for near-Mars cases only.

These connections are for cases where spacecraft is connected to 10°F capsule

Table 2-3. Internode Connections for Spacecraft (Cont)

1. Radiation				
Node i	Node j	F_e	$F_{ai \rightarrow j}$	A_i (ft^2)
23	28	0.765	0.40	3.35
23	30	0.90	0.35	3.35
24	29	0.765	0.40	1.6
24	30	0.90	0.45	1.6
25	28	0.765	0.40	1.675
25	30	0.90	0.35	1.675
26	29	0.765	0.40	0.80
26	30	0.90	0.45	0.80
27	30	0.020	1.0	2.955
31	30	0.80	1.0	8.624
32	30	0.67	1.0	4.651

2. Conduction		
Node i	Node j	C_{i-j}(Btu/hr-^{o}F)
1	2	0.3680
1	3	0.1677
1	4	0.0770
1	7	0.230
2	5	0.0155
2	8	0.0470
3	6	0.108
3	9	0.327
4	5	1.044
4	6	0.4994

Table 2-3. Internode Connections for Spacecraft (Cont)

2. Conduction		
Node i	Node j	C_{i-j}(Btu/hr-^{o}F
5	15	0.0490
5	21	0.3414
6	17	0.098
6	19	0.049
6	23	0.6828
6	25	0.3414
7	8	0.124
7	9	0.056
9	27	0.790
#9	33	0.0725
***9		6.25 Watts Heat Leak to Capsule
15	16	0.02765
16	22	0.03725
17	18	0.0553
18	24	0.0745
19	20	0.02765
20	26	0.03725
21	22	0.1155
21	28	1.495
22	29	2.823

*** This connection is for near-Mars cases only

These connections are for cases where spacecraft is connected to 10^{o}F capsule

Table 2-3. Internode Connections for Spacecraft (Cont)

2. Conduction		
Node i	Node j	C_{i-j} (Btu/hr-^{o}F)
23	24	0.231
23	28	2.991
24	29	5.647
25	26	0.1155
25	28	1.495
26	29	2.823

Table 2-4. Case Description

Case 1
Near Earth

1. $\epsilon_{node\ 1} = 0.05$
2. $q_{node\ 1}$ = 99.2 watts
3. Solar flux = 442 Btu/hr-ft^2
4. Spacecraft - capsule interface adiabatic

Case 2
Near Earth

1. $\epsilon_{node\ 1} = 0.30$
2. $q_{node\ 2}$ = 456.8 watts
3. Solar flux = 442 Btu/hr-ft^2
4. Spacecraft - capsule interface adiabatic

Table 2-4. Case Description (Cont)

Case 3
Near Mars

1. $\epsilon_{node\ 1}$ = 0.05
2. $q_{node\ 1}$ = 181.6 watts
3. Solar flux = 200 Btu/hr-ft^2
4. Heat Leak through spacecraft - capsule interface to space included

Case 4
Near Mars

1. $\epsilon_{node\ 1}$ = 0.30
2. $q_{node\ 1}$ = 356.8 watts
3. Solar flux = 200 Btu/hr-ft^2
4. Heat leak through spacecraft - capsule interface to space included

Case 5
Near Earth

1. $\epsilon_{node\ 1}$ = 0.05
2 $q_{node\ 1}$ = 150.4 watts
3. Solar flux = 442 Btu/hr-ft^2
4. Heat leak through spacecraft - capsule interface to 10^{o}F capsule boundary included

Table 2-5. Results for Detailed Thermal Analysis of Spacecraft

Node	Case 1 Temp (^oF)	Case 2 Temp (^oF)	Case 3 Temp (^oF)	Case 4 Temp (^oF)	Case 5 Temp (^oF)
1	113.4	116.5	61.7	48.5	120.6
2	109.8	112.2	48.4	38.0	113.1
3	107.5	109.5	34.8	26.3	108.2
4	107.5	109.4	35.8	28.2	108.5
5	108.3	109.9	35.8	29.2	109.1
6	108.2	110.0	35.8	28.8	109.1
7	108.2	110.4	41.2	31.6	110.0
8	108.0	110.0	40.2	31.1	109.4
9	101.6	103.6	13.2	4.3	98.5
10	109.2	111.2	37.0	28.4	109.7
11	112.1	113.9	38.7	31.1	113.0
12	110.0	111.9	37.6	29.7	112.0
13	109.4	111.3	37.7	29.7	110.4
14	124.7	126.3	45.6	38.4	125.3
15	100.3	101.1	30.3	26.0	100.7
16	106.2	106.4	31.8	30.4	106.3
17	99.4	100.5	29.6	24.6	99.9
18	104.5	104.8	30.9	28.9	104.7
19	100.3	101.1	30.3	25.7	100.7
20	106.2	106.5	31.8	30.2	106.3
21	115.3	115.5	37.0	36.2	115.4
22	124.1	124.1	41.2	41.2	124.1
23	115.3	115.5	37.0	36.1	115.4
24	124.1	124.1	41.2	41.2	124.1
25	115.3	115.5	37.0	36.1	115.4
26	124.1	124.1	41.2	41.2	124.1
27	89.9	91.7	7.1	-1.4	87.0
28	160.0	160.0	65.0	65.0	160.0
29	145.0	145.0	53.0	53.0	145.0
30	-460.0	-460.0	-460.0	-460.0	-460.0
31	230.2	230.2	106.4	106.3	230.2
32	161.9	161.9	50.4	50.3	161.9
33	-	-	-	-	10.0

Cases 4 and 5 represent Mars orbit conditions where the capsule has been separated from the spacecraft but the uninsulated aft biobarrier remained attached. Previous calculations had indicated that 50 watts would be conducted from the spacecraft at $40^{\circ}F$ to the aft biobarrier, and this heat leak was incorporated in the analysis. This previous analysis indicated that the biobarrier would become very cold, and so the radiation connection from node 10 was assumed to be the same as directly to space. These cases show that appreciable temperature differences can exist within the spacecraft structure, primarily in the region directly affected by the heat leak connections.

Cases 1, 3, and 5 were computed with the assumption that the external equipment bay radiating panels have a constant emittance of 0.05. In an actual design, the emittance of these panels will be automatically adjusted by louvers to accommodate power changes without the large temperature changes shown. For such a louvered thermal control system, the 0.05 emittance assumed is below the normally expected closed louver emittance. This value was chosen for the analysis, however, to represent the Phase IV test configuration which does not include the extra detail of louvers. Instead, the external panel surface is uncoated aluminum. The reason for this is to minimize the noninsulation heat losses, so that there will be less uncertainty in the net loss attributed to the insulation system after correcting the total heater power for the equipment panel emission.

In order to demonstrate the effect of equipment bay panel emittance, cases 2 and 4 were performed for an emittance of 0.3. Checking the results shows that the chief effect of equipment bay panel emittance is to shift the power scale by the increment representative of the change in emittance, although a slightly low choice of power for case 4 tends to confuse this comparison. For the actual Phase IV test conditions, however, there will be some uncertainty in the amount of external radiant heat flow that will occur from the equipment bay panels, due to uncertainties in surface emittance and degree of thermal interaction with the back of the spacecraft solar array and the capsule outer surface that is within "view" of the panels. Low panel emittance reduces this heat flow, and so reduces the absolute amount of heat flow uncertainty that could occur from this effect.

2.2.3 INSULATION REQUIREMENTS

From data compiled in the Phase I portion of this program, an outer cover sheet of 2 mil gold on Kapton was recommended. Subsequent experiments with vapor deposited gold on Kapton have resulted in an unsatisfactory surface. Because of this processing problem, the gold coating has been deleted as a requirement for the outer cover sheet.

Substituting clear 2 mil Kapton for Kapton metallized on the inside surface will cause the outer surface to rise $45^{\circ}F$ to $207^{\circ}F$ when the sun is directly incident. Concurrently, the first Mylar underlayer will be increased from about $160^{\circ}F$ to $261^{\circ}F$ for those areas which may be insulated during maneuvers. At the normally sun facing end of the spacecraft, the clear Kapton will reach about $202^{\circ}F$ instead of $162^{\circ}F$ for the metallized case. The 1/2 mil Kapton underlayer temperature will be increased from about $160^{\circ}F$ to $236^{\circ}F$. For the same insulation thickness, the increased temperature at the normally sun facing end would increase the heat flux through the actual spacecraft insulation around the engine nozzle by 59%. This effect is not expected to be particularly significant because the insulation at that location has been sized to accommodate the much higher temperatures imposed by the engine nozzle during the orbit insertion firing.

Based upon the use of clear 2 mil Kapton as the outer cover sheet, the insulation requirements given in Table 2-6 were evolved.

Table 2-6. Insulation Requirements

Location	Number of Layers
Side of spacecraft	20 layers gold on 1/4 mil Mylar 1 layer clear 2 mil Kapton
Capsule	24 layers gold on 1/4 mil Mylar 1 layer clear 2 mil Kapton
Interface-Capsule to spacecraft	20 layers gold on 1/4 mil Mylar
Spacecraft Between thrust chamber nozzle and solar panel	19 layers gold on 1/2 mil Kapton 1 layer clear 2 mil Kapton
Between base mounted solar array and spacecraft	10 layers gold on 1/2 mil Kapton

2.3 INSULATION PROCESS DEVELOPMENT

The materials testing effort in Phase I indicated the unreliability of aluminized insulation materials relative to the ethylene oxide decontamination cycle. Vapor deposited gold insulation, because of the chemical inertness of the gold and acceptable optical properties, became a prime candidate.

A literature survey and industry inquiries indicated minimal industrial experience relative to the vacuum deposition of gold on polymer substrates for aerospace applications. Gold on Mylar material was supplied by one vendor for evaluation during Phase I. The material was wrinkled by hand and fabricated into a blanket. It met all of the optical property and thermal conductivity requirements, in addition to surviving the ethylene oxide cycles. However, the adhesion of the gold to the substrate was marginal. It thus became necessary to find a means of increasing adhesion in order that the material could accommodate mechanical wrinking without degradation. An alternate task was to locate another vendor who could supply material with the required adhesion properties. Two additional considerations further influenced the source of supply for material. One of these was the necessity to obtain material widths of 40 inches or more to allow the fabrication of large blankets and, hence, obtain an efficient insulation system. The second item was cost.

2.3.1 MATERIAL REQUIREMENTS

Tests conducted during Phase I relative to the heat loads imposed on the aft end of the spacecraft by the orbit insertion motor dictated the use of vapor deposited gold on Kapton for this area. Further, an outer layer of 2 mil Kapton was selected for overall protection of the blankets during the application process. Kapton was required in a width of 36 inches or more.

Guidelines, prior to the development of a material specification, were provided for procurement of these goldized materials. These are shown in Table 2-7.

Table 2-7. Guidelines for Goldized Material

Property / Material	Mylar	Kapton	
	Blanket Layers	Blanket Layers	Outside Protective Layer
Width (Inches)	56	36	36
Emittance, ϵ_N	0.05 max	0.05 max	0.05 max
Transmission at 0.52 micron wave-length (5)	10 max	10 max	10 max
Resistance (ohms/square)	1.3 max	1.3 max	1.3 max
Polymer film	25 gage Type S Dupont	25 gage* Type H Dupont	200 gage Type H Dupont
Adhesion (250 Scotch Tape Test)	Pass	Pass	Pass

*Later changed to 50 gage since 25 gage Kapton was not commercially available

2.3.2 SAMPLE EVALUATION

Four vendors furnished samples of gold on Mylar. The samples were evaluated against the guideline requirement, with the results given in Table 2-8. Using material from vendor 1, whose costs at the time were in line with the program requirements, it was found that heat treating the gold on Mylar for up to 48 hours at $275^{\circ}F$ and Kapton for up to 100 hours at $500^{\circ}F$ in single sheets resulted in acceptable adhesion properties. Further effort using material as received from the vendor on rolls indicated that uniform adhesion could not be obtained without adequate air circulation within the roll. Techniques for loosely wrapping the material were then investigated.

Additional samples furnished by vendor 1 were not of good quality. At this time the National Metallizing Division of the Standard Packaging Corporation, identified in Table 2-8 as vendor 4, had done additional work on their process and a meeting was arranged. Acceptable samples were furnished with good adhesion characteristics. In addition, their costs were reduced to a value which was substantially lower than the other vendors. On this basis, the material order was placed with vendor 4. Similarly, acceptable samples of gold on 1/2 mil Kapton were also obtained from this same vendor. Difficulties with obtaining acceptable adhesion of gold on 2 mil Kapton necessitated the use of uncoated Kapton for the outer cover. The results of this change relative to thermal effects were discussed in an earlier section.

2.4 MATERIALS TESTING

During Phase II, additional thermal conductivity tests were performed with vapor deposited gold on 1/4 mil Mylar and 1/2 mil Kapton. Tests were conducted to establish requirements for depositing gold on Mylar and Kapton, as a function of cleaning and vacuum deposition techniques. Acceptance tests were performed for reflectance, normal emittance (ϵ_N), transmission, resistivity, solar absorptance (α_S), and adhesive properties as a function of gold thickness on Mylar and Kapton.

Evaluation of candidate tapes for insulation blanket assembly was completed.

Table 2-8. Vendor Material Property Data

Vendor	Resistance (ohms/square)	Emittance, ϵ_N	Transmission at 0.52 μ (%)	Adhesion: 250 Scotch Tape Test	Cost*
1	1.00	0.038	3	Failed	1
2	1.00	0.042	6	Passed	Would not agree to meet spec.
3	0.91	0.047	5	Passed	3
4 First Submission	0.73	0.067	0	Failed	2
4 Second Submission	0.86	0.040	Requirement Deleted	Passed	1**

*Lowest numbers indicate lowest costs.

**Second submission of vendor 4 resulted in lowest costs.

2.4.1 THERMAL CONDUCTIVITY TESTS

Three thermal conductivity tests were performed on samples from vendor 1. The materials were die crinkled by General Electric. The samples were as follows:

Sample 1	1/4 mil Mylar, gold coated on one side.
Sample 2	Similar to sample 1 with nine 1/8 inch diameter holes per square foot to allow for venting.
Sample 3	1/2 mil Kapton, gold coated on one side with hole pattern similar to sample 2.
Sample 4	Same as sample 3 except material is from vendor 4.

The results of the tests are given in Table 2-9. The results for samples 1 and 2 compare favorably with one test performed on 1/4 mil gold on Mylar during Phase I. It may also be noted that the vent hole patterns had no appreciable effect on the insulation performance.

The poor performance of sample 3 has been attributed to the quality of the gold coating. Its adherence was poor as attested by the many clear spots in the test sample. Thus, good adherence is necessary if acceptable thermal performance is to be obtained after processing and handling of the insulation material.

A fourth test was made with gold coated Kapton material from vendor 4. This material had good gold adherence as evidenced by it successfully passing the scotch tape test. However, when the material was crinkled as deeply as sample 3, some gold removal was noted. In an endeavor to prevent gold removal, the crinkling die was enlarged, which improved the gold coating quality after the crinkling operation. However, it resulted in less crinkle and, therefore, less stack-up height. The performance per layer of sample 4 is slightly better than that of sample 3, but not as good as would be expected with a more deeply crinkled material. The test was performed on the material of sample 4 with its relatively low crinkle height because it is representative of the material used to manufacture the Kapton insulation blankets at the base of the full scale test fixture.

Table 2-9. Thermal Conductivity Test Results

Description	Sample Number 1	2	3	4
	1/4 mil Mylar. Gold coated one side. Vendor (1)	Similar to (1) with nine 1/8 in. dia holes per sq ft Vendor (1)	1/2 mil Kapton. Gold coated one side holes similar to (2) Vendor (1)	1/2 mil Kapton. Gold coated one side. Four 1/8 in. dia holes per sq ft Vendor (4)
Temperature (^oF)				
Warm side	75.5	73	72	69
Cold Side	-323	-323	-322	-321
Number of layers	24	24	24	19
Thickness (in.)	0.625	0.625	0.625	0.3125
Pressure (torr)	2.5×10^{-5}	2.5×10^{-5}	2.5×10^{-5}	2.5×10^{-5}
Density (lb/ft^3)	0.98	0.97	1.61	3.11
Heat flow ($Btu/hr\text{-}ft^2$)	0.345	0.344	0.723	0.85
Conductivity ($Btu/hr\text{-}ft\text{-}^oF$)	4.5×10^{-5}	4.52×10^{-5}	9.56×10^{-5}	5.67×10^{-5}
Effective emittance	0.00245	0.00249	0.00527	0.00637
$\rho k \left(\frac{Btu\text{-}lb}{hr\text{-}ft^4\text{-}^oF}\right)$	4.42×10^{-5}	4.39×10^{-5}	15.4×10^{-5}	17.6×10^{-5}

2.4.2 TAPE AND ADHESIVE TESTS

Tests conducted during Phase I indicated that candidate pressure-sensitive tapes (Permacel EE 6600 and 3M 850) did not pass heat sterilization (576 hours at 275°F). A tape investigation program was initiated in Phase II to select tapes that would withstand heat sterilization effects. This effort was further expanded to include Velcro hook and pile bonding adhesives for use with the Tinger fasteners. A list of candidate tapes and hook and pile bonding adhesives that were evaluated is given in Table 2-10.

In Figure 2-16 a schematic is shown of the heat sterilization facility used for this test. A stainless steel container was placed in a temperature controlled oven and samples were attached to the top of the container. A recorder indicated temperature in the container during the test. Six heat sterilization cycles were run, each of 96 hours duration. Varying degrees of discoloration of the adhesives was noted after test,with solvent activated adhesive discolored the worst. A sample of Velcro with no adhesive was also included in the test, and no discoloration was noted.

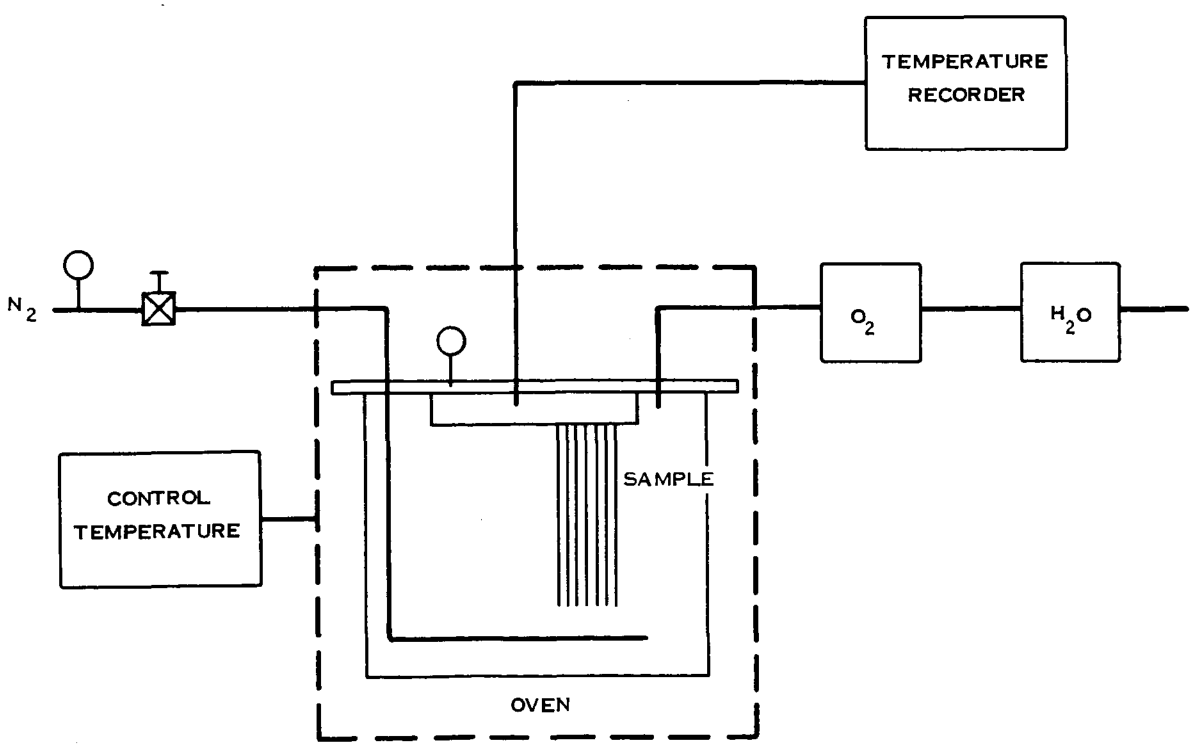

Figure 2-16. Heat Sterilization Facility

Table 2-10. Tape Candidates

Vendor	Type	Film	Adhesive	Manufacturer's Specified Operating Range
Tech Floro	603-1	1 mil Kapton	Silicone PS*	$-450^{o}F$ to $750^{o}F$
3M	Y91845	1 mil Kapton	Silicone PS	$-200^{o}F$ to $550^{o}F$
Permacel	EE6379	1 mil Kapton	Silicone PS	to $400^{o}F$
Velcro	SA0142		Solvent Activated	to $325^{o}F$
Velcro	PS0100		PS	to $325^{o}F$
Velcro	SA0140		Pliobond	to $325^{o}F$
Velcro	SA0140		Resiweld	to $325^{o}F$

*PS = Pressure sensitive

The samples were subjected to a lap shear test on an Instrom machine at 0.2 inch per minute. The results are given in Table 2-11. Lap shear strength is seen to increase after heat sterilization, when compared to a control sample. For Velcro hook and pile, little change took place as a result of heat sterilization. Tests were also performed with pressure-sensitive tapes at -200°F. Lap shear strength decreased by approximately 15% compared to the control samples.

Peel test values were not obtained from the Velcro adhesives, but it became obvious from handling the samples that the pressure sensitive adhesive was quite superior especially in respect to the solvent activated. Consequently for applications that must be subjected to heat sterilization, pressure sensitive adhesive should be used.

On the basis of these tests, Tech Floro tape will be used for application of insulation to the full scale test fixture. Pressure sensitive Velcro hook and pile appears to be satisfactory for use with the Tinger fastener. Additional information relative to the Velcro hook and pile will be available after completion of the long term vacuum storage test.

2.4.3 ADHESION INVESTIGATION

Tables 2-12 and 2-13 summarize the results of a laboratory effort to improve the adhesion of vapor deposited gold on Mylar and Kapton. It was concluded from this work that good adhesion could be obtained if adequate process control is maintained prior to and during metal deposition.

2.5 TEST ENGINEERING

2.5.1 PHASE IV TEST PROCEDURE

The procedure to be followed during the Phase IV full scale thermal model tests has been issued as document PVTIS 27, Test Procedure - Phase IV Thermal Model Test - Planetary Vehicle Thermal Insulation Systems Program. This document has been approved by JPL.

Table 2-11. Tape Test Results

Tape	Control	Lap Shear, (psi) Heat Sterilization	Low Temperature ($-200^{o}F$)
Tech Floro	30	41.0	26.5
3M Y91845	17	23	14
Permacel EE6379	18	21	15
Velcro and Hook Pile		Color After Test	
Solvent activated	10	10* Black	
Pressure sensitive	10	11* Light gray	
Pliobond	11	10* Tan	
Resiweld	11	12* Tan	

*Adhesive did not fail, the pile gave

Table 2-12. Gold on 1/4 Mil Mylar

Sample Ident.	Cleaning Technique	Deposition Variables			Adhesion	ϵ^N_{Au}	Res (ohm/sq)	Photovolt % Trans @ 0.52 μ	Beckman % Trans @ 0.5 μ	Comment
		Pressure	Source	Chamber						
1	Methanol wipe. Glow discharge 1.4 Kv, 125 ma, 14 min.	1×10^{-4}	W-coil	CVC	Good	0.069	6.3	44	32	
2	Dry wipe with lens tissue. Glow discharge 1.4 Kv, 125 ma, 14 min.	1×10^{-4}	W-coil	CVC	Good					
3	Methanol wipe. Glow discharge 1.4 Kv, 125 ma, 4 min.	1×10^{-4}	W-coil	CVC	Good	0.132	10.8	45	42	
4	Dry wipe with lens tissue Glow discharge 1.4 Kv, 125 ma, 4 min.	1×10^{-4}	W-coil	CVC	Good					
5	Methanol wipe. Glow discharge 1.4 Kv, 125 ma, 5 min.	1×10^{-4}	W-coil	CVC	Poor	0.023	0.63	4.2	3	Adhesion still poor after exposure to 300°F for 30 min.
6	Dry wipe with lens tissue	1×10^{-4}	W-coil	CVC	Good	0.134	3.3	49	42	Scratched area on sample
7	Dry wipe with lens tissue	1×10^{-4}	W-coil	CVC	Fair	0.024	0.82	13	9	Good adhesion on uncontaminated areas
8	Methanol wipe	1×10^{-4}	W-coil	CVC	Good	0.045	1.3	26	19	
9	Methanol wipe	1×10^{-4}	W-coil	CVC	Fair	0.026	0.48	2.6	1.7	Good adhesion on uncontaminated areas
10	Methanol wipe	1×10^{-4}	W-boat	CVC	Good	0.022	0.25		0.8	
11	Methanol wipe	1×10^{-4}	W-boat	CVC	Good	0.036	0.46		12	
12	Methanol wipe	1×10^{-4}	W-boat	CVC	Good	0.025	0.21		0	Some shadowed areas
13	Methanol wipe. Glow discharge 10 min.	2×10^{-5}	W-boat	Edwards	Good		0.46		1.0	Substrate at 60°C during deposition
14	Methanol wipe. Glow discharge 10 min.	1×10^{-5}	W-boat	Edwards	Good					
15	Methanol wipe. Glow discharge 10 min.	1×10^{-5}	W-boat	Edwards	Good					
16	Methanol wipe. Glow discharge 10 min.	1×10^{-5}	W-boat	Edwards	Good		0.10			
17	Methanol wipe	1×10^{-5}	W-boat	Edwards	Good					
18	Methanol wipe	1×10^{-5}	W-boat	Edwards	Good		2.6	45	32	
19	Methanol wipe	1×10^{-5}	W-boat	Edwards	Good		1.6	32	21	
20	Methanol wipe	1×10^{-5}	W-boat	Edwards	Good		0.47	2.5	1.2	
21	Methanol wipe	1×10^{-5}	W-boat	Edwards	Good		0.30	0.35	0	
22	Methanol wipe	1×10^{-5}	W-boat	Edwards	Good		0.25	0.10	0	
23	Acetone wipe. Glow discharge 10 min.	3×10^{-5}	W-boat	Edwards	Good				0.4	Substrate at 70°C during deposition
24	Acetone wipe. Glow discharge 10 min.	2×10^{-5}	W-boat	Edwards	Good					

Table 2-12. Gold on 1/4 Mil Mylar (Cont)

Sample Ident.	Cleaning Technique	Deposition Variables			Adhesion	ϵ_N Au	Res (ohm/sq)	Photovolt % Trans @ 0.52 μ	Beckman % Trans @ 0.5 μ	Comment
		Pressure	Source	Chamber						
25	Genasolve wipe. Glow discharge 10 min.	2×10^{-5}	W-boat	Edwards	Good		0.26		0	7 mo. separate depositions, 1050Å each; substrate at 80°C during deposition
26	Cobean wipe. Glow Discharge 10 min	2×10^{-5}	W-boat	Edwards	Good		0.18		0	7 mo. separate depositions, 1050Å each; substrate at 70°C during deposition
27	Dis H_2O rinse. Glow discharge 10 min.	3×10^{-5}	Ta-boat	Edwards	Poor				16	Tantalum boat reacted with gold; substrate at 70°C during deposition
28	Acetone wipe. Glow discharge 10 min	1×10^{-5}	Ta-boat	Edwards	Poor					Tantalum boat reacted with gold; substrate at 60°C during deposition
29	As received. Glow discharge	2×10^{-5}	W-boat	Edwards	Poor					
30	Dry wipe	2×10^{-5}	W-boat	Edwards	Fair					Good adhesion on approximately 70% of sample
31	Alconox + H_2O rinse. Glow discharge 10 min.	2×10^{-5}	W-boat	Edwards	Fair					Good adhesion on approximately 90% of sample
32	Alconox + H_2O rinse	5×10^{-6}	W-boat	Edwards	Poor					
33	Alconox + H_2O rinse + Methanol wipe + Glow discharge 10 min.	4×10^{-5}	W-boat	Edwards	Good					
34	Alconox + H_2O rinse + Methanol wipe + Glow discharge 10 min.	3×10^{-5}	W-boat	Edwards	Good					
35	Alconox + H_2O rinse + Acetone wipe + Glow discharge 10 min.	3×10^{-5}	W-boat	Edwards	Good					
36	Methanol wipe + Alconox + H_2O rinse	1×10^{-5}	W-boat	Edwards	Poor					
37	Dis H_2O rinse	3×10^{-6}	W-boat	Edwards	Poor					
38	Methanol wipe. Glow discharge	2×10^{-5}	W-boat	Edwards	See Remarks					Poor adhesion after evaporation; adhesion was good after exposure to 300°F for 15 min.

Table 2-13. Gold on Kapton

Sample Ident.	Thickness	Cleaning Technique	Deposition Variables		Adhesion	ϵ_N Au	Approx Thick (Å)	Res (ohm/sq)	Photovolt % Trans @ 0.52 μ	Beckman Peak % Trans	Film	
			Pressure	Substrate Temp (°C)							α_s	ϵ_N
39	1 mil	Methanol wipe	1×10^{-4}		Poor							
40	1 mil	Methanol wipe. Glow discharge 18 min.	1×10^{-4}		Poor							
41	1 mil	Methanol wipe. Glow discharge 8 min.	1×10^{-4}		Poor							
42	1 mil	Alconox + H_2O rinse + methanol wipe. Glow discharge 8 min.	1×10^{-4}		Poor							
43	1 mil	Alconox + H_2O rinse	1×10^{-4}		Poor							
44	1 mil	Methanol wipe	1×10^{-4}		Poor							
45	1 mil	Methanol wipe	3×10^{-5}	25	Poor		2100					
46	1 mil	Methanol wipe	3×10^{-5}	25	Poor		2100					
47	1 mil	Methanol wipe	3×10^{-5}	25	Poor		2100					
48	1 mil	Methanol wipe	3×10^{-5}	25	Poor		2100					
49	1 mil	Genasolve wipe. Glow discharge 20 min.	5×10^{-6}	65	Good		1000	0.4	1.3			
50	1 mil	Genasolve wipe. Glow discharge 20 min.	1×10^{-5}	95	Good		2100					
51	1 mil	Methanol wipe. Glow discharge 20 min.	1×10^{-5}	95	Good		2100	0.17	0.1			
52	1 mil	Acetone wipe. Glow discharge 20 min.	1×10^{-5}	95	Good		2100	0.2	0.3			
53	1 mil	Cobean wipe. Glow discharge 20 min.	1×10^{-5}	75	Good		2100					
54	1 mil	Acetone wipe	1×10^{-5}	100	Good		2100					
55	1 mil	Methanol wipe	1×10^{-5}	100	Good		2100					
56	2 mil	Methanol wipe. Glow discharge 20 min.	1×10^{-5}	140	Good	0.127	100	8.4	41	57	0.591	0.793
57	2 mil	Methanol wipe. Glow discharge 20 min.	1×10^{-5}	150	Good		175	7.8	34-37	Scratches on Au coating		
58	2 mil	Methanol wipe. Glow discharge 20 min.	2×10^{-5}	135	Good	0.026	250	1.5	22.5	17	0.398	0.773
59	2 mil	Methanol wipe. Glow discharge 20 min.	2×10^{-5}	150	Good		500	0.94	12.0	7.5	0.374	
60	2 mil	Methanol wipe. Glow discharge 20 min.	2×10^{-5}	160	Good		1000	0.40	0.70	0	0.335	

Table 2-13. Gold on Kapton (Cont)

Sample Ident.	Thickness	Cleaning Technique	Deposition Variables: Pressure	Deposition Variables: Substrate Temp (^oC)	Adhesion	ϵ_N Au	Approx Thick. (Å)	Res. (ohm/sq)	Photovolt % Trans @ 0.52 μ	Beckman Peak % Trans	Film α_s	Film ϵ_N
61	2 mil	Methanol wipe. Glow discharge 20 min.	2×10^{-5}	160	Good	0.028	1550	0.27	0.14	0	0.341	0.769
62	2 mil	Methanol wipe. Glow discharge 20 min.	2×10^{-5}	160	Good	0.028	2100	0.20	0.05	0	0.342	0.773
63	1/2 mil	Methanol wipe. Glow discharge 20 min.	9×10^{-6}	170	Good	0.124	100	12.0	63	39		
64	1/2 mil	Methanol wipe. Glow discharge 20 min.	1×10^{-5}	160	Good	0.070	175	5.0	55	32		
65	1/2 mil	Methanol wipe. Glow discharge 20 min.	2×10^{-5}	150	Good	0.032	250	1.7	38	26		
66	1/2 mil	Methanol wipe. Glow discharge 20 min.	2×10^{-5}	75	Good	0.027	350	1.5	30	18		
67	1/2 mil	Methanol wipe. Glow discharge 20 min	2×10^{-5}	150	Good		500				Scratches on Au Coating	
68	1/2 mil	Methanol wipe. Glow discharge 20 min.	2×10^{-5}	100	Good	0.025	500	1.2	23	12.5		
69	1/2 mil	Methanol wipe. Glow discharge 20 min.	3×10^{-5}	125	Good	0.024	750	0.6	5.5	3.5		
70	1/2 mil	Methanol wipe. Glow discharge 20 min.	2×10^{-5}	150	Good	0.021	1000	0.42	1.6	1.2		
71	1/2 mil	Methanol wipe. Glow discharge 20 min.	3×10^{-5}	160	Good	0.018	1550	0.32	0.25	0		
72	1/2 mil	Methanol wipe. Glow discharge 20 min.	3×10^{-5}	160	Good	0.018	2100	0.19	0.15	0		
73	1/2 mil	Methanol wipe. Glow discharge 20 min.	3×10^{-5}	125	Good	0.022	2600	0.15	0.05	0		

2.5.2 SECOND SERIES OF DEPRESSURIZATION TESTS

Tests to demonstrate the capability of insulation blanket designs to withstand ascent depressurization were conducted during Phase I. These tests showed that improvements were required to provide adequate venting.

A venting analysis was performed for 24 layer insulation blankets which assumed 1/8 or 1/4 inch diameter holes spaced to give 4, 9, or 16 holes per square foot. This analysis showed that 1/4 inch diameter holes would not reduce the venting pressure difference appreciably with respect to 1/8 inch diameter holes, for nearly all of the pressure difference is caused by flow through the wrinkled passages formed between the insulation layers. The analysis gave maximum pressure differences across the blanket of 0.009, 0.031, or 0.106 pound per square foot for the 16, 9, or 4 holes (1/8 inch diameter) per square foot, respectively. Further analysis indicated that pressure levels of these amounts would be insufficient to cause the outer 2 mil Kapton cover sheet to tear, even if this layer transmitted all of the pressure loading to the support posts. Consequently, it appeared likely that satisfactory venting of blankets of 4 foot width would occur within the range of 4, 9, or 16 holes (1/8 inch diameter) per square foot. The second depressurization test series was planned to evaluate the effect of that range of hole spacing on insulation expansion and structural integrity. In addition, static tests were performed to determine the amount of expansion to be expected for a given pressure difference. The effect of reducing the maximum insulation span between support posts was also evaluated.

The test procedure has been described in detail in Planetary Vehicle Thermal Insulation Systems Phase I Summary Report, General Electric Company Report No. 67SD4289, dated 3 March 1967. Briefly, the test specimens were mounted in the air lock of a 39 by 54 foot thermal vacuum chamber. The desired pressure versus time profile was obtained by a manually operated valve which dumped air into the evacuated main chamber. The test configuration is shown in Figure 2-17, and the specimens listed as follows:

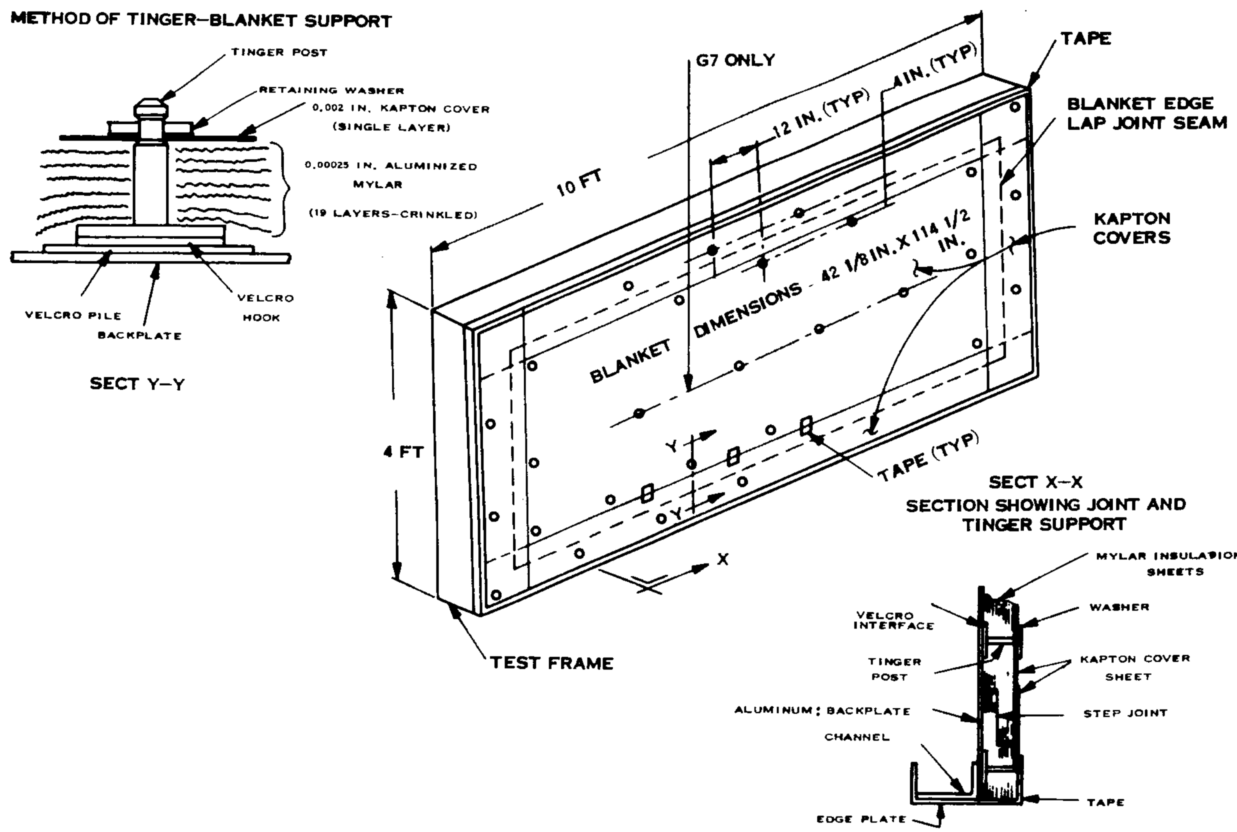

Figure 2-17. Depressurization Test Specimen

Blanket Assembly 47R211796	No. of Vent Holes per Square Foot	Tinger Support	
		Perimeter Only	Perimeter and Center Span
G5	4	X	
G6	9	X	
G7	4		X
G8	16	X	

The depressurization expansions are plotted in Figures 2-18 and 2-19 which correlate the expansion observations with chamber pressure. The maximum expansion of each test blanket is plotted in Figure 2-20.

The results of the static blanket loading tests are shown in Figure 2-21. The minimum blanket loading, i.e., that loading caused by its own weight when the blanket was held horizontally, produced more deflection than was observed during depressurization. Blanket weight results in a loading of about 0.05 pound per square foot. Thus the depressurization

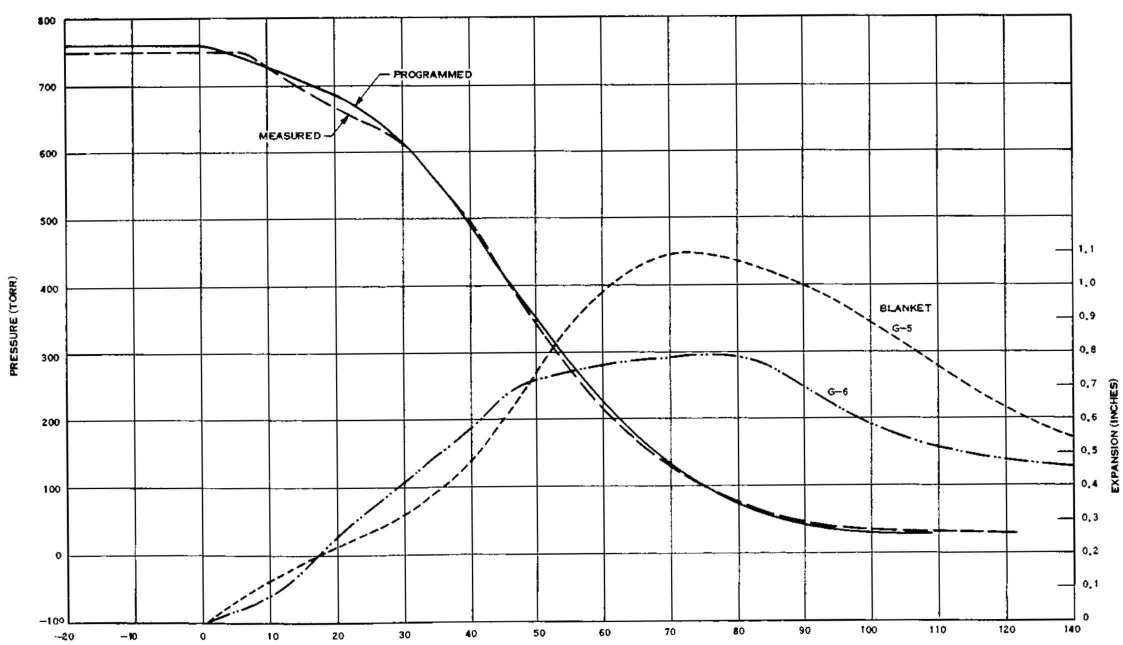

Figure 2-18. Depressurization Test Results: Test 1

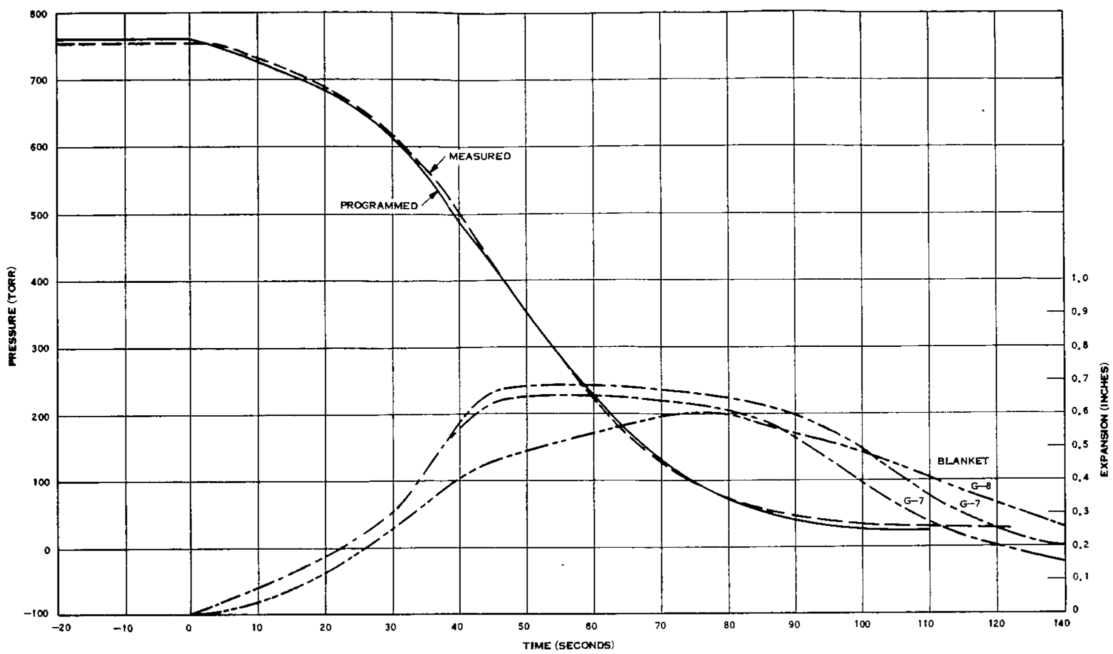

Figure 2-19. Depressurization Test Results: Test 2

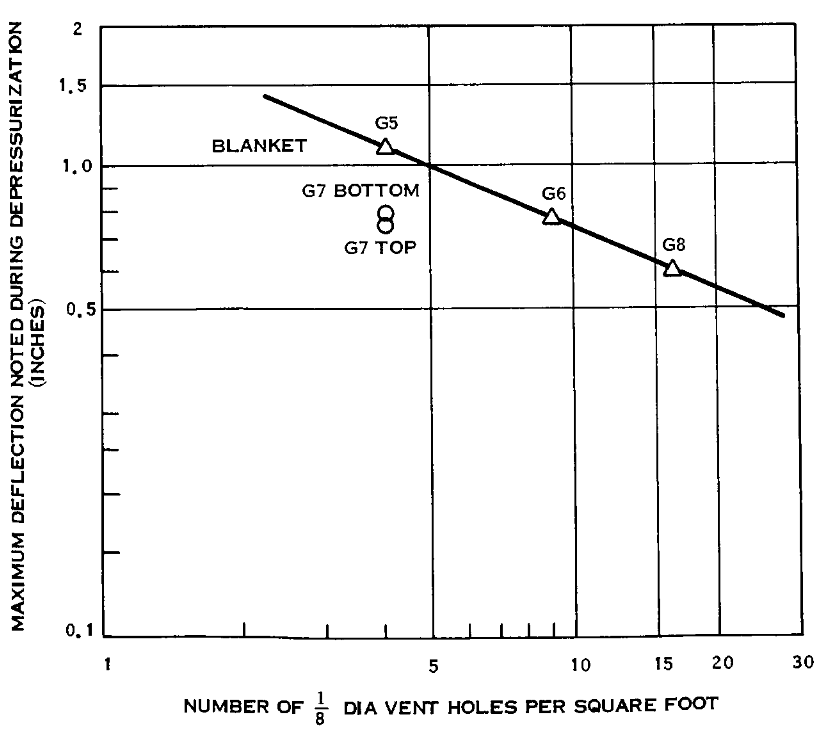

Figure 2-20. Maximum Deflection vs Number of Vent Holes per Square Foot

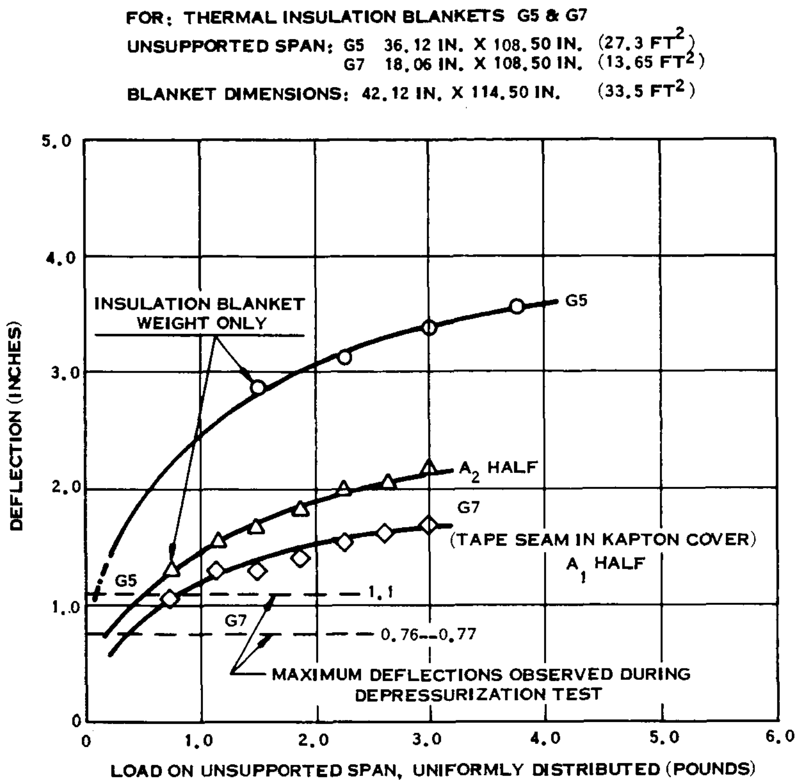

Figure 2-21. Static Load-Deflection Curves: Kapton Cover Sheet

tests indicate that the analysis that predicted about 0.1 psf for four 1/8 inch diameter holes per square foot was conservative, with the actual venting pressure buildup limited to much less than that amount.

Based on the above tests, it was decided that four 1/8 inch diameter holes per square foot, together with the step type of insulation blanket joint, will be sufficient to prevent any pressure loading damage during launch. In addition, limiting unsupported spans to a maximum of 2 feet will restrict blanket expansion to 1 inch. Tinger fasteners with 1 foot spacing, placed alternately along both sides of the joint, will satisfactorily support the insulation.

2.5.3 INITIAL SHOCK, ACOUSTIC, AND VIBRATION TESTS

Dynamic mechanical tests of gold coated Mylar and Kapton insulation material assemblies were planned in two series, with insulation exposure to six cycles of ethylene oxide decontamination after the first series. The mechanical tests were performed with the test fixture described in Section 2.1.2.1, and were conducted as described in the following discussion.

2.5.3.1 Shock Test

The insulation shock test was performed on an Avco model SM 220 shock machine at the Associated Testing Laboratories, Inc., Wayne, New Jersey, according to General Electric Test Procedure PVTIS 19. The test fixture was mounted to the platform of the shock machine, and an accelerometer was mounted near the center of the base plate of the test fixture. The accelerometer was connected through a bandpass filter to a Memo Scope. The cutoff settings of the band pass filter were 0.2 cps and 900 cps. The shock machine was then calibrated for the required shock pulse. The shock pulse approximated a one-half sine wave with a peak intensity of 200 g ±10% and a time duration of 2 milliseconds ±15%. A depiction of the calibration shock pulse may be seen in Figure 2-22.

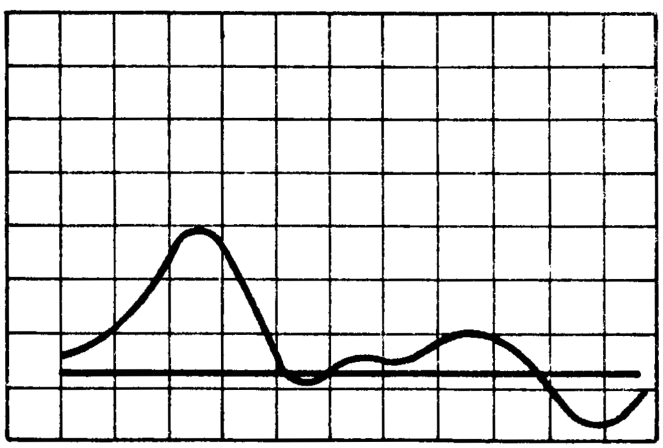

ACCELEROMETER SENSITIVITY:	0.735 PK MV/PK G
OSCILLOSCOPE VERTICAL SETTING:	50 MV/DIVISION (70G/DIVISION)
OSCILLOSCOPE HORIZONTAL SETTING:	0.5 MS/DIVISION
PEAK INTENSITY:	200G
TIME DURATION:	2 MS

Figure 2-22. Calibration Shock Pulse

After the shock machine was calibrated, the insulation blanket samples were mounted to the test fixture at the locations shown in Figure 2-23. The blanket samples were then subjected to one shock impact in a direction perpendicular to the test fixture base plate. The direction of drop is identified in Figure 2-23. The shock pulse recorded during the impact may be seen in Figure 2-24. The shock pulse obtained from the Memo Scope was within the specified limits of 200 g ±10% and 2 milliseconds ±15%. Photographs of the blanket samples prior to and at the completion of the shock test may be seen in Figures 2-25 through 2-28.

Inspection after the shock test showed that some tears had developed at the support post holes in both the outer 2 mil Kapton cover sheet and in the 1/4 mil Mylar underlayers. Had these tears occurred on a flight vehicle, it is not likely that blanket performance would have been noticeably affected. However, the tears were sufficiently numerous to suggest that some remedial action be taken. None of the attachment posts were dislocated.

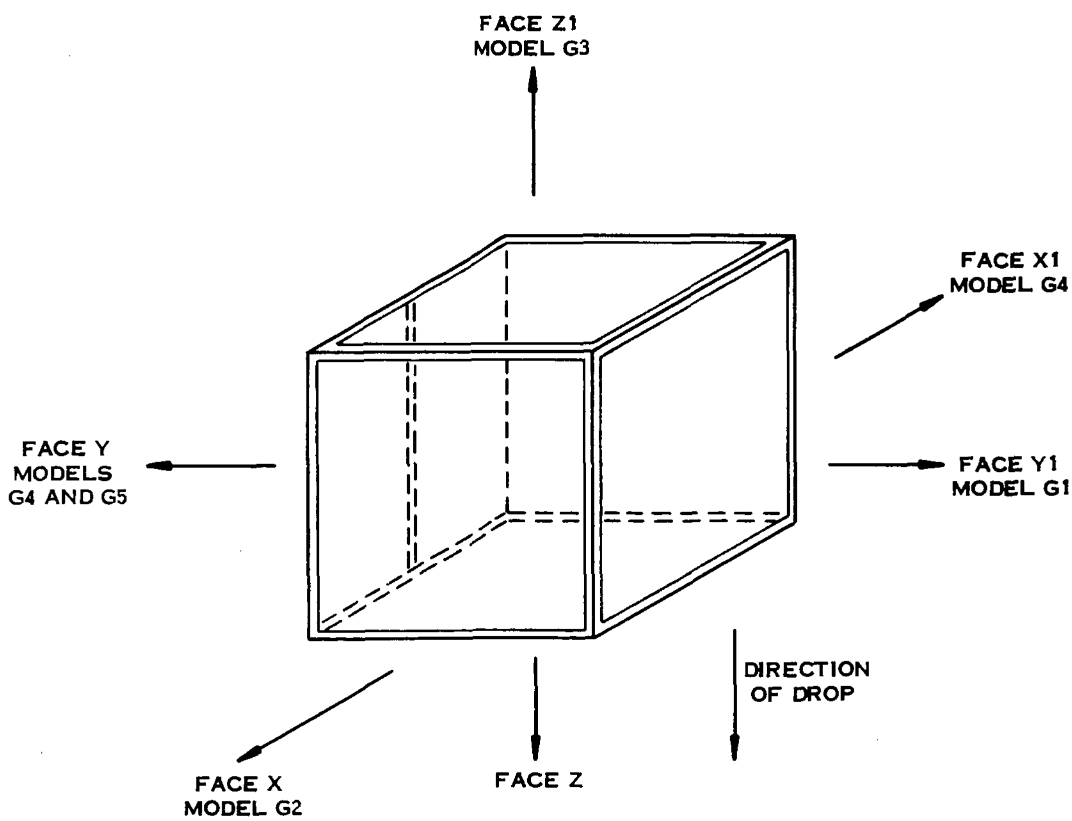

Figure 2-23. Location of Blanket Samples on Test Fixture

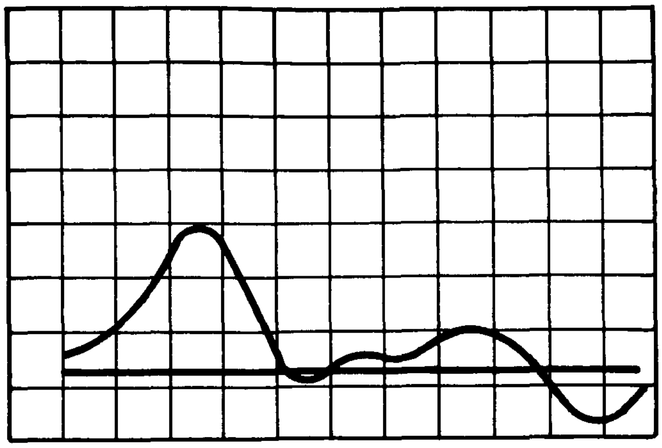

ACCELEROMETER SENSITIVITY: 0.735 PK MV/PK G

OSCILLOSCOPE VERTICAL SETTING: 50 MV/DIVISION (70G/DIVISION)

OSCILLOSCOPE HORIZONTAL SETTING: 0.5 MS/DIVISION

PEAK INTENSITY: 200G

TIME DURATION: 2 MS

Figure 2-24. Test Shock Pulse

2.5.3.2 Acoustic Test

Following the shock test, the insulation blankets mounted on the same test fixture were exposed to acoustic excitation at Noise Unlimited, Inc., Somerville, New Jersey.

Figure 2-29 compares the excitation levels achieved with the test objective. Although the test did not achieve the specified levels, particularly below 250 cycles per second, it is felt that the intent of the test was achieved. The average overall intensity was within 4 db of the desired 151.5 db level. This intensity was maintained for 7-1/4 minutes.

Examination after the test did not reveal any additional damage to the insulation blankets beyond that sustained during the shock test. Also significant is the fact that dummy blankets installed on the fixture for facility checkout did not sustain any damage during approximately 30 minutes of high intensity noise.

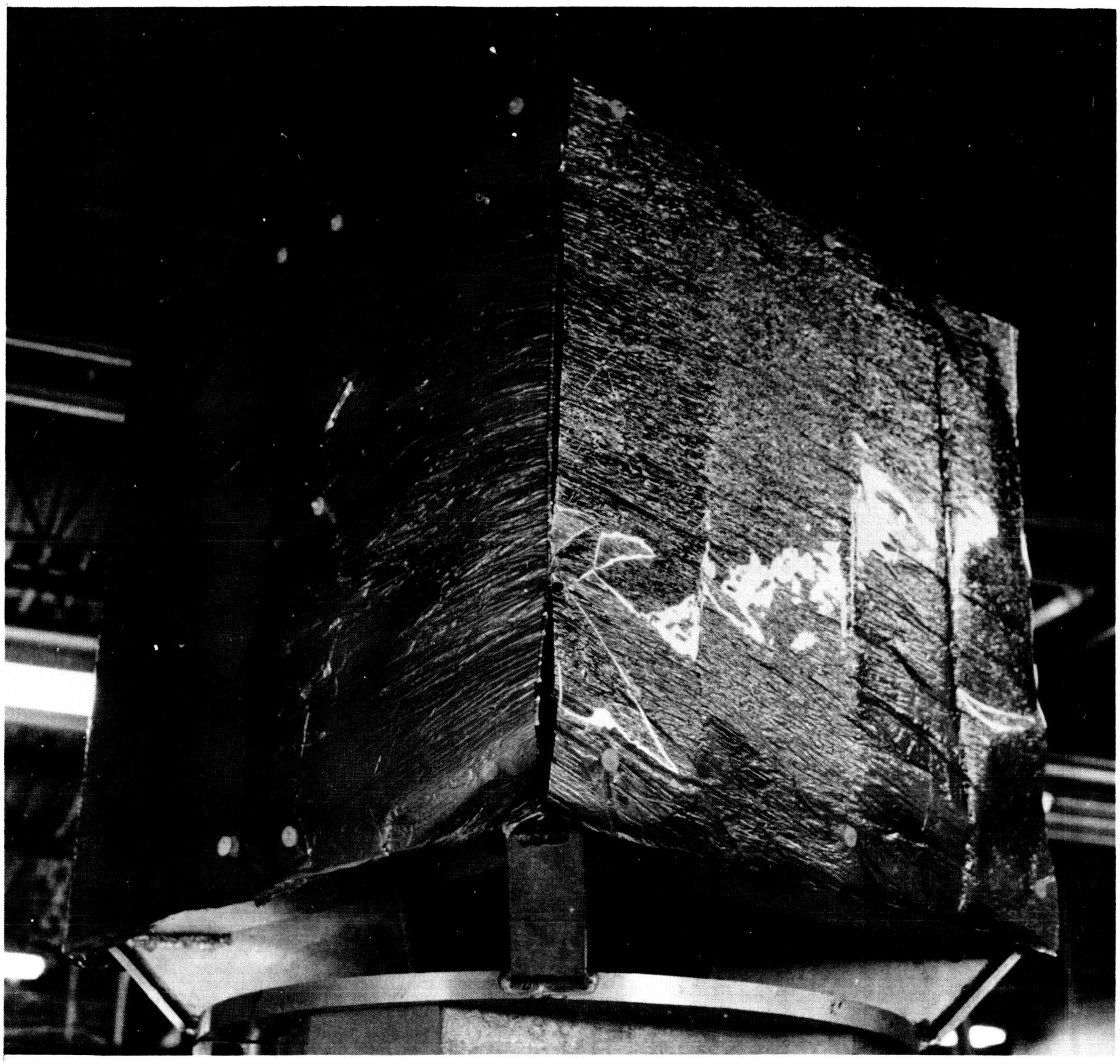

FIXTURE FACE	BLANKET MODEL NO.
X	G2
Y	G4 AND G5

Figure 2-25. Preshock Test Photograph: Blankets G2, G4, and G5

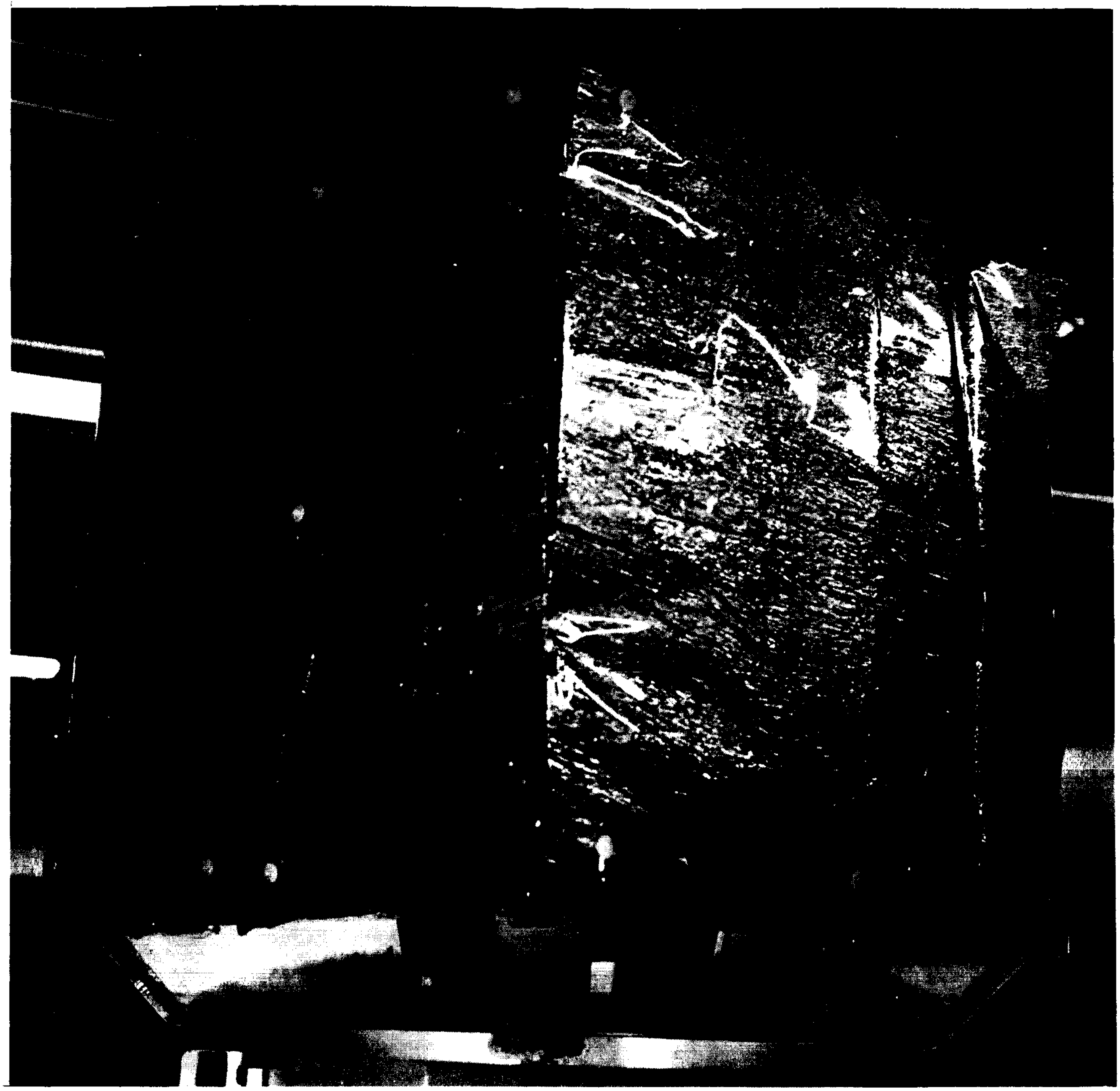

FIXTURE FACE	BLANKET MODEL NO.
X	G2
Y	G4 AND G5

Figure 2-26. Postshock Test Photograph: Blankets G2, G4, and G5

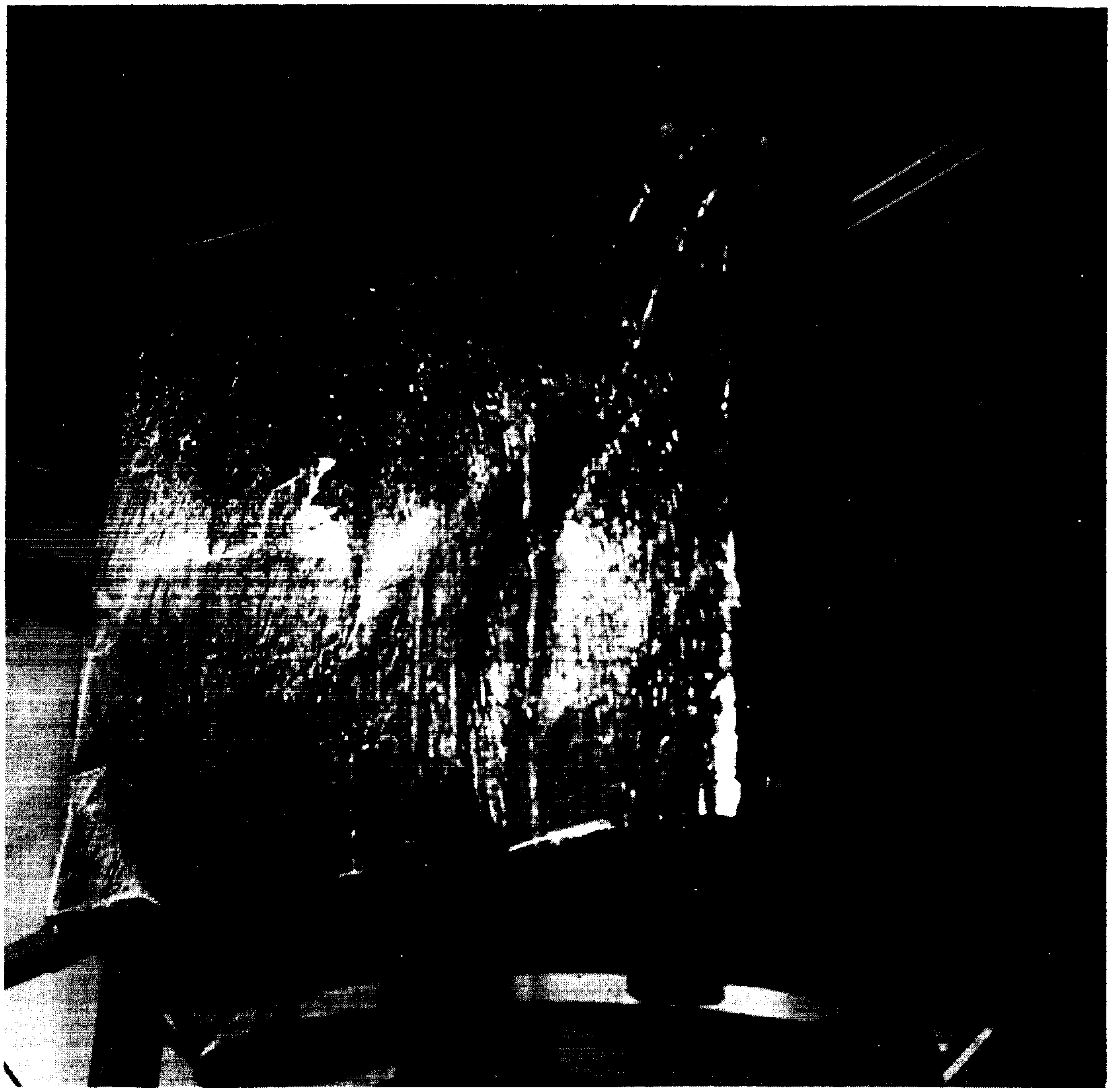

FIXTURE FACE	BLANKET MODEL NO.
X1	G4
Y1	G1

Figure 2-27. Preshock Test Photograph: Blankets G4 and G1

FIXTURE FACE	BLANKET MODEL NO.
X1	G4
Y1	G1

Figure 2-28. Postshock Test Photograph: Blankets G4 and G1

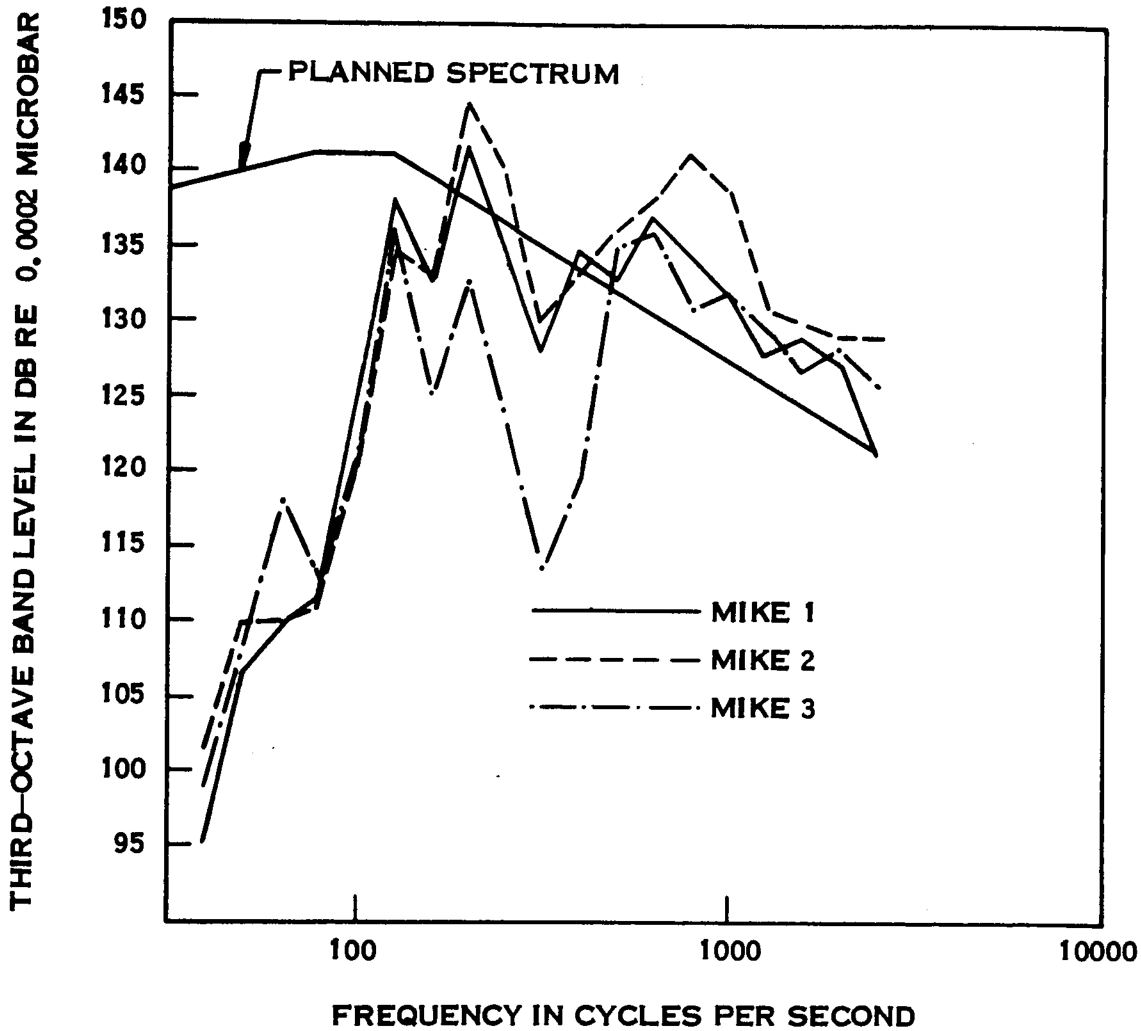

Figure 2-29. Acoustic Levels

2.5.3.3 Vibration Test

After the acoustic exposure, the test fixture was installed in the General Electric Dynamic Simulation Laboratory at Valley Forge, Pa. on a MB Model C210 exciter. The insulation blankets were subjected to broad band random vibration in the vertical direction. A test level of 15 g rms for a period of 120 seconds was maintained. Figure 2-30 shows the averaged response of six accelerometers.

Inspection after test showed that insulation blanket damage had not increased beyond that noticed after the shock test. Neither were the dummy insulation blankets damaged during an approximate 30 minute exposure to 10 to 15 g rms during test facility checkout.

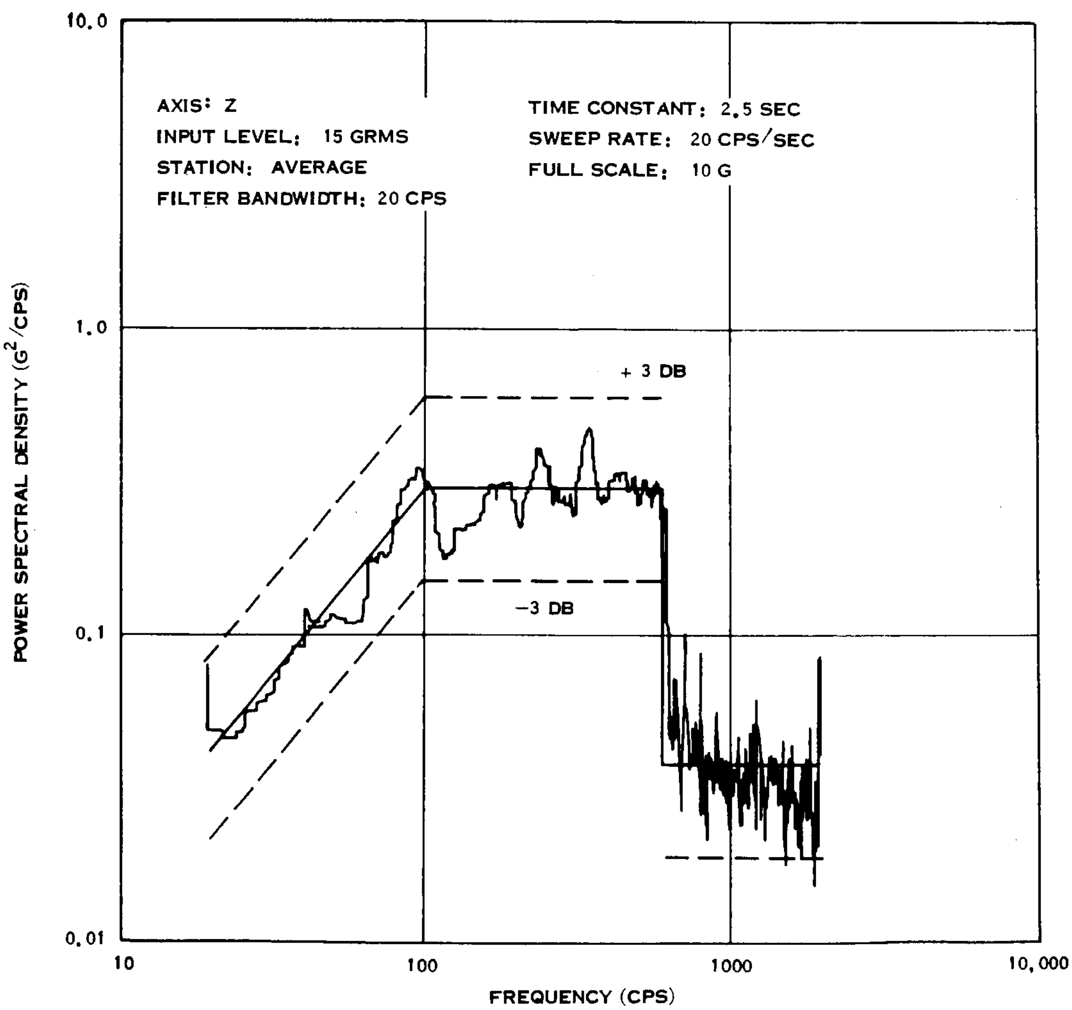

Figure 2-30. Vibration Levels

2.5.3.4 Ethylene Oxide Decontamination Exposure

In accordance with the test plan, the insulation blankets were subjected to six 30 hour ethylene oxide cycles per JPL Specification VOL-50530 ETS following the first series of shock, acoustic, and vibration tests. Subsequent examination of the gold coated Mylar and Kapton material did not reveal any signs of surface degradation. Restricted inspection between the multilayers without removing the blanket fasteners did not disclose any areas where the materials were stuck together as had been found with aluminized materials during Phase I.

2.5.3.5 Conclusions from Mechanical Tests

From the above tests it was determined that a change in insulation blanket design was needed to prevent material tearing at the support posts. As mentioned in Section 2.1.1.3.1, support post holes in the blankets will be made 0.296 inch in diameter. This has been enlarged from the original size of 0.250 inch because of tearing caused by insertion and removal of the support post. The blankets for the shock, acoustic, and vibration tests had been made with 0.250 inch diameter holes. It is believed that the enlarged holes will prevent tears at assembly and will remove the tear sites that may subsequently be enlarged during shock exposure. An evaluation of this change was made during the second shock test, since a dummy set of nonmetalized blankets was constructed with the larger hole size. These dummy blankets were used during check out calibration of the facility with loads at least as severe as the actual test.

2.5.4 SECOND SERIES OF SHOCK, ACOUSTIC, AND VIBRATION TESTS

The same set of gold coated Mylar and Kapton insulation blanket assemblies discussed in Section 2.5.3 were subjected to a second series of mechanical excitation tests to determine if the intervening decontamination treatment discussed in Section 2.5.3.4 had debilitating effects. These insulation assemblies at this point included a number of tears at support post holes. These tears had first appeared after the initial shock test, and in some instances had been increased with subsequent handling as the blankets were attached and removed from the test fixture. It was decided not to attempt any repair of the tears prior to the second series of tests, and consequently to determine if the tears were important to blanket integrity.

The second shock test was similar to the initial test described in Section 2.5.3.1. During the equipment checkout for this second test, a set of dummy blankets made of clear Mylar was installed and subjected to two shocks approximating 200 g each. These dummy blankets had 0.296 inch diameter post holes instead of 0.25 inch holes in the gold coated blankets. Inspection of the dummy blankets after removal from the fixture did not reveal any tears in the Mylar. Thus enlargement of the post holes solved the tearing problem. The insulation blankets for the full scale thermal tests will have the enlarged holes.

After shock machine checkout to establish the desired pulse contour, the gold coated blankets were installed on the fixture and subjected to the 200 g shock. Examination after the second shock test did not indicate any noticeable enlargement of the previous tears. However, some holes in blanket G2 had tears that were not in evidence after the first test. After the first test, the tears were primarily at post holes near the top of the fixture, tearing from the holes toward the adjacent edge. The tears at the new locations are also toward the adjacent edge. This leads to the conclusion that at the second installation, the G2 blanket was turned around so that untorn holes from the bottom were located at the top. During the second shock, these untorn holes then developed tears as the blanket material was restrained by the upper posts. No new tears appeared in the other blankets, nor did the tears that were there appear enlarged.

The second acoustic test exposure followed the same procedure as the first, and no further damage to the insulation blankets was noted. Similarly, the second random vibration exposure did not produce any additional blanket damage or cause any of the fasteners to loosen.

The results of these tests indicated that enlarging the support post holes eliminates tearing of the insulation during shock loads. Acoustic and random vibration of the multilayer Mylar and Kapton insulation blankets did not reveal any degrading effects either before or after ethylene oxide exposure. It may then be concluded that these insulation materials are insensitive to the mechanical environments expected during boost flight.

SECTION 3

CONCLUSIONS

The results of the Phase II effort have led to the following definitive conclusions:

a. The number of layers of insulation material specified in Table 2-6 should provide adequate thermal protection throughout all mission phases.

b. Tech Fluoro tape and pressure sensitive Velcro hook and pile appear to be satisfactory for applying and fastening the insulation to a space vehicle that must undergo dry heat sterilization.

c. Vent holes and restraining fasteners are required to prevent excessive ballooning of large insulation blankets. Four 1/8 inch diameter holes per square foot and maximum unsupported spans of 2 feet result in minimal ballooning.

d. The initial shock test demonstrated that 0.25 inch diameter holes in the insulation material for 0.23 inch diameter tinger posts resulted in some tearing at the post holes, an amplification of damage initiated by post insertion and removal. No further adverse effects were noted during the acoustic and shock tests prior to ethylene oxide exposure.

SECTION 4
RECOMMENDATIONS

On the basis of the work performed in Phase II, it is recommended that the following vent hole and fastener patterns be incorporated into the blanket design:

> Four 1/8 inch diameter holes per square foot, fasteners spaced no more than 12 inches apart along a joint, and a maximum unsupported distance of 2.0 feet will eliminate tearing of insulation material during depressurization, and will restrict ballooning to less than one inch.

The results of the shock tests indicate that support post holes in the insulation blankets will be enlarged to 0.296 inch to minimize assembly tearing which subsequently amplifies during shock. Since only the shock test produced any adverse effects on the insulation material, acoustic and vibration tests should not be required in the future for multilayered, metallized Mylar and Kapton insulation blankets.

The insulation blankets for Phase III fabrication should be comprised of the number of layers of material as specified in Table 2-6.

SECTION 5

NEW TECHNOLOGY

No reportable items of new technology are deemed to have resulted from the effort reported herein.

DIN: 67SD4405-S

1 NOVEMBER 1967

SUPPLEMENT TO

VOYAGER THERMAL INSULATION SYSTEMS

PHASE II SUMMARY REPORT

LONG TERM VACUUM STORAGE TEST AND VIBRATION EFFECTS EVALUATION ON MULTI-LAYER SUPER INSULATION BLANKETS

BY

R.W. CARR

C.S. LANKTON

PREPARED FOR

JET PROPULSION LABORATORY
PASADENA, CALIFORNIA
UNDER JPL CONTRACT NO. 951537

GENERAL ELECTRIC

MISSILE AND SPACE DIVISION
Valley Forge Space Technology Center
P.O. Box 8555 • Philadelphia 1, Penna.

This report was prepared by the General Electric Company under Contract No. 951537, Planetary Vehicle Thermal Insulation Systems, for the Jet Propulsion Laboratory. It is a supplement to the Phase II Summary Report, dated 11 September 1967. The work was administered under the technical direction of the Advanced Engineering Section, Engineering-Mechanics Division of the Jet Propulsion Laboratory, with Mr. Donald Ting acting as Technical Director.

Submitted by: A. D. Cohen

A.D. Cohen, Program Manager (PVTIS)
General Electric Company

Approved by: Donald Ting

Donald Ting, Technical Director (PVTIS)
Jet Propulsion Laboratory

ABSTRACT

Super insulation blankets were subjected to a sixty day exposure to vacuum levels in the 10^{-8} torr range while radiating to walls cooled by liquid nitrogen. At the end of the sixty day time period, the blankets were subjected to broad-band vibration levels of 3.77 G to 4.66 G RMS while at vacuum/cryogenic conditions. There was no apparent physical damage to the insulation and no measurable change in the thermal performance.

TABLE OF CONTENTS

LIST OF ILLUSTRATIONS

SECTION 1

INTRODUCTION

As part of the subject program, it was required to demonstrate that the super insulation material, when assembled into blankets, could survive the expected vibration levels caused by firing of the orbit insertion motor after several months of exposure to space vacuum and temperature conditions. A secondary objective was to measure the thermal performance of the insulation material after initial temperature stabilization and again after vibration to determine if any significant change in thermal performance occurred. For this test, the materials were exposed to vacuum levels in the 10^{-8} torr range and to a sink temperature below $-280^{o}F$. At the conclusion of the exposure period, and while the specimen was under vacuum/low temperature conditions, it was vibrated at the levels that approximate those shown in Figure 1-1 which are representative of vibration levels expected from a liquid rocket engine.

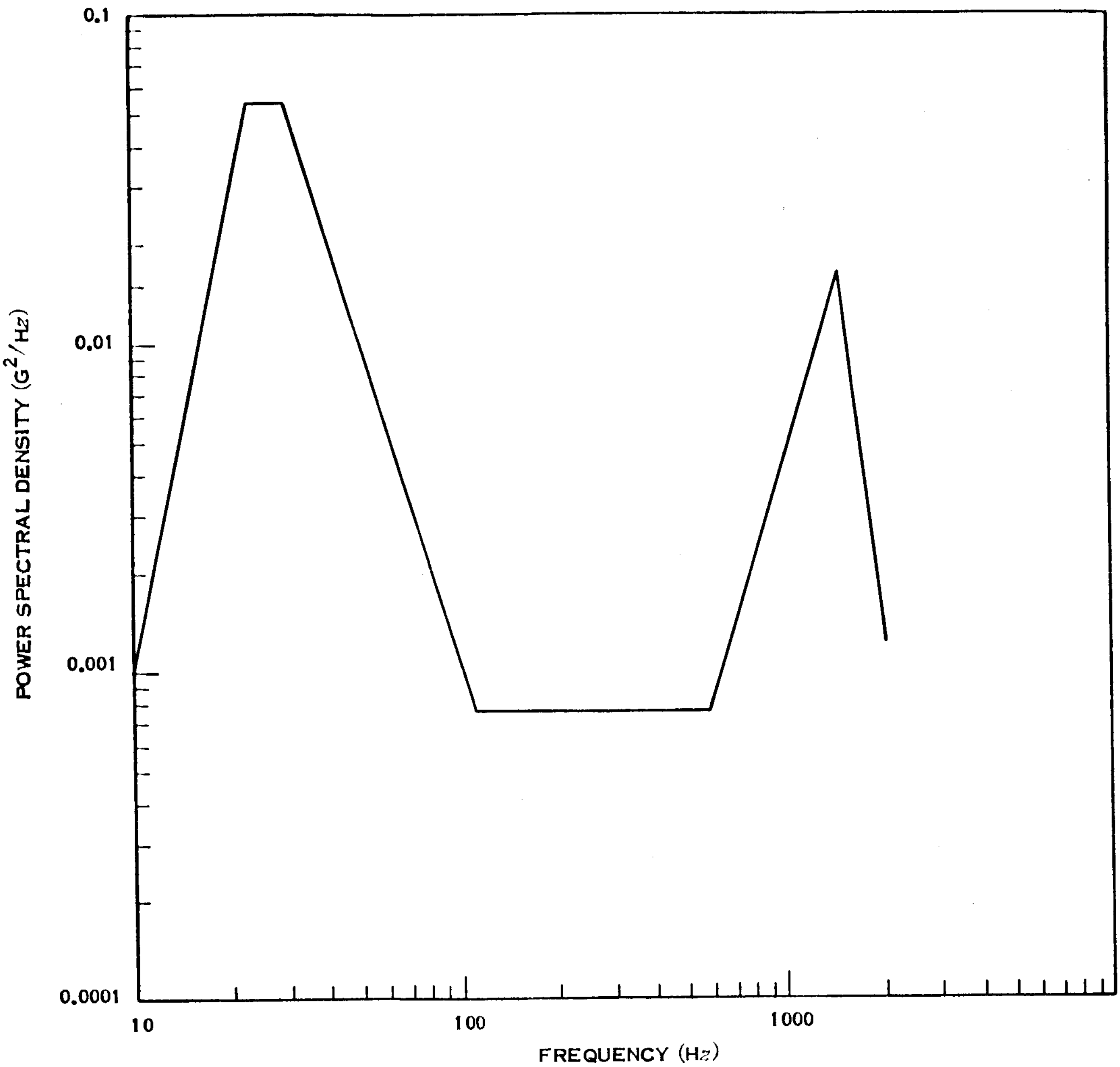

Figure 1-1. Random Vibration Spectrum

SECTION 2

TECHNICAL DISCUSSION

2.1 TEST FIXTURE DESCRIPTION

The test fixture was a 14-in. diameter by 14-in. long right circular cylinder as shown in Figures 2-1 and 2-2.

2.2 TEST BLANKET DESCRIPTION

The test blankets are as shown in Figures 2-3 through 2-7. The 1/4-mil gold coated Mylar and 1/2-mil gold coated Kapton were crinkled by pulling the sheet material through a Teflon die. The sheets were perforated prior to crinkling with nine 1/8-in. diameter holes per square foot. The uncoated 2 mil Kapton cover sheets were drilled with the same hole pattern. Holes to accommodate the Tinger fasteners were 0. 30 inches in diameter. The Tinger fasteners are described in Figure 2-8. The blankets were restrained on the posts by nylon split-washers snapped into the machined shoulder on top of the Tinger.

The blankets were taped at the joints with one inch wide, one mil Kapton tape coated with pressure sensitive cement.

The following materials and sources of supply were used.

1/4-mil, gold coated Mylar	National Metallizing
1/2-mil, gold coated Kapton	National Metallizing
2 mil Kapton cover	DuPont DeNemours, Inc.
Tinger Fasteners	General Electric Company
Velcro nylon hook and pile tape	Velcro Corp.
Adhesive backed Kapton Tape	Technical Fluorocarbons Eng., Inc.

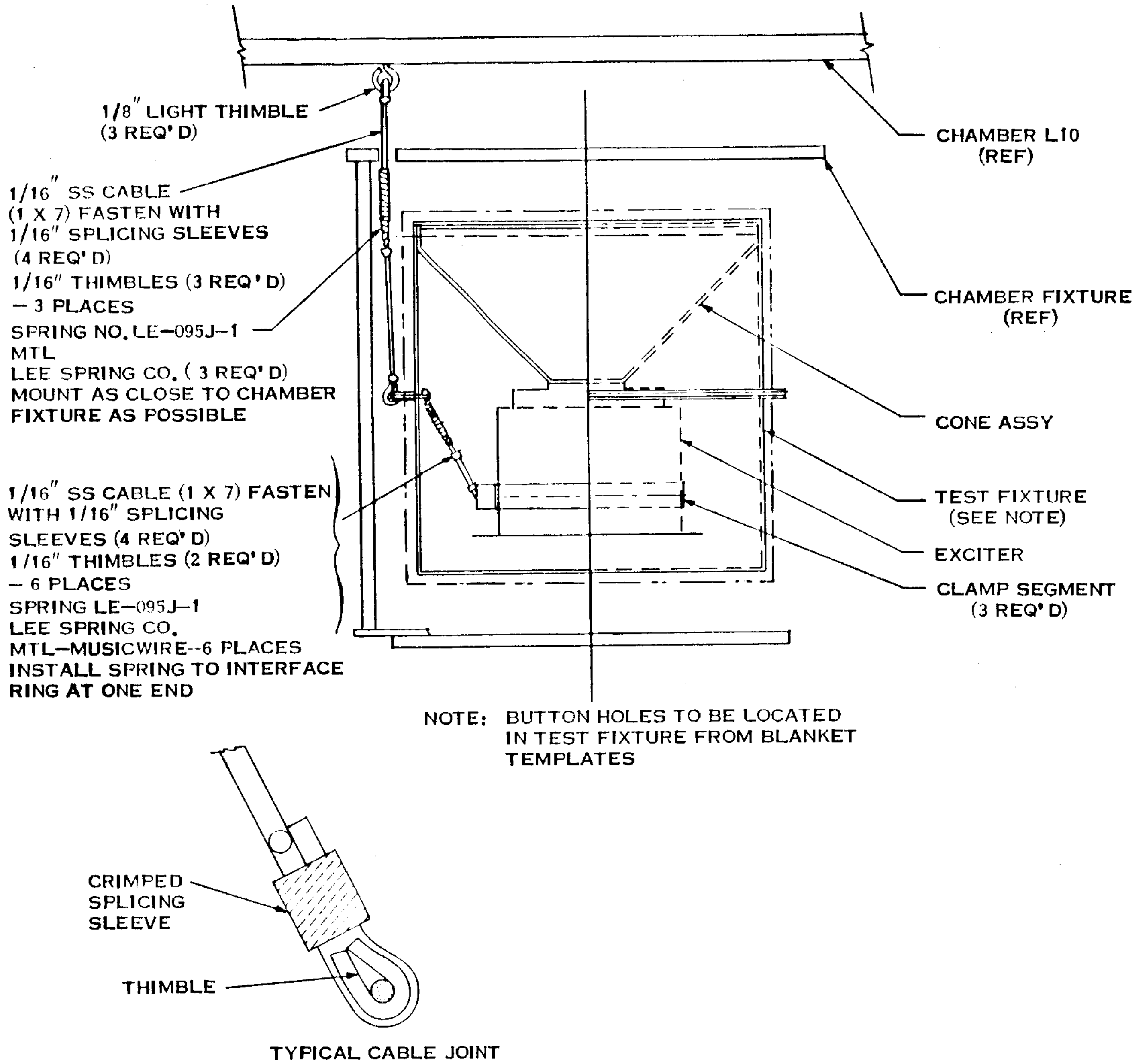

Figure 2-1. Long Term Thermal Vacuum Test Fixture

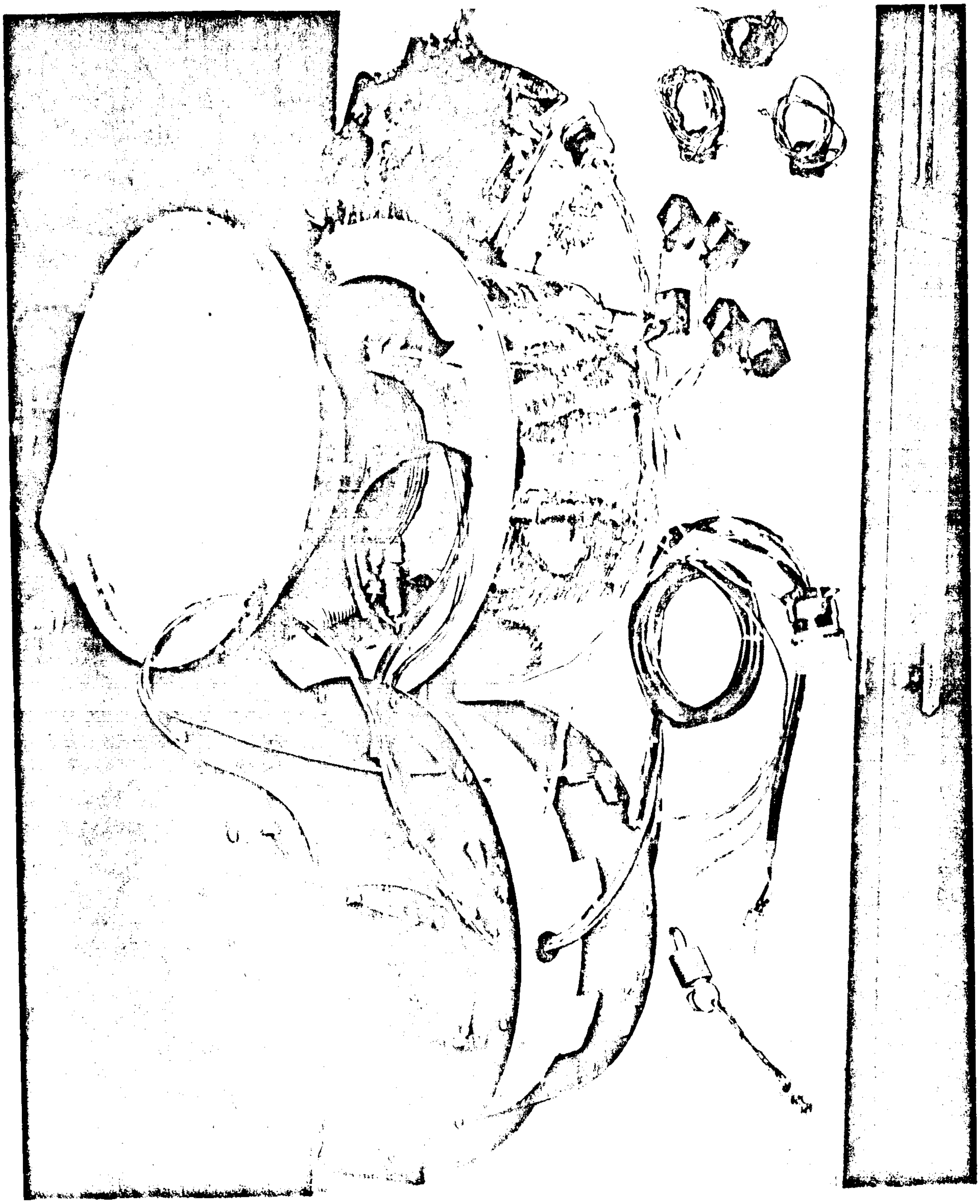

Figure 2-2. Dismantled Test Fixture

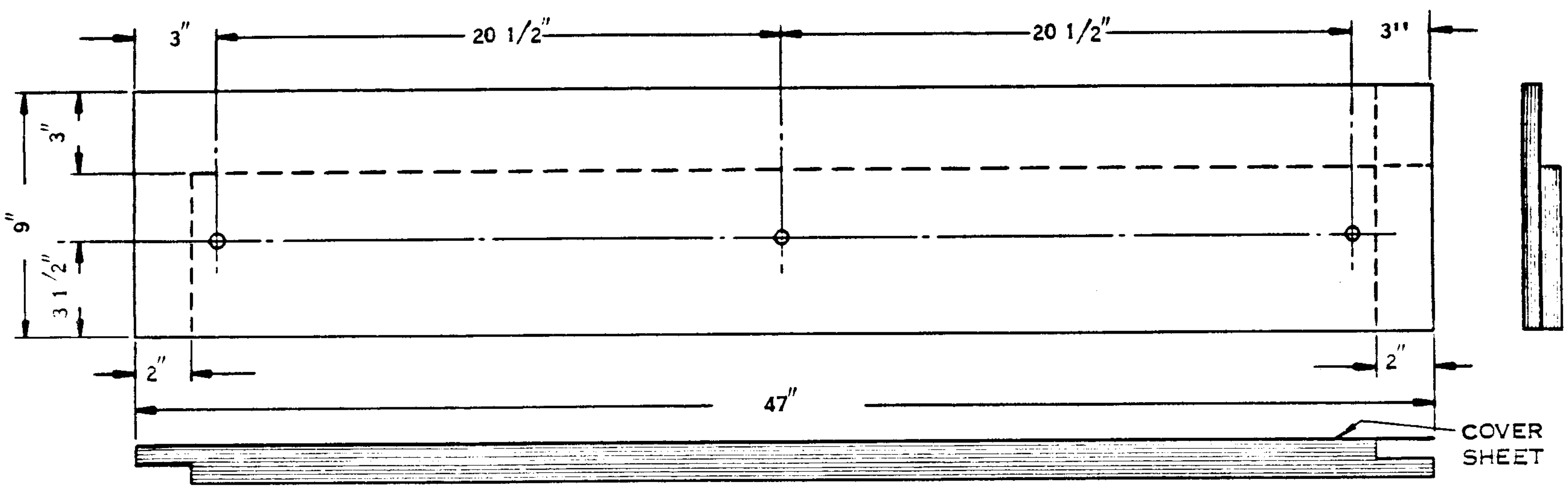

G1 { 19 LAYERS GOLD COATED 1/2 MIL KAPTON
1 LAYER COVER SHEET 2 MIL KAPTON }

G2 { 19 LAYERS GOLD COATED 1/4 MIL MYLAR
1 LAYER COVER SHEET 2 MIL KAPTON }

NOTES:

1. 1/2 MIL KAPTON AND 1/4 MIL MYLAR TO BE PERFORATED AND CRINKLED
2. 2 MIL KAPTON TO BE PERFORATED

Figure 2-3. Body Insulation Blanket

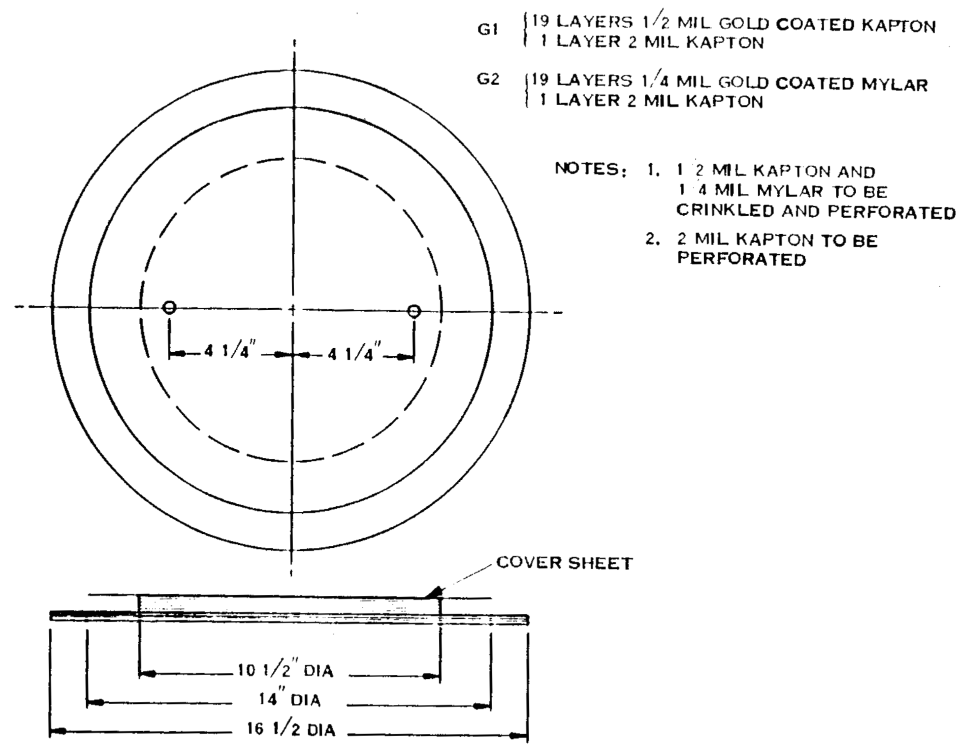

Figure 2-4. End Insulation Blanket

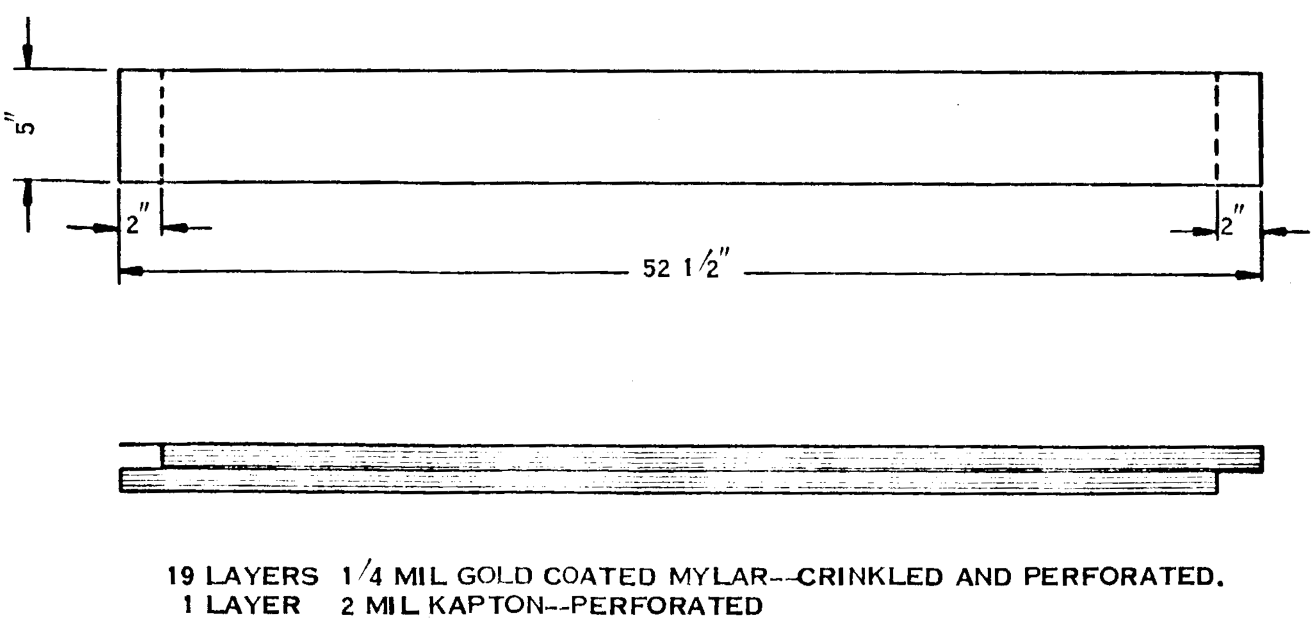

Figure 2-5. Flange Insulation Blanket

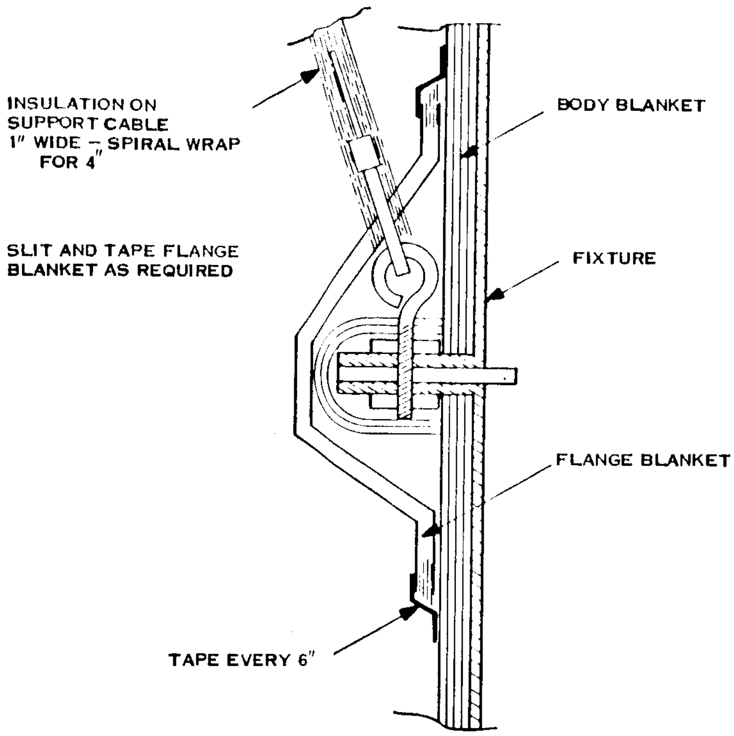

Figure 2-6. Flange Insulation Detail

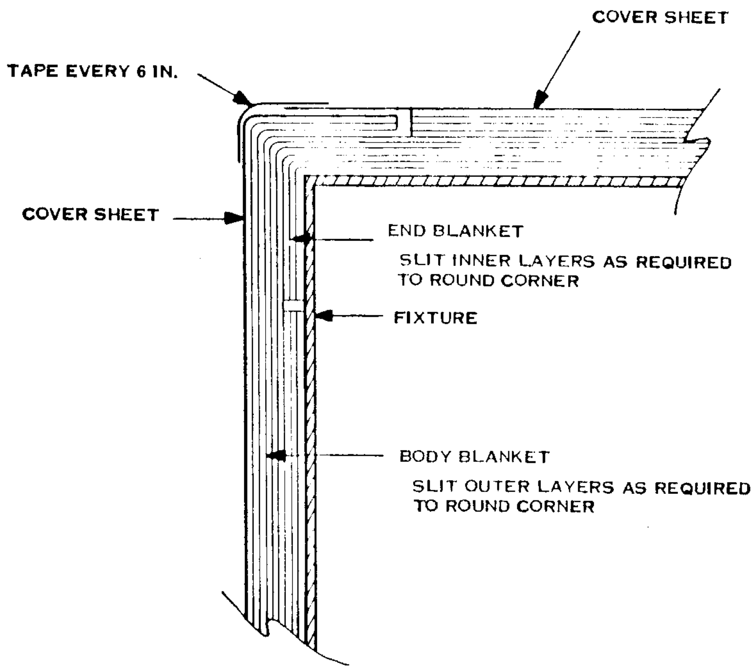

Figure 2-7. Corner Insulation Detail

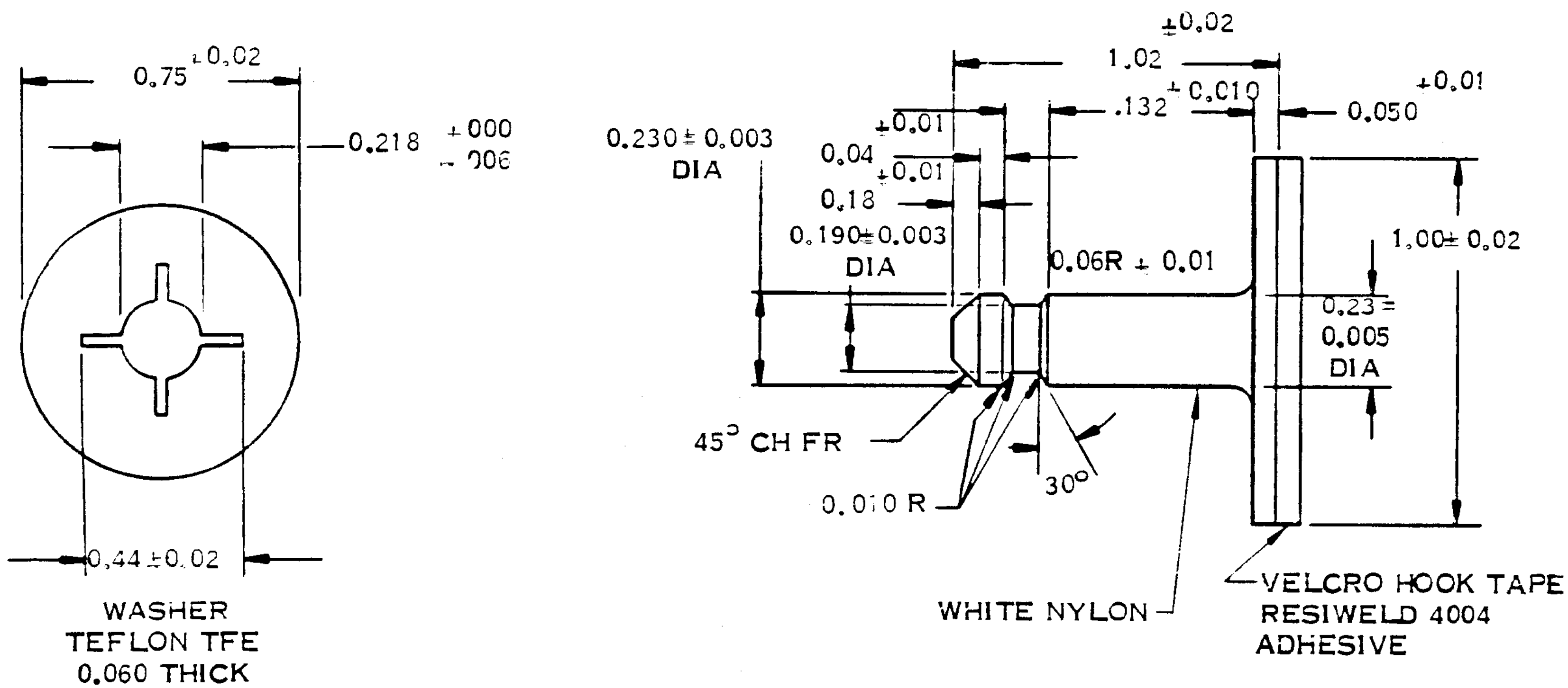

Figure 2-8. Tinger Fasteners

2.3 TEST FACILITY AND EQUIPMENT

The test was performed in a 2 ft by 2 ft thermal vacuum chamber located at the Valley Forge facility. Photographs of the test fixture and vibration exciter are shown in Figures 2-9 and 2-10.

2.4 TEST RESULTS

2.4.1 TEST CONDITIONS

The vacuum level throughout the test was maintained between 1.6×10^{-7} and 2.5×10^{-8} torr. Shroud temperatures were below $-280^{O}F$ during the test. A reference internal temperature of the test model was held between $+36^{O}F$ and $+51^{O}F$ with variations of $+10^{O}F$ to $-9^{O}F$ from the reference location. The total exposure to the test conditions was 1440 hours (60 days) before vibration excitation,plus four days for evaluation of thermal conductance change.

2.4.2 VIBRATION TEST

Prior to starting the vacuum test, the vibration spectrum was run under ambient pressure and temperature conditions to check out operation of the vibration set-up. The vibration levels simulated, as closely as possible, vibration levels measured in static tests of the LEMDE thrust chamber assembly. The total vibration time was three and one-half minutes. An inspection of the insulation system indicated no visible damage after the excitation.

At the conclusion of the sixty day thermal vacuum exposure, and with vacuum and temperature conditions maintained, the model was again subjected to vibration. Figures 2-11 and 2-12 depict the power spectral density for the control accelerometer and accelerometer No. 2, respectively. Two accelerometers were used for redundancy purposes, in case of failure of one of the units. The frequency spectrums were essentially unchanged from the values recorded prior to the start of the vacuum exposure cycle. As may be seen from Figure 2-11, the overall vibration spectrum showed reasonable correlation with the specified levels. Several peaks at 160, 460, 550, 650, 730, and 840 cycles are considerably above the

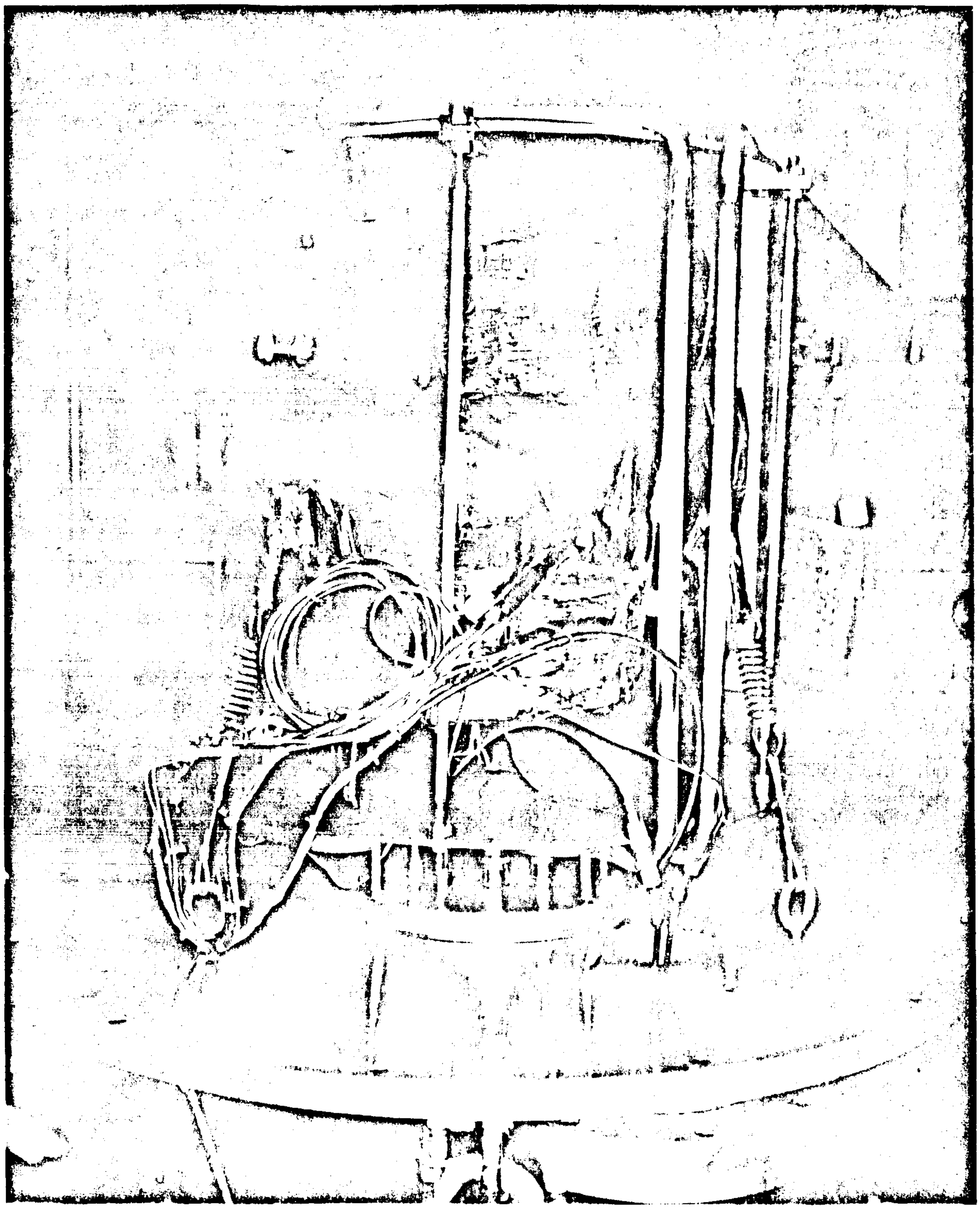

Figure 2-9. Assembled Insulated Test Fixture

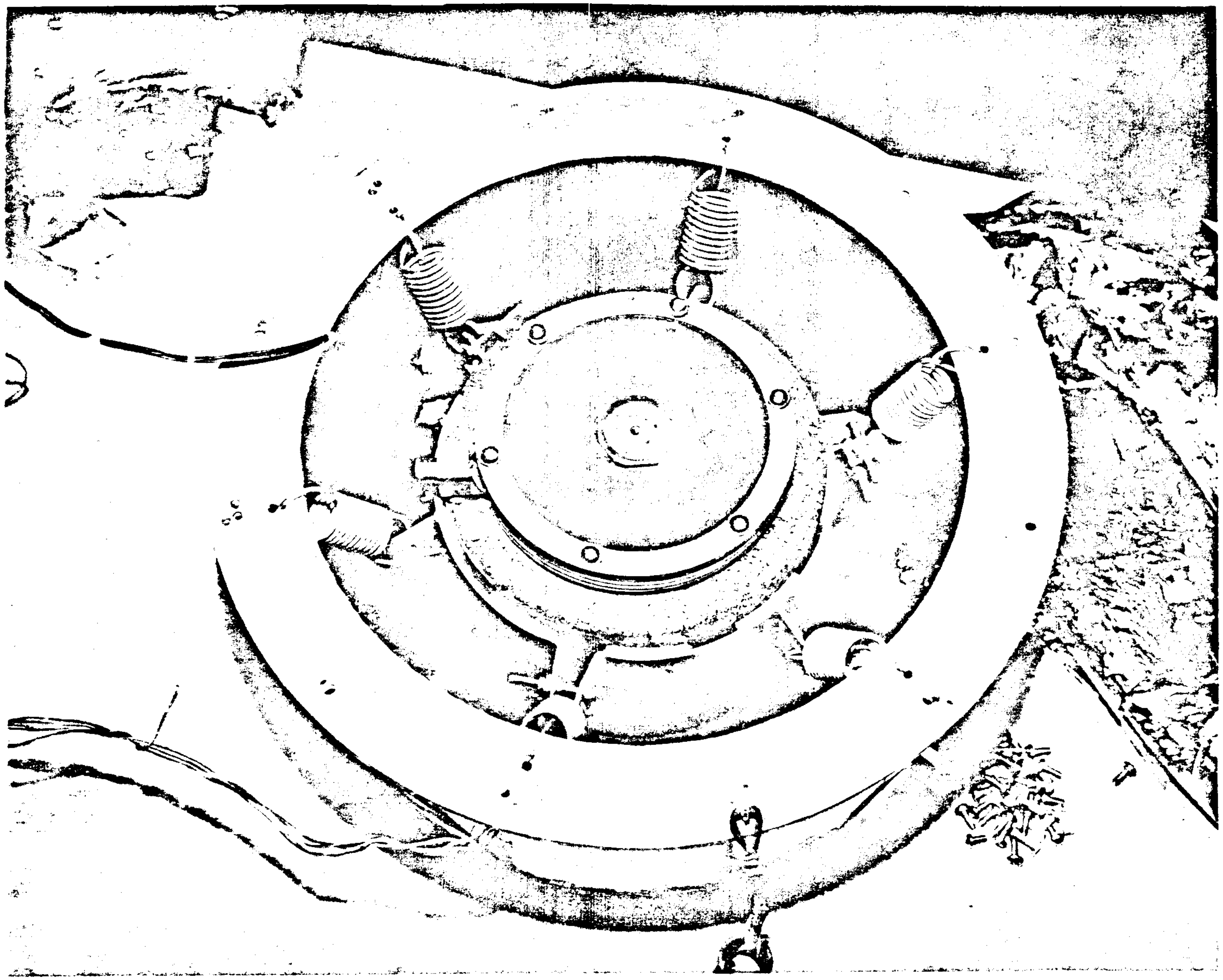

Figure 2-10. Exciter Mounting

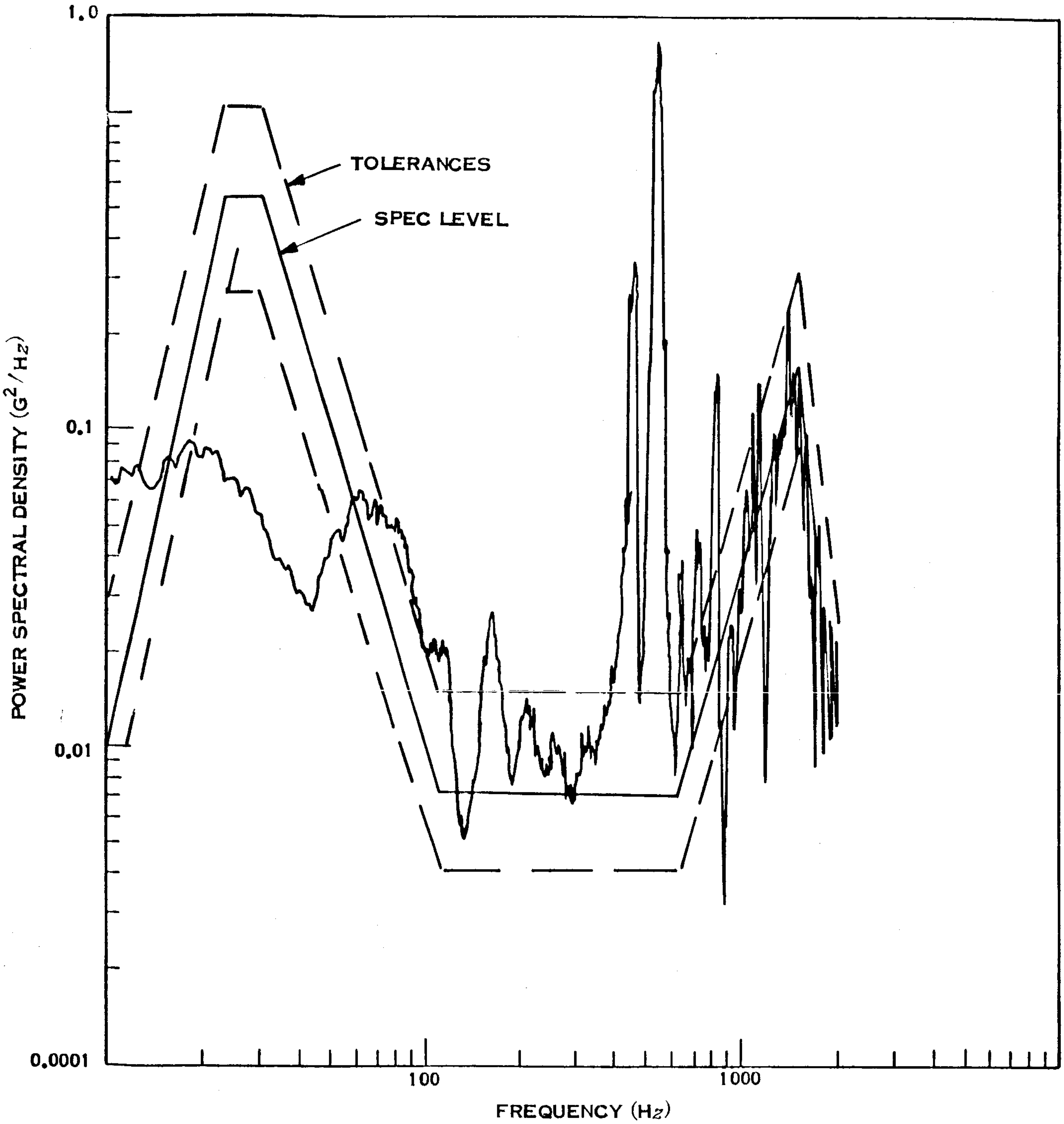

Figure 2-11. Power Spectral Density-Control Accelerometer

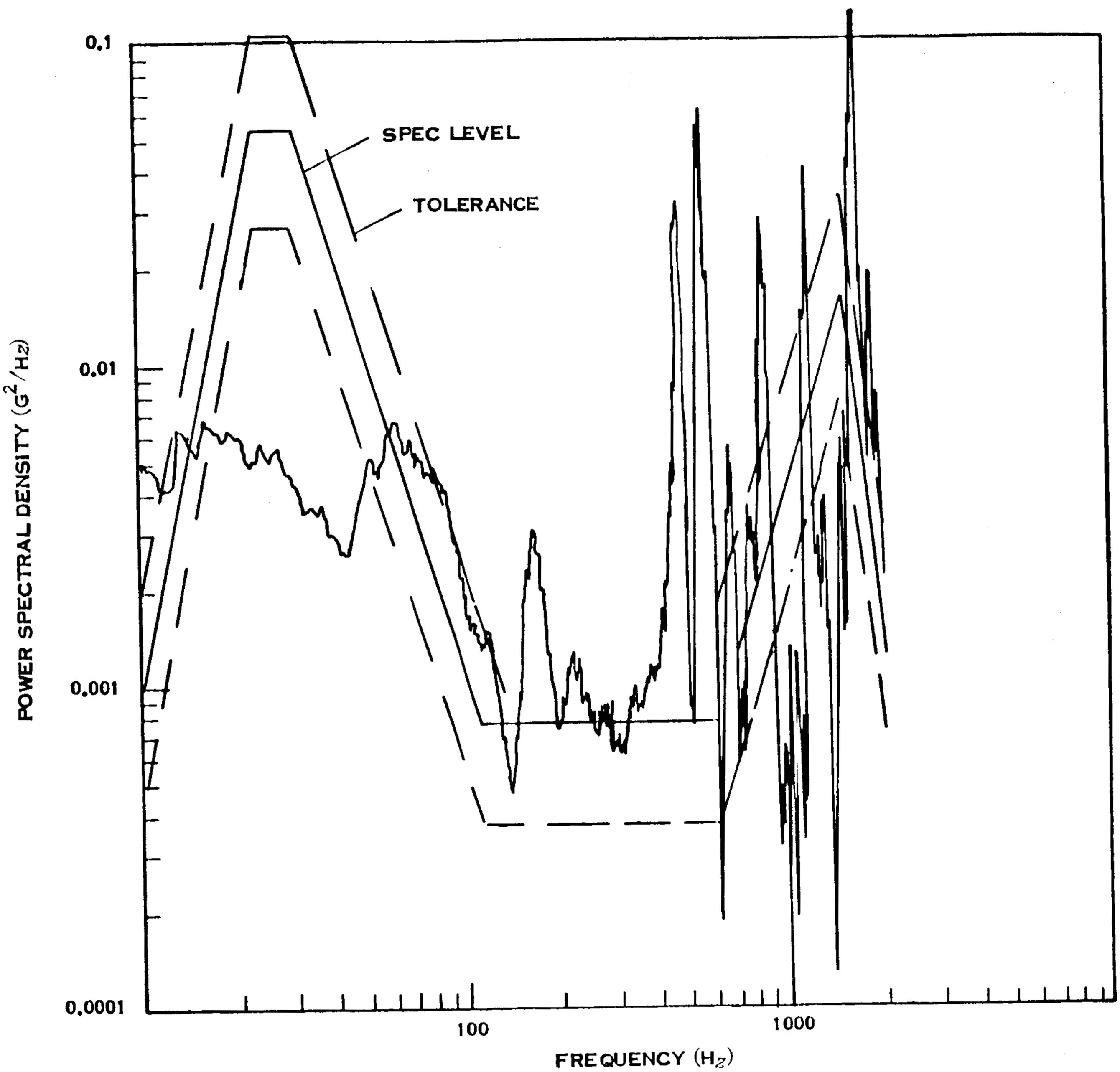

Figure 2-12. Power Spectral Density-Accelerometer No. 2

specification levels and peaks at 900, 960, 1700, and 1800 cycles are below specification levels. These correspond to resonances in the test fixture, which were confirmed by a plot of acceleration/exciter voltage versus frequency.

Total vibration time for the vacuum vibration test was five minutes and 18 seconds, with 120 seconds at the specified test levels.

2.4.3 INSULATION THERMAL PERFORMANCE

The long term vacuum test provided an opportunity to obtain data on the effectiveness of the multilayer insulation design proposed for the full scale tests. The performance of the insulation on the 14-inch long cylinder should be appreciably worse than that applied to the full scale fixtures because of the increased length of joint seams and increased number of support posts per unit area on the smaller model. In addition, the support cables and electrical lead wires will cause a greater proportionate thermal leakage in the small model than will similar disturbances in the full scale test.

During test with liquid nitrogen-cooled chamber walls, 3.7 watts power was required to maintain the model at about $40^{o}F$. At this condition, thermocouples mounted on the cylinder ends adjacent to the heaters read about $45^{o}F$, and thermocouples near the central parting flange were about $35^{o}F$. The 3.7 watts power value is an average over one day's time, with the actual values up to 0.2 watts above that at night and about the same amount below during the day due to plant line voltage fluctuation.

The lead wire bundle included six 24-gage copper-constantan thermocouple lead wire pairs, six 20-gage copper heater power wires, two accelerometer coaxial cables, and the shaker power cable. This bundle was wrapped with insulation to about 5 inches from the model, and included a thermocouple 2.5 inches from the model. The couple read about $-65^{o}F$ during test. Calculations show that at least 0.5 watts could leak through this bundle at these conditions.

The model was supported by three 1/16-in. diameter steel cables. Thimbles were used at each eyebolt in the model flange. The cables and thimbles penetrated the "belly band" of insulation used to cover the flange area of the model. There is no readily available data on the thermal loss through this type of insulation penetration, but is estimated that the leak is probably as much as 0.7 watts total for the three cables. Thus, the heat loss directly through the insulation is estimated to be 2.5 watts (3.7 - 0.5 - 0.7).

Including both sides of the one-inch wide central flange, the model has 7.08 square feet of surface area. This gives a heat loss of about 0.35 watts per square foot. If the heat loss were that much from the 472 square foot full scale capsule fixture, it would result in 165 watts loss. This is higher than the calculated capsule loss of 106 watts at 40^{O}F, but it would be within the values specified by JPL as design requirements for the program.

Data was taken after completion of the vibration cycle and no measurable change in thermal performance was noted.

SECTION 3

CONCLUSIONS

The results of the vacuum/vibration test have led to the following conclusions:

a. The insulation material, Velcro mounting pad material, tingers, and tape exhibited no noticeable damage or change in physical appearance or function after exposure to vacuum and vibration.

b. The insulation system as installed on the fixture exhibited no measurable change in thermal performance after exposure to the vibration.

SECTION 4
RECOMMENDATIONS

It is recommended that this test be considered a materials qualification test for the ability of the materials listed in Section 2.2 to withstand the vacuum and thermal environments encountered during the planetary transfer orbit followed by the vibration levels expected from the firing of the orbit insertion rocket engine.

SECTION 5
NEW TECHNOLOGY

No reportable items of new technology are deemed to have resulted from the effort reported herein.